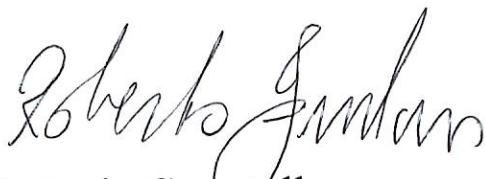


UNIVERSITA' VITA-SALUTE SAN RAFFAELE

**CORSO DI DOTTORATO DI RICERCA
INTERNAZIONALE IN MEDICINA MOLECOLARE
Curriculum in Neuroscienze E Neurologia Sperimentale**

**Regulatory neutrophils during
neuroinflammation**

DoS: MD PhD., Roberto Furlan 
Second Supervisor: Prof. Marco Antonio Cassatella

Tesi di DOTTORATO di RICERCA di Susanna Manenti

matr. 015568

Ciclo di dottorato XXXV

SSD MED/26

Anno Accademico 2021/2022

RELEASE OF PHD THESIS

Il/la sottoscritto/I the undersigned Susanna Manenti
Matricola / registration number 015568
nata a/ born at Gallarate (VA), Italia
il/on 23/03/1995

autore della tesi di Dottorato di ricerca dal titolo / author of the PhD Thesis titled
“Regulatory neutrophils during neuroinflammation”

AUTORIZZA la Consultazione della tesi / AUTHORIZES the public release of the thesis
 NON AUTORIZZA la Consultazione della tesi per 12 mesi / DOES NOT AUTHORIZE the
public

release of the thesis for 12 months
a partire dalla data di conseguimento del titolo e precisamente / from the PhD thesis date,
specifically

Dal / from 16/12/2022 Al / to 16/12/2023

Poiché /because:

l'intera ricerca o parti di essa sono potenzialmente soggette a brevettabilità/ The whole project
or part of it might be subject to patentability;

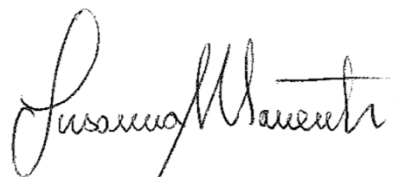
ci sono parti di tesi che sono già state sottoposte a un editore o sono in attesa di
pubblicazione/ Parts of the thesis have been or are being submitted to a publisher or are in
press;

la tesi è finanziata da enti esterni che vantano dei diritti su di esse e sulla loro pubblicazione/
the thesis project is financed by external bodies that have rights over it and on its publication.

E' fatto divieto di riprodurre, in tutto o in parte, quanto in essa contenuto / Copyright the
contents of the thesis in whole or in part is forbidden

Data /Date 29/11/2022

Firma /Signature



DECLARATION

This thesis has been:

- composed by myself and has not been used in any previous application for a degree.
- Throughout the text I use both 'I' and 'We' interchangeably.
- has been written according to the editing guidelines approved by the University.

Permission to use images and other material covered by copyright has been sought and obtained. For the following image/s (specify), it was not possible to obtain permission and is/are therefore included in thesis under the "fair use" exception (Italian legislative Decree no. 68/2003).

All the results presented here were obtained by me, except for:

- 1) *Mass spectrometry (CyTOF) experiment. For instance: CyTOF experiments (Results, paragraph I.VI, figure 25), were performed in collaboration with Dr. T Croese, Department of Brain Sciences, Weizmann Institute of Science, Rehovot, Israel.*

Moreover, I hereby declare that:

Chapter IV of the Introduction "PD-1/PD-L axis" has been already published. Chapter IV was adapted from the review written by our lab, Manenti et al. *PD-1/PD-L Axis in Neuroinflammation: New Insights* published in *Frontiers in Neurology* in June 2022¹.

All sources of information are acknowledged by means of reference.

Acknowledgements

I would like to thank Dr. Roberto Furlan, for the opportunity to join his lab and complete this PhD. He has been a great mentor, with wise advice and brilliant solutions even when I was not able to see one. He always believed in me and gave me everything that was necessary to finish this project in the best possible environment.

Special thanks go to the present and past member of Furlan's group (KNUT) for all the technical and psychological support that they have provided in the last three years. In particular, I would like to thank Annamaria Finardi and Alessandra Mandelli for their professional expertise in mouse experiments, flow cytometry and basically everything else. This project will never be completed without them.

I thank my second advisor, Professor Marco Antonio Cassatella, for guiding me through the complex world of neutrophils and for his punctual advice. I would also like to thank him for helping me to start collaborating with Prof. Sergio Daniel Catz, in whose lab I spent six months during my second year, and where I learned a lot on microscopy and mouse neutrophils.

I thank Professor Mathias Gunzer, Professor Xuemei Zhong and Professor Matteo Iannacone for kindly sharing the transgenic mouse models that were fundamental for the final experiments and for the publication of this study.

I thank dr. Tommaso Croese for starting this project with me during my master's thesis and for transmitting to me the love for research. I also thank him for performing the CyTOF experiments at the Weizmann Institute in Israel, which helped in the characterization of human neutrophils.

Finally, I thank all the lab members of the Neuroimmunology Unit.

Dedication

Ai miei genitori.

Abstract

The onset and progression of neurological disorders have recently been linked to neutrophils. The neutrophil-to-lymphocyte ratio has been proposed as a clinical marker for both ischemic stroke and multiple sclerosis (MS). A few recent studies have revealed the existence of neutrophils with immunosuppressive and protective roles in the preclinical model of MS, Experimental Autoimmune Encephalomyelitis (EAE). However, the identification and characterization of neutrophils with regulatory functions in patients with MS are still lacking. Here, we identified a subpopulation of neutrophils characterized by the expression of the regulatory ligand PD-L2 (or CD273) in both MS patients and mice with EAE. PD-L2⁺ neutrophils are more frequent during the active stages of human MS as well as during experimental neuroinflammation in EAE mice. In this study, we extensively characterized the expression of surface markers typically associated with immunosuppressive functions in humans using multiparametric flow and mass cytometry. By performing *ex vivo* co-culture experiments, we observed the cell-to-cell interactions between neutrophils and lymphocytes and confirmed their suppressive action on T cell proliferation. We then described the kinetics of PD-L2⁺ neutrophils in EAE mice and hypothesized the preferential recruitment of this population in the CNS through the CXCR2 axis. Finally, using transgenic mutant mice, we aimed to deplete this neutrophil population to understand its relative importance in the context of the disease. Overall, we speculate that PD-L2 may be a suitable candidate for identifying regulatory neutrophils in both MS and EAE, paving the way for innovative approaches to noninvasive diagnosis and cell therapies.

TABLE OF CONTENTS

TABLE OF CONTENTS	1
ACRONYMS AND ABBREVIATIONS.....	3
LIST OF FIGURES AND TABLES.....	5
INTRODUCTION.....	9
I. NEUROINFLAMMATION	9
<i>I.I Pathogenesis of neuroinflammation</i>	9
<i>I.II Glial cells crosstalk in neuroinflammation</i>	10
II. MULTIPLE SCLEROSIS	14
<i>II.I MS as a neuroinflammatory autoimmune disease</i>	14
<i>II.II Other circulating cellular subsets involved in the pathogenesis of MS</i>	16
<i>II.III Clinical features of MS</i>	19
<i>II.IV EAE as an experimental model of MS</i>	23
III. NEUTROPHILS	27
<i>III.I Neutrophil biology</i>	27
<i>III.II Heterogeneity of neutrophils subsets and immunoregulatory functions</i>	29
<i>III.III Neutrophil in EAE and MS</i>	31
IV. PD1/PD-L1 PD-L2 AXIS	35
<i>IV.I Biology of the PD-1/PD-L axis</i>	35
<i>IV.II PD-L1 and PD-L2 expression in the CNS of EAE mice</i>	37
<i>IV.III Transgenic PD-1^{-/-}, PD-L1^{-/-} and PD-L2^{-/-} in EAE model</i>	38
<i>IV.IV PD-1/PD-L axis in MS</i>	39
AIM OF THE WORK.....	43
RESULTS	45
I. HUMAN RESULTS	45
<i>I.I PD-L2 expression on circulating immune cells in neurological patients and healthy donors</i> 45	
<i>I.II PD-L2⁺ neutrophils are increased in patients with an active form of MS, but not in other autoimmune diseases</i>	47
<i>I.III PD-L2⁺ neutrophils are a group of mature cells sedimenting in the NDNL</i>	48
<i>I.IV PD-L2 neutrophils express markers typically associated with regulatory functions</i>	50
<i>I.V Anti-inflammatory cytokines are detectable in the supernatants of PD-L2 neutrophils co-cultured with T lymphocytes</i>	51
<i>I.VI PD-L2⁺ neutrophils are inducible ex vivo after stimulation with cytokines</i>	53
<i>I.VII Multiparametric flow cytometry and CyTOF mass spectrometry show that PD-L2⁺ neutrophils express markers typically associated with regulatory features</i>	58

<i>I.VIII PD-L2 neutrophils inhibit T cell proliferation and IFN-γ release in the supernatant of coculture</i>	59
<i>I.IX Blocking PD-1 axis, the inhibitory effect of PD-L2 neutrophils is partially restored</i>	60
<i>I.X Neutrophils and CD3 cells form conjugates in vitro</i>	62
<i>I.XI Quantification of soluble hPD-L2 in plasma and CSF of patients with MS</i>	65
II.I MOUSE RESULTS - WILD TYPE MICE	67
<i>II.I.I PD-L1 and PD-L2 expression on immune cells during EAE</i>	67
<i>II.I.II CXCR2 seems to be fundamental for the recruitment of PD-L2⁺ neutrophils</i>	71
<i>II.I.III PD-L2 expression cannot be induced in murine neutrophils after ex vivo stimulation</i>	72
<i>II.I.IV DT toxicity</i>	74
II.II MOUSE RESULTS – TRANSGENIC MOUSE MODELS	75
<i>II.II.I PZTD mouse model</i>	75
<i>II.II.II Catchup mouse model (CRE specific for Ly6G locus)</i>	79
<i>II.II.III Depletion of PD-L2⁺ myeloid cells (LysM⁺) during EAE</i>	81
DISCUSSION	83
MATERIALS AND METHODS	91
I. HUMAN SAMPLES	91
<i>I.I Whole blood analysis with multiparametric flow cytometry</i>	91
<i>I.II Neutrophils and PBMCs isolation</i>	93
<i>I.III Ex-vivo neutrophil stimulation</i>	93
<i>I.IV CyTOF Mass Spectrometry analysis</i>	94
<i>I.V Cell proliferation assay</i>	97
<i>I.VI May-Grünwald Giemsa Staining on neutrophils</i>	98
<i>I.VII Immunofluorescence</i>	99
<i>I.VIII Lymphocytes/Neutrophils conjugates</i>	100
II. MOUSE SAMPLES	101
<i>II.I EAE induction</i>	101
<i>II.II Intracardiac perfusion</i>	102
<i>II.III Multiparametric analysis of mouse tissues by flow cytometry</i>	102
<i>II.IV RT-PCR</i>	104
<i>II.V Tissue immunofluorescence staining</i>	104
<i>II.VI Isolation of murine neutrophils</i>	105
<i>II.VII Transgenic mouse models</i>	105
III. STATISTICAL ANALYSIS	109
REFERENCES	110

ACRONYMS AND ABBREVIATIONS

AD *Alzheimer's Disease*

APCs *Antigen Presenting Cells*

ATP *Adenosine TriPhosphate*

BBB *Blood Brain Barrier*

BM *Bone Marrow*

CAMs *CNS-associated macrophages*

CCL *C-C-motif Chemokine Ligand*

CFA *complete Freund's adjuvant*

CIS *Clinically isolated syndrome*

CNS *Central Nervous System*

CSF *Cerebrospinal Fluid*

CXCL *C-X-C-motif Chemokine Ligand*

CXCR *C-X-C-motif chemokine receptor*

DAMPs *Damage-Associated Molecular Patterns*

EAE *Experimental Autoimmune Encephalomyelitis*

FOXP3 *Forkhead box P3*

GFAP *Glial Fibrillary Acidic Protein*

GM-CSF *granulocyte-macrophage colony-stimulating factor*

GWAS *genome-wide association study*

ICS *Intra Cellular Staining*

IFN *Interferon*

IL *Interleukin*

LDNs *low-density neutrophils*

MBP *Myelin Basic Protein*

MHCII *Major Histocompatibility Complex type II*

MMP *Matrix Metalloproteinase*

MOG *Myelin Oligodendrocyte Glycoprotein*

MPO *Myeloperoxidase*

MRI *Magnetic Resonance Imaging*

MS *Multiple Sclerosis*
NDNs *Normal Density Neutrophils*
NETs *Neutrophil Extracellular Traps*
NO *Nitric Oxide*
NK *Natural Killer (cells)*
PAMPs *Pathogen-Associated Molecular Patterns*
PD-1 *Programmed cell death protein-1*
PD-L *Programmed cell death protein-1 ligand*
PLP *Proteolipid Protein*
PMNs *Polymorphonuclear Neutrophils*
PP-MS *Primary Progressive Multiple Sclerosis*
PRRs *pattern recognition receptors*
ROS *Reactive Oxygen Species*
RR-MS *Relapsing-Remittent Multiple Sclerosis*
SC *Spinal Cord*
SP-MS *Secondary Progressive Multiple Sclerosis*
TGF *Transforming Growth Factor*
Th *T helper (cells)*
TLR *Toll-like receptors*
TNF *Tumor Necrosis Factor*

LIST OF FIGURES AND TABLES

FIGURE 1. POSITIVE AND NEGATIVE ASPECTS OF NEUROINFLAMMATION.	10
FIGURE 2. ABERRANT RESPONSES OF THE IMMUNE SYSTEM IN THE PERIPHERY.	15
FIGURE 3. LYMPHOID-MYELOID INTERACTIONS IN MS.	18
FIGURE 4. HETEROGENEITY OF MULTIPLE SCLEROSIS COURSES.	19
FIGURE 5. TYPES OF MS	22
FIGURE 6. EAE CLINICAL COURSES.	25
FIGURE 7. NEUTROPHIL ACTIONS IN INFECTION AND INFLAMMATION.	28
FIGURE 8. NEUTROPHILS GRANULES AND SECRETORY VESICLES.	29
FIGURE 9. REGULATORY OR ACTIVATING NEUTROPHIL INTERACTIONS WITH T CELLS AND DCs.	31
FIGURE 10. IMMUNE CHECKPOINT FUNCTION DURING ACTIVATION OR INHIBITION PATHWAYS.	37
FIGURE 11. PD-1/PD-L AXIS IN NEUROINFLAMMATION. ERROR! BOOKMARK NOT DEFINED.	
FIGURE 12. VISUAL REPRESENTATION OF THE AIM OF WORK.	44
FIGURE 13. PD-L2 EXPRESSION ON CIRCULATING IMMUNE CELLS.	46
FIGURE 14. PERCENTAGE OF PD-L2 NEUTROPHILS ON TOTAL CD16 CD66B NEUTROPHILS IN PATIENTS AND HEALTHY CONTROLS.	48
FIGURE 15. NEUTROPHILS MATURATION STAGES.	49
FIGURE 16. PD-L2 NEUTROPHILS IN DIFFERENT CENTRIFUGATION LAYERS. BIOSCIENCES).	50
FIGURE 17. PERCENTAGE OF EXPRESSION OF REGULATORY MARKERS ON PD-L2⁺ NEUTROPHILS COMPARED TO PD-L2⁻ NEUTROPHILS.	51
FIGURE 18. CYTOKINES RELEASED IN THE SUPERNATANT OF CO-CULTURE BETWEEN SORTED NEUTROPHILS AND T LYMPHOCYTES.	52
FIGURE 19. ICS OF IL4 IN PD-L2⁺ AND PD-L2 NEGATIVE NEUTROPHILS.	53
FIGURE 20. DOSE RESPONSE AND KINETICS OF NEUTROPHILS RESPONSE TO IL-4 EX VIVO STIMULATION.	54

FIGURE 21. MAY-GRUNWALD GIEMSA STAINING OF NEUTROPHILS ISOLATED FROM HEALTHY DONORS, STIMULATED WITH IL-4 FOR 18 HOURS, OR NOT STIMULATED (RPMI ONLY).....	55
FIGURE 22. PERCENTAGE OF NEUTROPHILS EXPRESSING PD-L2 AFTER EX VIVO STIMULATION FOR 18H, ALONE OR IN COMBINATION.....	55
FIGURE 23. KINETICS OF NEUTROPHILS RESPONSE TO GM-CSF AND IFN-γ EX VIVO STIMULATION.....	56
FIGURE 24. HUMAN NEUTROPHILS WITH OR WITHOUT STIMULATION.	57
FIGURE 25. CYTOF RESULTS.....	59
FIGURE 26. IMMUNOSUPPRESSIVE ASSAYS: CO-CULTURE BETWEEN NEUTROPHILS AND ACTIVATED T CELLS.	60
FIGURE 27. THE SUPPRESSIVE FUNCTION OF PD-L2 NEUTROPHILS IS PARTIALLY REVERTED IN THE PRESENCE OF PD-1 BLOCKING ANTIBODY.....	61
FIGURE 28. ACTIVATION STATUS OF T LYMPHOCYTES IN CO-CULTURES WITH OR WITHOUT NEUTROPHILS.	62
FIGURE 29. NEUTROPHIL/CD3 CONJUGATES.	63
FIGURE 30. STACKS OF NEUTROPHIL/CD3 CONJUGATES.	64
FIGURE 31. ANALYSES OF NEUTROPHILS/LYMPHOCYTES CONJUGATES.....	65
FIGURE 32. SOLUBLE PD-L2 FOUND IN THE SERUM.....	66
FIGURE 33. SOLUBLE PD-L2 FOUND IN THE CSF.....	66
FIGURE 34. EAE.....	67
FIGURE 35. INFILTRATING AND RESIDENT CELLS IN THE CNS EXPRESSING PD-L1 OR PD-L2 IN EAE.....	68
FIGURE 36. PD-L2 AND PD-L1 NEUTROPHILS IN BLOOD AND LYMPHOID ORGANS.	69
FIGURE 37. REPRESENTATIVE IMAGES OF PD-L2 NEUTROPHILS INFILTRATING THE CNS OF EAE MICE AT 14 D.P.I.	70
FIGURE 38. HEATMAPS OF TRANSCRIPT EXPRESSION IN BRAINS, SPINAL CORDS, AND LYMPH NODES IN EAE MICE AT DIFFERENT TIME POINTS.....	71
FIGURE 39. PD-L2⁺ NEUTROPHILS IN THE CNS AND CIRCULATING IN THE BLOOD.....	72
FIGURE 40. EX VIVO STIMULATION OF MOUSE NEUTROPHILS.	73
FIGURE 41. EAE COURSE WITH OR WITHOUT DT ADMINISTRATION.	74
FIGURE 42. PERITONEAL WASHOUT OF PZTD HETEROZYGOUS MICE.....	75

FIGURE 43. EAE IN PZTD TRANSGENIC MICE.....	76
FIGURE 44. GATING STRATEGY OF IMMUNE CELLS IN THE CNS OF PZTD MICE WITH EAE.	77
FIGURE 45. CO-LOCALIZATION OF ZSGREEN WITH DIFFERENT CELL POPULATION MARKERS IN PZTD MICE WITH EAE AT 14 D.P.I.	78
FIGURE 46. BLOOD ANALYSIS OF CATCHUP MICE.....	79
FIGURE 47. EAE IN CATCHUP MICE.	80
FIGURE 48. INFILTRATING NEUTROPHILS IN CATCHUP MICE WITH EAE AT 14 D.P.I. .	81
FIGURE 49. EAE IN PZTD X LYSM MICE.	83
FIGURE 50. SCHEMATIC PROTOCOL FOR THE ISOLATION OF NEUTROPHILS AND PBMCs FROM WHOLE BLOOD.	93
FIGURE 51. SCHEMATIC PROTOCOL USED FOR CELL PROLIFERATION ASSAY.	97
FIGURE 52. CLINICAL SCORES USED TO EVALUATE EAE.	101
FIGURE 53. GENETIC STRATEGY USED FOR THE GENERATION OF PZTD MICE.....	106
FIGURE 54. GENETIC STRATEGY USED FOR THE GENERATION OF CATCHUP MICE. ..	107

TABLE 1. DEMOGRAPHIC AND CLINICAL CHARACTERISTICS OF THE STUDY COHORT.	45
TABLE 2. IMMUNE CHECKPOINT ANALYSIS ON WHOLE BLOOD FROM NEUROLOGICAL PATIENTS.	92
TABLE 3. REGULATORY MARKERS IN CIRCULATING NEUTROPHILS ON WHOLE BLOOD FROM PATIENTS WITH MS AND HEALTHY DONORS.	92
TABLE 4. PANEL USED FOR THE QUANTIFICATION OF PD-L2 AND PD-L1 EXPRESSION ON NEUTROPHILS AFTER OVERNIGHT EX VIVO STIMULATION.	94
TABLE 5. CYTOF ANTIBODY PANEL USED FOR THE CHARACTERIZATION OF PD-L2⁺NEUTROPHILS.	96
TABLE 6. PANEL OF ANTIBODIES USED TO QUANTIFY THE CELL PROLIFERATION AFTER 3,5 DAYS OF CO-CULTURES OF LYMPHOCYTES WITH NEUTROPHILS.	98
TABLE 7. PRIMARY ANTIBODIES USED FOR IF ON HUMAN LEUKOCYTES.	100
TABLE 8. PANEL OF ANTIBODIES USED TO ANALYZE PD-L1 AND PD-L2 EXPRESSION ON DIFFERENT POPULATION OF LEUKOCYTES IN MICE WITH EAE.	103
TABLE 9. MOUSE PANEL FOR CXCR2 EXPRESSION ON CIRCULATING NEUTROPHILS AND CNS INFILTRATING CELLS IN EAE MICE.	103
TABLE 10. PRIMARY ANTIBODIES USED FOR IF ON MOUSE TISSUES.	105
TABLE 11. PANEL OF ANTIBODIES USED TO CHARACTERIZE INFILTRATING CELLS IN THE CNS OF PZTD MICE WITH EAE AT 14 D.P.I.	106
TABLE 12. PANEL OF ANTIBODIES USED TO CHARACTERIZE CIRCULATING CELLS IN THE BLOOD OF CATCHUP MICE.	107
TABLE 13. PANEL OF ANTIBODIES USED TO ANALYZE DIFFERENT CELL POPULATIONS IN PZTD X LYSM MICE WITH EAE.	108

INTRODUCTION

I. Neuroinflammation

1.1 Pathogenesis of neuroinflammation

Neuroinflammation is defined as an inflammatory response occurring within the Central Nervous System (CNS), specifically in the brain or the spinal cord (SC). Neuroinflammation occurs through a complex, highly multicellular pathophysiological process that evolves according to the type and duration of the disease. The trigger can be of various types such as infections, traumatic brain injury, toxic metabolites, neurodegenerative diseases and aging². In response to inflammatory stimulation, CNS-resident cells (microglia and astrocytes), endothelial cells and infiltrating peripheral immune cells, release a plethora of pro-inflammatory cytokines, chemokines, reactive oxygen species (ROS) and secondary messengers (prostaglandins and nitric oxide) that spread and maintain the inflammatory process. The extent of neuroinflammation depends on the context, duration, and course of the primary stimulus³ (Figure 1). Although often associated with negative and maladaptive effects, neuroinflammatory responses have several positive effects. In fact, brief and controlled responses are usually associated with a beneficial effect on the organism (e.g., induction of sickness behaviors after an infection). Following a mild and localized CNS insult, a focused immune response consisting of rapid activation of glial cells can contain the spread of inflammation and enhance the production of neurotrophic factors (such as interleukin-1 (IL-1) and IL-4). This may induce repolarization of macrophages/microglia (M2) and promote neuronal recovery and axonal regrowth^{4,5}. However, chronic and uncontrolled neuroinflammation leads to maladaptive responses characterized by uncontrolled glial activation with significant release of pro-inflammatory cytokines, infiltration of peripheral immune cells, edema and increased permeability of the brain-blood barrier (BBB)^{6,7}. Myeloid cells and lymphocytes are the main mediators of cytokine release and tissue damage, thereby boosting the inflammatory cascade.

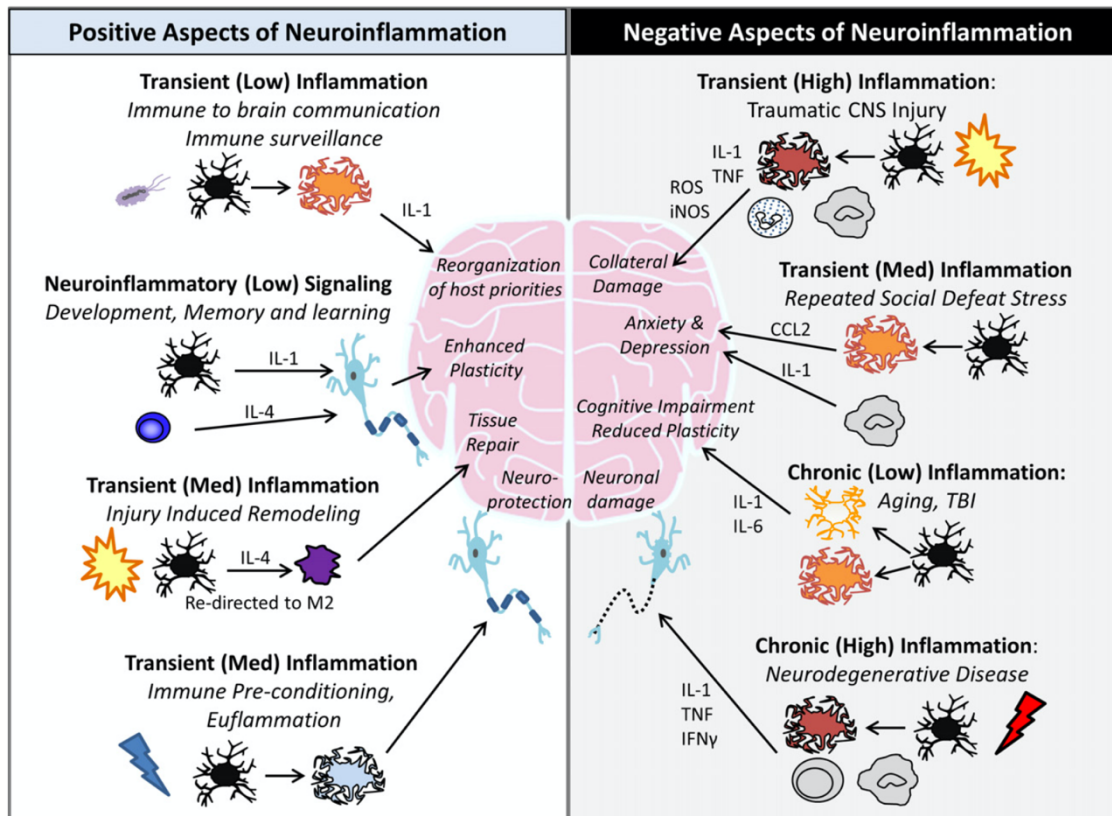


Figure 1. Positive and negative aspects of neuroinflammation. On the left side of the panel, examples of the positive aspects of neuroinflammation, usually observed when the process is brief and controlled. Among these, induction of sickness behaviors, development, memory, and learning. On the right side of the panel, examples of the maladaptive inflammatory responses. Chronic neuroinflammation is characterized by an increase in the release of cytokines (IL-1 and TNF), ROS, and other secondary messengers. These byproducts appear following CNS-trauma and are accompanied by significant recruitment and trafficking of peripheral macrophages and neutrophils to the site of injury (DiSabato, D. J., Quan, N., & Godbout, J. P. (2016). *Neuroinflammation: the devil is in the details. Journal of neurochemistry*, 139, 136-153).

I.II Glial cells crosstalk in neuroinflammation

Microglia and astrocytes are the main innate immune cells in the brain and SC, representing the initiators of immune responses within the CNS. They release immunomodulators and express immune pattern recognition receptors (PRRs), such as Toll-like receptors (TLRs), NOD-like receptors, complement receptors, mannose receptors and scavenger receptors⁸. The interaction among microglia, astrocytes and CNS-infiltrating cells is often bivalent and for many aspects is still unclear. Owing to

their sensing functions in the CNS, glial cells must constantly crosstalk with neurons and other glial cells to adapt to changes. As a result, several cytokines, chemokines, growth factors, and adenosine triphosphate (ATP) are released and these interactions play a key role in CNS development, structural organization, and homeostasis. In contrast, a breakdown in cellular communication can lead to neurological diseases such as Multiple Sclerosis (MS) and Alzheimer's Disease (AD).

Microglial cells are known as the resident macrophages of the CNS that originate from the yolk sack. Under normal conditions, microglia display a resting phenotype and constantly monitor the CNS environment by interacting with neurons, oligodendrocytes, and astrocytes. In response to injury, microglia undergo morphological changes and proliferate at the injury site. They also express several factors, including immune mediators, when activated⁹. In physiological conditions in the adult brain, microglia play a role in innate immunity by maintaining neuronal plasticity and homeostasis in the CNS. The development of two-photon microscopy combined with the availability of fluorescent transgenic mice has allowed the appreciation for microglia constantly surveying the microenvironment through their sensosomes¹⁰. In case of injury, microglial cells upregulate receptors such as CXCR1 and Trem2 and transform into highly phagocytic cells that help in removing dead cells and debris. As a result, microglial cells release cytokines (such as TNF and IL-1 β) and neurotrophic factors (brain-derived neurotrophic factor (BDNF), Neurotrophin-3 (NT-3) and nerve growth factor (NGF)), promoting remyelination and axonal regeneration^{11,12}. Microglial dysfunction, however, has been linked to pathogenesis and progression of multiple diseases. In MS, the interaction with infiltrating lymphocytes induces microglial activation, stimulating the production of pro-inflammatory cytokines and ROS, which contributes to neuronal damage. Microglial cells can also act as antigen-presenting cells, fueling the effector activity of T lymphocytes in a positive-feedback loop¹³.

For years the dual role of microglia has been found in the two classical phenotypes of activation, known as the pro-inflammatory M1 phenotype and the anti-inflammatory and protective M2 phenotype. However, it is now clear that there is great plasticity and heterogeneity in their phenotypes, which are based on location, type, and stage of the disease^{9,14}. The pro-inflammatory phenotype is generally characterized by the activation

of mitogen-activated protein kinases (MAPK, ERK1/2 and p38), expression of major histocompatibility complex type II cell surface glycoprotein (MHCII), secretion of pro-inflammatory cytokines (TNF- α , IL-1 β , IL-6 and IL-12) and ROS production. Most of these factors are neurotoxic and induce intracellular signal transduction in astrocytes, resulting in cell activation¹⁵. In contrast, the anti-inflammatory phenotype is characterized by the expression of heparin-binding lectin (Ym1), cysteine-rich protein FIZZ-1, mannose receptor CD206 and arginase 1 (Arg1)¹⁶.

Astrocytes, on the other hand, maintain the homeostasis of ions and neurotransmitters, supply neuronal metabolic substrates, and maintain BBB integrity¹⁷. The role of activated astrocytes in neuroinflammatory diseases has long been considered purely detrimental. However, it is important to note that the role of astrogliosis during neuroinflammation is complex and multifaceted, characterized by progressive states of activation. Astrocytes can be either beneficial or harmful depending on their reactive grade and the surrounding microenvironment. Following microglial activation, NO production induces an increase in glycolytic enzymes in astrocytes, which consequently amplifies ROS production and hypoxia-inducible factor (HIF)-1 α release¹⁸. Consequently, the production of ROS by BBB-forming astrocytes determines vasodilatation and leukocyte recruitment¹⁹. Activated astrocytes undergo morphological changes and cytoskeletal rearrangements and overexpress glial fibrillary acidic protein (GFAP)²⁰. During high-grades activation, reactive astrocytes form a glial scar that surround the injury sites (*astrogliosis*), acting as a barrier against the spread of damage and limiting the infiltration of peripheral leukocytes²¹. Recent data suggest that astrocytes may play multiple roles in the formation and repair of lesions in MS. On the one hand, astrocytes produce the chemokines CCL2 (C-C motif chemokine ligand 2) and CXCL10 (C-X-C chemokine ligand 10) at the rim of demyelinated areas, recruiting and activating astrocytes and microglia in an autocrine and paracrine manner. This enhances axonal injury through microglia-derived metalloproteinase (MMP)-9 and other toxic molecules^{22,23}. Moreover, in the chronic phase of the disease, the *glial scar* formed by astrocytes around lesions notably hampers remyelination processes²⁴. In contrast, TNF- α released by activated glial cells following axonal damage induces CXCL12 production by astrocytes, resulting in oligodendrocyte precursor cell recruitment to demyelinated areas and enhanced remyelination processes²⁵.

In addition to resident microglia, **other myeloid cells** within the injured CNS contribute to acute neuroinflammation. There are several specialized infiltrating macrophages in the CNS borders, whose origins and roles in the steady state and disease remain largely unknown. Additionally, once monocytes differentiate into brain macrophages, their surface markers are almost indistinguishable from those of microglia by histology³. These macrophage populations are known as CNS-associated macrophages (CAMs) and include dural, leptomeningeal, perivascular and choroid plexus macrophages²⁶⁻²⁸. Located along cerebrospinal fluid (CSF) gateways, their strategic position suggests a role in the drainage of antigens and metabolite exchange, supporting their involvement in immune surveillance of CNS^{29,30}. There is some evidence that CAMs might have a protective function in MS by limiting the presence of antigens in the central nervous system, thereby controlling local autoimmune reaction³¹. MS lesions, however, exhibit a significant number of activated macrophages as well as in its principal animal model, Experimental Autoimmune Encephalomyelitis (EAE), where there is a significant activation of CAMs^{26,32}.

II. Multiple sclerosis

Multiple sclerosis (MS) is the most common immune-mediated inflammatory disease of the CNS affecting young adults. It is estimated that approximately 2.5 million people are diagnosed with MS worldwide. The impact of the socioeconomic relevance of MS is increasing, as the average age of the disease's onset is between 20 and 40 years, and approximately 50% of the patients need constant use of a wheelchair 25 years after diagnosis³³. Although the etiopathological causes underlying MS remain uncertain, it is now understood that MS is a complex multifactorial disorder in which genetic susceptibility interacts with environmental factors (diet, sunlight exposure/vitamin D) and infectious agents³⁴. In genome-wide association studies (GWASs), more than 100 distinct genetic regions have been associated with MS. Genetic variation accounts for about 30% of disease risk overall³⁵. Although the non-genetic contribution has a larger impact on the development of the disease, less progress has been made in unraveling the environmental determinants of MS due to the complexity of the interpretation of large and sometimes confounding epidemiological data³⁶.

II.1 MS as a neuroinflammatory autoimmune disease

The multifactorial nature of MS reveals a complex pathophysiological process that engages different cellular subpopulations and evolves during disease progression. The hallmarks of MS include inflammation, gliosis, demyelination and axonal loss³³. The developmental mechanisms of the disease can be summarized in three main steps: an autoimmune reaction is triggered against myelin antigens in the periphery; immune cells are recruited into the CNS through a damaged BBB; and T cells are reactivated through contact with specific interactions with antigen-presenting cells (APCs) in the CNS, which ultimately leads to chronic inflammation³⁴.

More extensively, MS is generally considered a predominantly T cell-mediated autoimmune disease and this assumption is supported by evidence mainly derived from its principal animal model, EAE. Infiltrating T cells are detectable in the CNS lesions of patients at the early stages of the disease³⁷ and the HLA mutations associated with MS are thought to reflect the presentation of specific CNS self-antigens to aberrant T cells. CD4⁺ T helper lymphocytes (**Th1 and Th17**) are the main lymphocyte subsets involved in MS as they mount aberrant responses against self-antigens, particularly myelin³⁸.

It is still under debate, however, which of its specific antigens could be the exact cause of the T cells' cross-reactivity. Myelin Basic Protein (MBP), Proteolipid Protein (PLP) and Myelin Oligodendrocyte Glycoprotein (MOG) are the most likely candidates. Different and often contradictory results have been obtained from studies on T-cell reactivity to myelin antigens, which can be partially explained by disease heterogeneity between patients and genetic differences in HLA loci. Moreover, myelin antigens are recognized by an increased number of circulating reactive T cells in patients with MS, but also by a few circulating T cells in healthy controls. A possible explanation is the so-called *epitope spreading* which implies that even if the trigger of the pathology is a single myelin antigen, along with disease progression demyelination leads to the release of previously inaccessible myelin components that fuel T cells' aberrant responses³⁹ (figure 2).

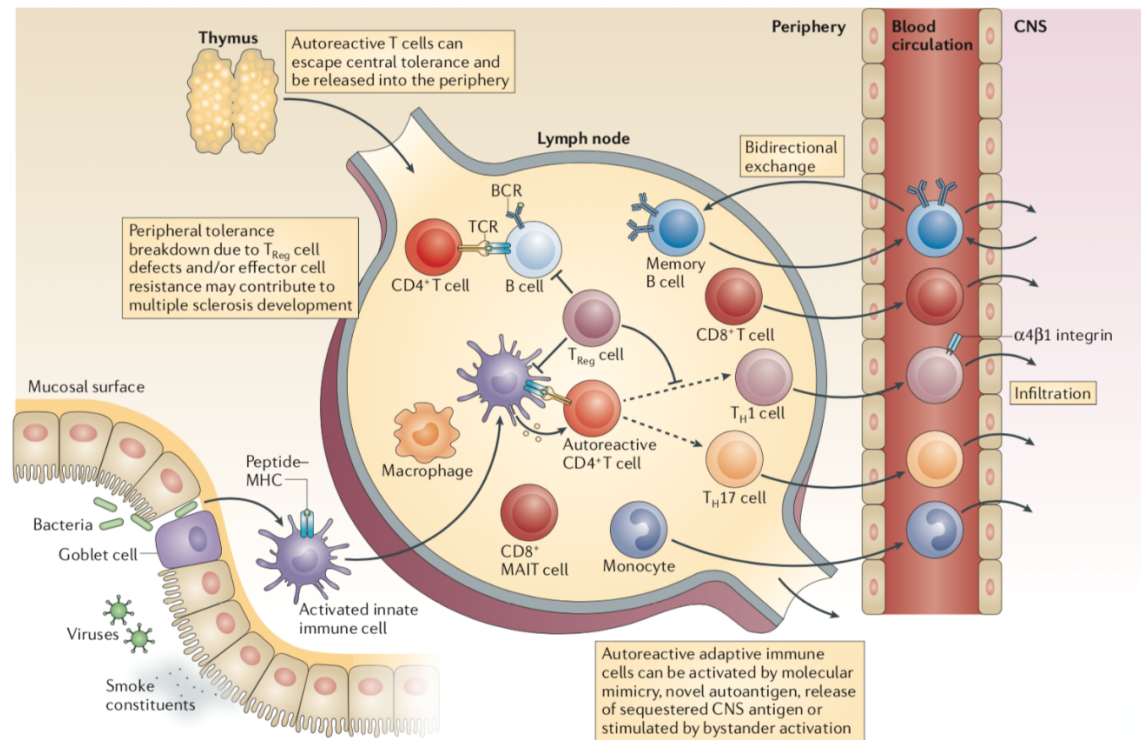


Figure 2. Aberrant responses of the immune system in the periphery. In the thymus, the most autoreactive T cells are discarded during central tolerance establishment. However, some of the autoreactive T cells escape the process of selection and are released into the periphery, leading to aberrant responses and autoreactivity. (Dendrou, C. A., Fugger, L., & Friese, M. A. (2015). *Immunopathology of multiple sclerosis. Nature Reviews Immunology*, 15(9), 545-558. License number: 5423140832715)

Subsequently, there is an increase in BBB permeability, following the overexpression of integrins and their relative ligands in lymphocytes and on endothelial cells, respectively. Moreover, cytokine production (such as TNF- α , IFN- γ and IL-17) by immune cells, expression of metalloproteases and release of reactive oxygen species (ROS) contribute to the impairment of BBB's integrity. In the third step, T cells are reactivated through interactions with specific antigens presented by the resident APCs. T cells reactivation also leads to an increase in cytokine production, which further increases BBB permeability and leads to a second wave of inflammatory cells in the parenchyma. Demyelination is the ultimate result of this process, rendered either by infiltrating macrophages or by TNF- α and NO secreted by T cells, microglia, and macrophages, with consequent cytotoxicity exacerbation⁴⁰.

To date, another theory that has been proposed is the so-called *inside-out* hypothesis: MS may be caused by primary infection or by a neuronal disturbance within the CNS. Therefore, inflammation could occur as a subsequent response, amplifying disease and worsening tissue damage.⁴¹

II.II Other circulating cellular subsets involved in the pathogenesis of MS

In addition to T helper CD4⁺ cells, another important subset of lymphocytes involved in MS is **CD8⁺ T cells**. They can be found in cortical demyelinating lesions of the white and gray matter of MS patients in greater numbers than CD4⁺ T cells, and their frequency positively correlates with axonal damage⁴². Antigen cross-presentation by monocyte-derived dendritic cells (DCs) in the central nervous system activates CD8⁺ T cells via *epitope spreading*⁴³. Moreover, in active lesions of patients with MS, up to a quarter of CD8⁺ T cells are able to produce IL-17 and are thus identified as mucosa-associated invariant T cells (**MAIT cells**).⁴⁴

In MS, **B cells** undergo clonal expansion and can be found in the meninges, parenchyma, and CSF of patients. The number of infiltrating B cells in the CNS changes significantly with disease progression and tends to increase with age, especially in patients with progressive forms of MS⁴². Intrathecal B cells release autoantibodies (immunoglobulins and especially IgG) that are increased in the CSF of patients and can be used as a diagnostic tool⁴⁵.

Additionally, although the reason is still poorly understood, **regulatory T cells** are reduced in number and dysfunctional in patients with MS⁴⁶. This assumption may help explain the emerging role of T and B autoreactive cells in the pathogenesis of MS. Regulatory cells, such as **Foxp3**⁺ CD4⁺ T (T_{reg}) cells and IL-10-producing T regulatory Type 1 (T_{R1}) cells, regulate peripheral tolerance and deplete immune cells mounting aberrant responses against self-antigens, under physiological conditions. If this tolerance is broken, autoreactive T and B cells directed to the CNS may become damaging effector cells through mechanisms such as molecular mimicry, novel autoantigen presentation or recognition of CNS antigens released in the periphery⁴⁷.

In recent years, **natural killer** cells (NK) have recently gained attention in the MS field, both as potent cytotoxic killers, as well as unique immunoregulators. NK cells are lymphocytes of the innate immune system (identified by the antigens CD56^{bright}CD16⁻ and CD56^{dim}CD16⁺) involved in the defense against malignancies and viral infections^{48,49}. The involvement of NK cells in MS was identified mainly through treatment with daclizumab, an IL-2 receptor alpha chain (IL-2R α ; CD25) blocking monoclonal antibody proven to be effective in MS due to its effects on NK cells^{50,51}. NK cells in MS are strongly influenced by environmental risk factors (e.g., EBV infections, smoking and obesity) and the characterization of *memory-like NK cells* provides evidence that NK cells can easily create an inflammatory environment⁵². At the same time, CD56^{bright} NK cells have been suggested to play a major role in controlling T cell responses and counteracting the autoimmune responses in MS⁵³.

APCs of myeloid origin, including **monocytes**, **macrophages**, and **dendritic cells**, have also been shown to play a crucial role in MS, along with lymphoid cells. (NDR: The role of microglia and neutrophils in MS, two other important innate myeloid populations, is discussed respectively in chapter I and in chapter III). In neuroinflammation, these myeloid cell populations serve as both antigen-presenting cells and effector cells. T cells and myeloid cells interact in a vicious cycle that exacerbates the pathology. There are now several disease-modifying therapies available for treating MS, and understanding their mechanism of action has largely focused on the adaptive immune system, but these treatments also affect myeloid cells, as summarized by Mishra et al⁵⁴. The action of MS

immunomodulators on myeloid cells contributes to the clinical efficacy of these therapeutic approaches.

Overall, the complex immune-mediated attack of CNS is almost entirely summarized in **Figure 3**.

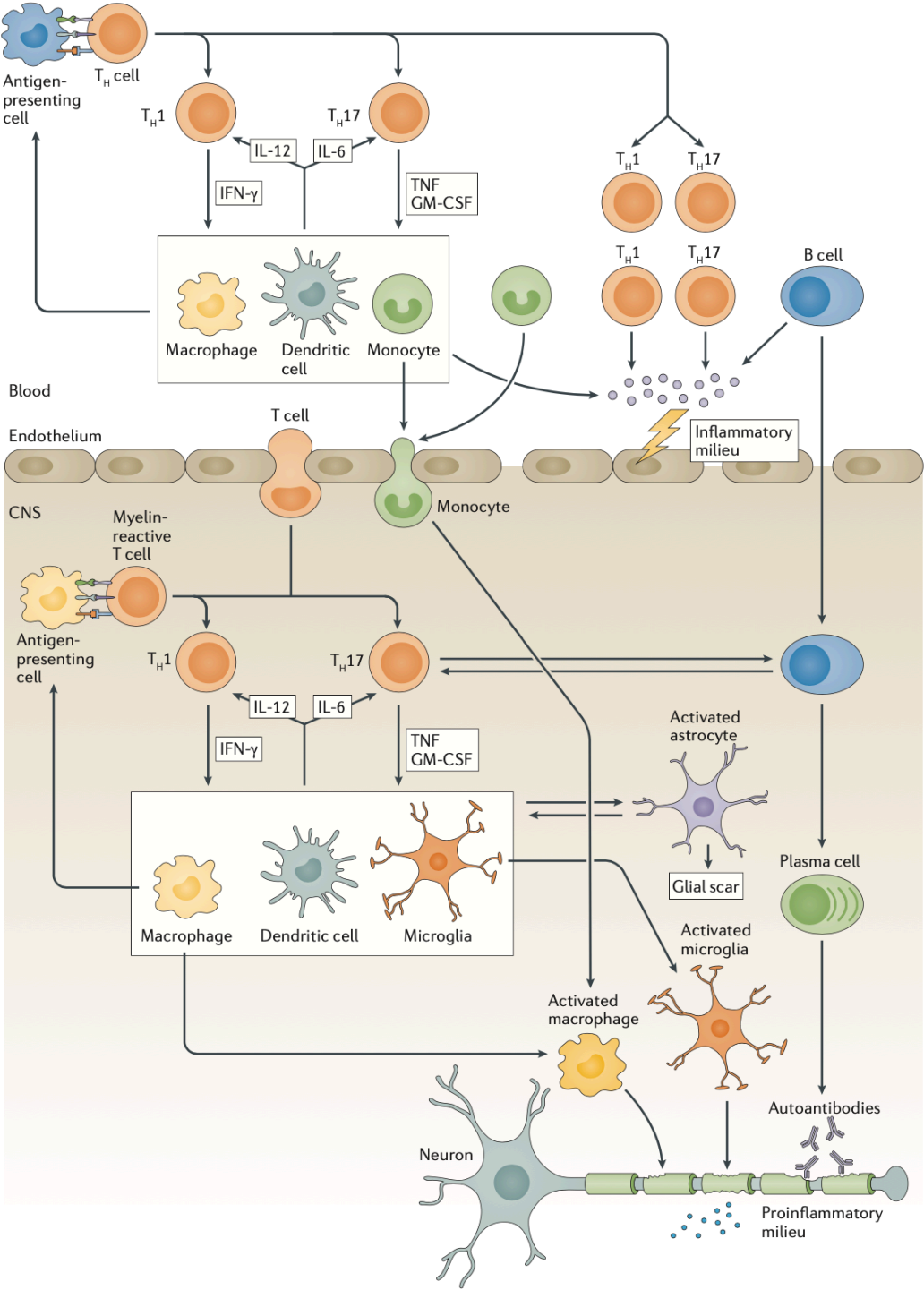


Figure 3. Lymphoid-myeloid interactions in MS. GM-CSF, granulocyte macrophage colony-stimulating factor; TH, T helper; TNF, tumor necrosis factor. (Mishra, M. K., & Yong, V. W.

(2016). *Myeloid cells—targets of medication in multiple sclerosis*. *Nature Reviews Neurology*, 12(9), 539-551. License number: 5423151124446)

II.III Clinical features of MS

MS is characterized by confluent demyelinated areas, both in the white and grey matter of the brain and spinal cord, called *plaques* or *lesions*⁵⁵. The initial presentation of the disease varies from patient to patient, according to both the location of the lesions and the type of symptom onset (relapsing or progressive). In the acute phase (active plaques), lymphocytes, macrophages, and microglia damage myelin and oligodendrocytes to varying degrees. The clinical evolution of MS is attributed to demyelination and neuroaxonal degeneration. Gliosis develops over time and plaques become burnt-out (inactive plaques) by demyelinated axons traversing the glial scar tissue. The remaining oligodendrocytes attempt to replace new myelin. Plaques can be partially remyelinated (shadow plaques) if the inflammatory process is arrested at an early stage. However, the progression of gliosis creates a barrier between myelin-producing cells and their axonal targets, making remyelination unsuccessful. Demyelination finally leads to blockage or delay in neuronal conduction, which results in the acute onset of neurological deficits⁵⁶.

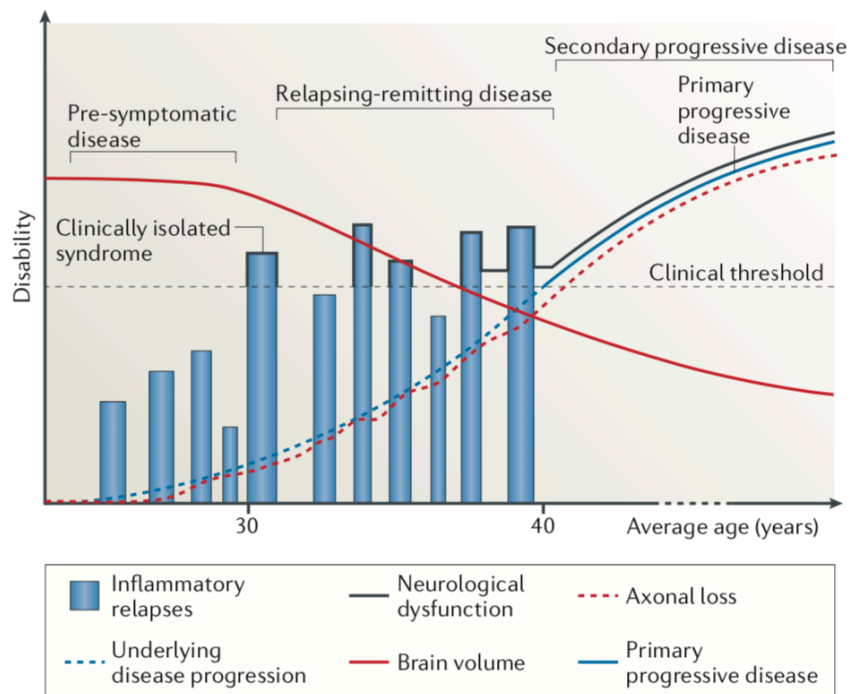


Figure 4. Heterogeneity of multiple sclerosis courses. (C. Dendrou et al, *Nature Reviews*, 2015, License number: 5423160313557)

In assessing a patient with suspected MS, it is critical to determine the onset and evolution of symptoms. Additionally, it is crucial to obtain details about previous neurological episodes that may indicate an earlier, unrecognized attack, thus helping to establish an appropriate diagnosis of the disease. The first episode of neurological dysfunction is called a Clinically Isolated Syndrome (CIS) and usually includes acute unilateral optic neuritis, partial myelitis, or brainstem syndrome (Figure 4).⁵⁷ In this context, Magnetic Resonance Imaging (MRI) is proven to be a powerful tool for MS diagnosis and disease monitoring, showing the presence of white matter lesions (some of which can be clinically occult) and their dissemination in space and in time.

The typical neurological manifestations related to demyelinating lesions are as follows:

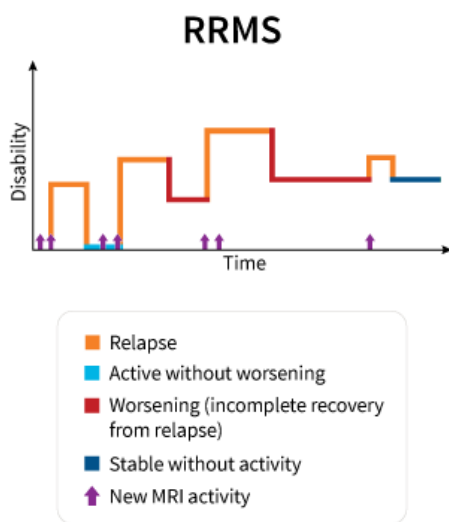
- **Visual impairments:** acute unilateral optic neuritis or double vision
- **Sensitive alterations:** paresthesia and dysphasia
- **Motor impairments:** spasticity in 85% of patients and can affect one or more limbs. E.g., Loss of balance and asymmetric limb weakness
- **Urinary and sexual deficits**
- **Paroxysmal symptoms:** E.g., Facial sensory loss or trigeminal neuralgia
- **Cerebellar ataxia and nystagmus**

Moreover, fatigue is one of the most common and invalidating symptoms in MS, regarding almost the 80% of patients. Its pathogenesis, not linked to demyelinating lesions, is still unclear, but several authors have suggested a possible correlation with high levels of circulating cytokines, such as IL-6⁵⁸. In addition to these clinical manifestations, growing interest has been found in psychiatric disturbances and cognitive impairment, which are highly associated with MS.

At first, MS clinical courses were classified in a consensus work by Lublin et al. in 1996⁵⁹, where they defined four different clinical phenotypes: *Relapsing Remittent* (RR-MS), *Primary Progressive* (PP-MS), *Secondary Progressive* (SP-MS) and finally *Relapsing Progressive* (RP-MS), similar to SP, but with a different progressive course *ab initio*. Moreover, some *benign forms* were identified among the relapsing remittent forms (10%), in which the disease leads only to a slight form of disability within 15 years from

the onset. Rarely, *malignant forms* of MS promptly become progressive and lead to complete disability within a few months.

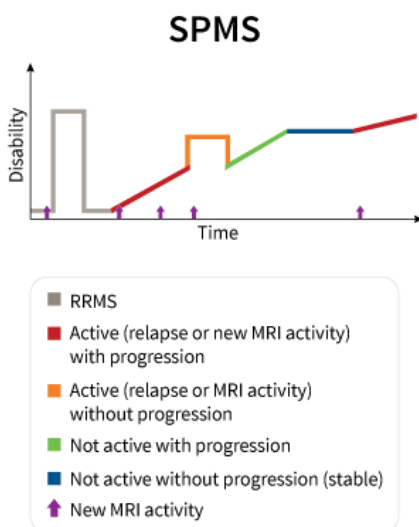
The classification has been recently updated (e.g. elimination of RP course and introduction of CIS)⁶⁰ and is still widely used by clinicians. In the new classification, all forms of MS are further subcategorized as either active or non-active, where active MS is defined as the occurrence of clinical relapse or the presence of new T2 or gadolinium-enhancing lesions on MRI over a specified period of time, e.g. one year⁶⁰.



Source: Lublin et al., 2014.

1) Relapsing Remittent Multiple Sclerosis

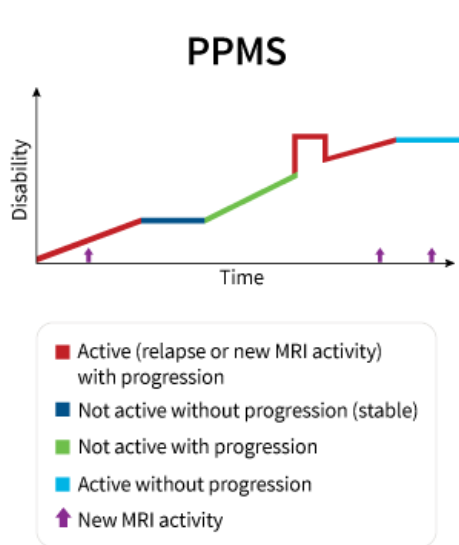
The 85% of the patients is affected by relapsing-remittent multiple sclerosis (RR-MS) whose primary cause at the onset is demyelination. Generally, the first manifestation of the disease happens in patients younger than 40 years old. The episode starts with an acute or subacute onset which lasts hours to days, with a maximal deficit within 4 weeks⁶¹. Exacerbations (*relapses*) of disease are followed by spontaneous period of partial or complete recovery (*remissions*).



Source: Lublin et al., 2014.

2) Secondary Progressive Multiple Sclerosis

A significant percentage of patients diagnosed with RR-MS gradually turns into a secondary progressive course, in which there is a constant worsening of neurologic functions over time. The disease results associated with gradual loss of neurological function and ascending paralysis, and it seems to be independent from inflammation. During early stages of SP-MS, relapses can occur, while their frequency decreases with the progression of the disease.



Source: Lublin et al., 2014.

3) Primary Progressive Multiple Sclerosis

The 15% of patients are diagnosed with primary progressive MS. Differently from RR-MS, the onset of PP-MS is generally due to neurodegeneration rather than demyelination. Its course is characterized by a progressive worsening of symptoms from the diagnosis, with constant transition towards disability. PP-MS can begin with an asymmetric paraparesis that evolves over months or years.

Figure 5. Types of MS (Lublin et al., 2014. Image source: www.nationalmssociety.org)

During the RR phase of the disease, clinical relapses occur every one to two years. MRI studies indicate that inflammatory lesions tend to form 10-20 times more often than clinical relapses in RR-MS, despite periods of active and quiescent disease. Currently, the *axonal hypothesis* states that SP-MS occurs when the nervous system can no longer compensate for ongoing tissue injury after overcoming a critical threshold. During this time, the disease becomes a mainly neurodegenerative process independent of ongoing inflammation, although it still causes additional damage⁶².

Although there is no cure for MS, patients with relapsing forms of MS, including SP-MS patients who continue to relapse, have access to a number of approved therapeutic agents that can reduce disease activity and delay disease progression⁵⁵. With regard to therapies, it is necessary to make a distinction between those aimed at minimizing acute attacks of MS and those aimed at reducing the progression of pathology. When treating relapses, therapy is usually meant to limit both the duration and entity of the episode. The treatment consists of a mixture of corticosteroid drugs such as intravenous (IV) high-dose methylprednisolone or dexamethasone. Corticosteroids are highly effective in limiting acute attacks owing to their powerful anti-inflammatory activity. However, the outcome of relapse remains unclear, and it does not delay disease progression. In the treatment of chronic MS, the therapy is based on disease-modifying drugs. The goal is to shorten the duration of acute exacerbations, decrease their frequency, and provide symptomatic relief. However, currently, there are no curative drugs for MS approved by FDA (Food

and Drug Administration), except for ocrelizumab, and research is ongoing to find a treatment that could halt further deterioration in a disease that has already entered a progressive stage^{55,63}.

II.IV EAE as an experimental model of MS

Several different animal models of demyelinating CNS diseases exist, but Experimental Autoimmune Encephalomyelitis (EAE) is commonly used for MS research. The origin of this model traces back to 1925, with the discovery of the immunization of rabbits with human spinal cord homogenate, leading to inflammation and paralysis⁶⁴. In 1933, Rivers reported that monkey could be immunized by injecting brain extracts and brain emulsions. Repeated intramuscular injections were followed by *an inflammatory reaction, accompanied by demyelination, in the central nervous system*⁶⁵.

The protocol was substantially improved in years by the addition of Freund's adjuvant to emulsify myelin antigens⁶⁶. Chronic demyelination and toxin-induced demyelination models, such as the cuprizone and Lysphosphatidylcholine (lysolecithin) models, are also available⁶⁷. Over the years, protocols for EAE induction have been considerably optimized and EAE is probably the best animal model for studying autoimmunity and demyelinating diseases of the CNS, such as MS.

EAE can be induced by immunization of susceptible species with CNS proteins and by the passive transfer of T lymphocytes that react to myelin antigens. The pathophysiology of EAE is mainly characterized by perivascular autoreactive CD4⁺ T cells that recognize CNS-specific antigens such as MBP, MOG and PLP. Immunized animals can produce encephalitogenic T cells, supporting the concept that auto-reactive immune cells are a natural part of immunity⁶⁸. Several species and strains of mice have been used and, to date, all mammalian species are potentially susceptible to EAE when properly immunized. However, mice are particularly favored as carriers, due to the diversity of the transgenic models, the numerous antibodies and immunomodulatory reagents available in this species that can be used to investigate the pathogenic mechanisms of EAE⁶⁹. Overall, the most common protocol for EAE induction consists of a first subcutaneous injection of an encephalitogenic peptide (myelin homogenate or a single myelin protein) emulsified with an equal volume of complete Freund's adjuvant (CFA) containing *Mycobacterium tuberculosis* to create an antigen depot. Then, two

additional intraperitoneal injections of pertussis toxin are administered on the same day of immunization and two days later.⁷⁰ *Bordetella Pertussis* helps boosting the immunization weakening the BBB, but also enhancing the cytokine production by T cells and induction of lymphocytosis⁷¹.

EAE's immunological, pathological, and symptomatic outcomes vary depending on the mode of sensitization, the immunogen, and the species and strain's genetic background⁶⁸.

- In Swiss Jim Lambert (**SJL**) **mice**, immunization is performed with a single injection of spinal cord homogenate that lead to an acute form of EAE (**Fig. 6a**).
- Alternatively, **SJL mice** are immunized with an injection of **PLP₁₃₉₋₁₅₁**, leading to a relapsing-remitting EAE. Within every relapse, autoreactive T-cells attack new myelin peptides, resulting in a monophasic acute course of disease resembling human RR-MS (**Fig. 6b**). In this model, lesions typically form in brainstem, optic nerve, and spinal cord, as well as in cerebellum and cortex. Pathology begins with perivascular and meningeal lymphocytes and neutrophils infiltration, followed by the spontaneous resolution of the inflammatory infiltrate. In addition, white matter damages and gliosis occur, leading to demyelination of axons⁶⁸.
- In **C57BL/6 mice**, immunization with **MOG₃₅₋₅₅** can induce a chronic, sustained form of EAE, characterized by a peak after the onset, followed by a moderate decrease in the severity that continues in a stable clinical progression (Figure 6c). The chronic form exhibits multifocal, confluent areas of inflammatory immune cells infiltration as well as demyelination in the peripheral white matter of the spinal cord.⁷² Macrophages and CD4⁺ lymphocytes are the most abundant cell types in the inflammatory infiltrate, although B cells, CD8 T cells, monocytes and neutrophils contribute to the pathogenesis of the disease⁶⁷. (**Fig. 6c**)

Although C57BL/6J and SJL/J mice are suitable models for the investigating the role of CD4⁺ T cells in the pathogenesis of EAE, some difficulties arise in isolating specific T cells from peripheral lymph nodes. In this context, the development of T-

cell receptor (TCR) transgenic mouse models over the past 20 years has greatly helped in the study of antigen-specific T cell responses⁶⁷.

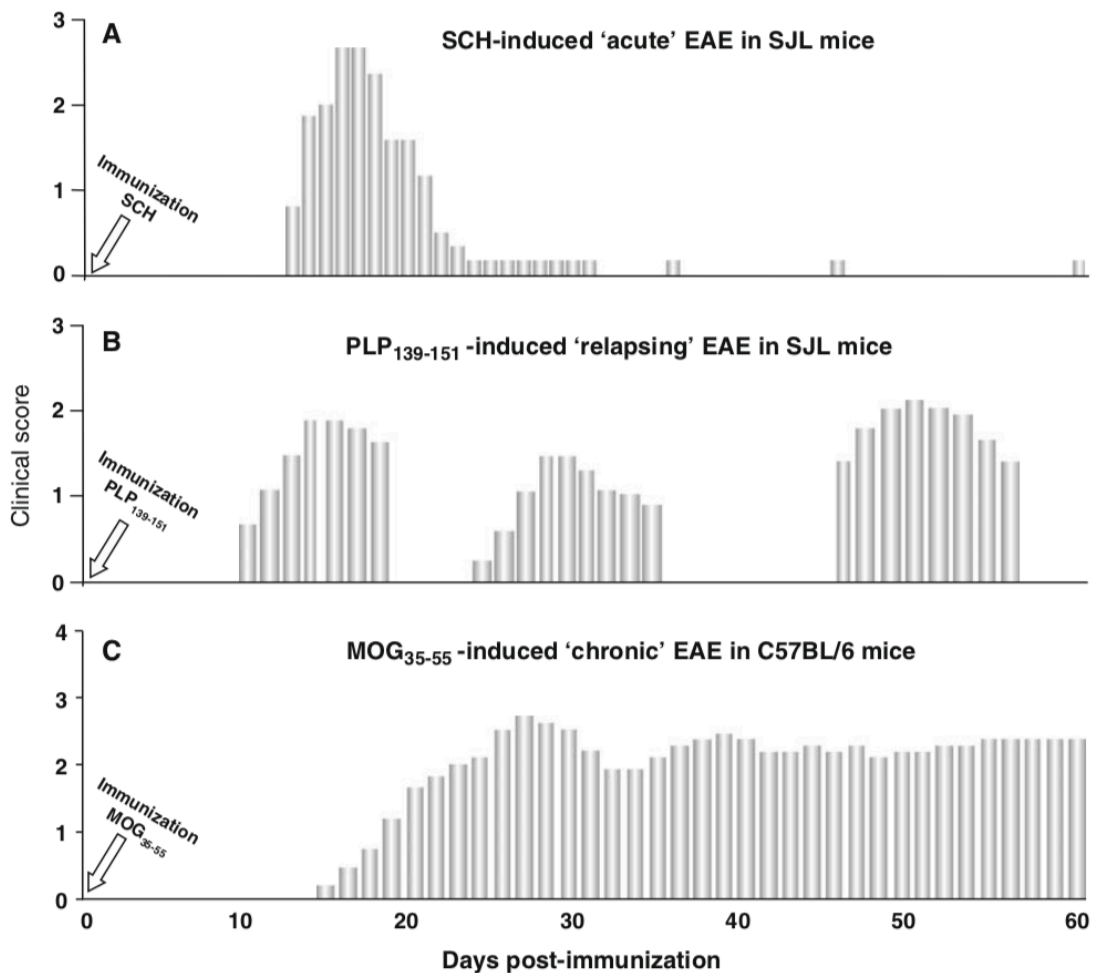


Figure 6. EAE clinical courses. (Adapted from Furlan et al. "Animal models of multiple sclerosis." *Neural Cell Transplantation*. Humana Press, Totowa, NJ, 2009. 157-173. License number: 5423511317584)

- Bettelli et al. (2003) were the first to generate a class II-restricted TCR transgenic mouse model, specific for the MOG₃₅₋₅₅ on the C57BL/6J background (**2D2 mice**).⁷³ In this model, CD4⁺ MOG-specific lymphocytes were not deleted or tolerated and were functionally competent. More than 30% of 2D2 mice spontaneously developed isolated optic neuritis, which is also the first clinical manifestation in a large percentage of MS patients, without any clinical nor histological evidence of EAE. This predilection for the development of optic

neuritis is probably due to the higher expression of MOG in the optic nerve than in the spinal cord. However, when 2d2 mice are immunized with the full immunization regimen of encephalitogenic peptide in combination with pertussis toxin, they developed more severe EAE than their non-transgenic littermates. This is associated with higher mortality, an early disease onset, and an increased number of CNS inflammatory foci. Overall, 2d2 mice provide a good model to investigate the role and nature of the MOG-specific self-reactive repertoire in EAE both *in vivo* and *in vitro*.

III. Neutrophils

III.I Neutrophil biology

Neutrophils, alternatively called polymorphonuclear leukocytes (PMNs), are the most abundant leukocytes circulating in the human blood. They are generally described as myeloid cells with a short half-life, a specific nuclear morphology, a defined granule content and the surface expression of specific markers, such as CD66b⁷⁴. An estimate of 10^{11} neutrophils are produced every day in the bone marrow under physiological conditions, although this number can increase by ten times during infections⁷⁵. Under steady-state conditions, neutrophils are released from the bone marrow and circulate for about half a day before infiltrating tissues and being removed from the blood. As the final effectors of the acute inflammatory response, these cells are key players in the defense against invading pathogens. Despite their beneficial antimicrobial functions, prolonged activation within the tissues can result in local injury. Neutrophil involvement has recently been linked to sterile inflammation, resulting in tissue damage under conditions such as autoimmunity, chronic inflammation, and cancer⁷⁶⁻⁷⁸. Despite having a short lifespan in the blood, neutrophils can live two to three times longer in tissues, with peaks of up to one week⁷⁵. Moreover, neutrophils show a tendency for *collective swarming* in tissues, a self-organized migration mechanism that leads to their accumulation and the formation of neutrophil clusters⁷⁹. According to current paradigms, neutrophil development starts with granulocyte-monocyte progenitors (GMPs) and proceeds through a continuum of maturation stages. Immature neutrophils are distinguished from others by their nuclear features, as they lack nuclear segmentation. Their maturation begins with the progranulocyte stage and proceeds through the myelocytes, metamyelocytes, bands, and mature neutrophil stages, resulting in slightly smaller cells with more nuclear constriction and less cytoplasmic RNA. Differentiation is stimulated by granulocyte-macrophage colony-stimulating factor (GM-CSF) and granulocyte colony-stimulating factor (G-CSF) signaling and lasts for approximately 14 days. Mature neutrophils, also called *segmented* neutrophils, have clear constrictions or segments⁸⁰. Neutrophils leave the bone marrow (BM) through the interaction of the chemokine receptor CXCR2 with the ligands CXCL1 and CXCL2 as well as the receptor CXCR4

with the ligand CXCL12⁷⁴. Aged neutrophils have hyper segmented nuclei, lose CD62L (L-selectin) expression and overexpress CD11b and CXCR4 over approximately six hours. In response to infections, neutrophils release a variety of preformed molecules that are stored in different intracellular granules. Granule proteins regulate adhesion, phagocytosis, transmigration, release of reactive oxygen species (ROS) and neutrophil extracellular trap (NETs) formation, which are composed of chromatin and secretory mediators that help trap bacteria⁸¹.

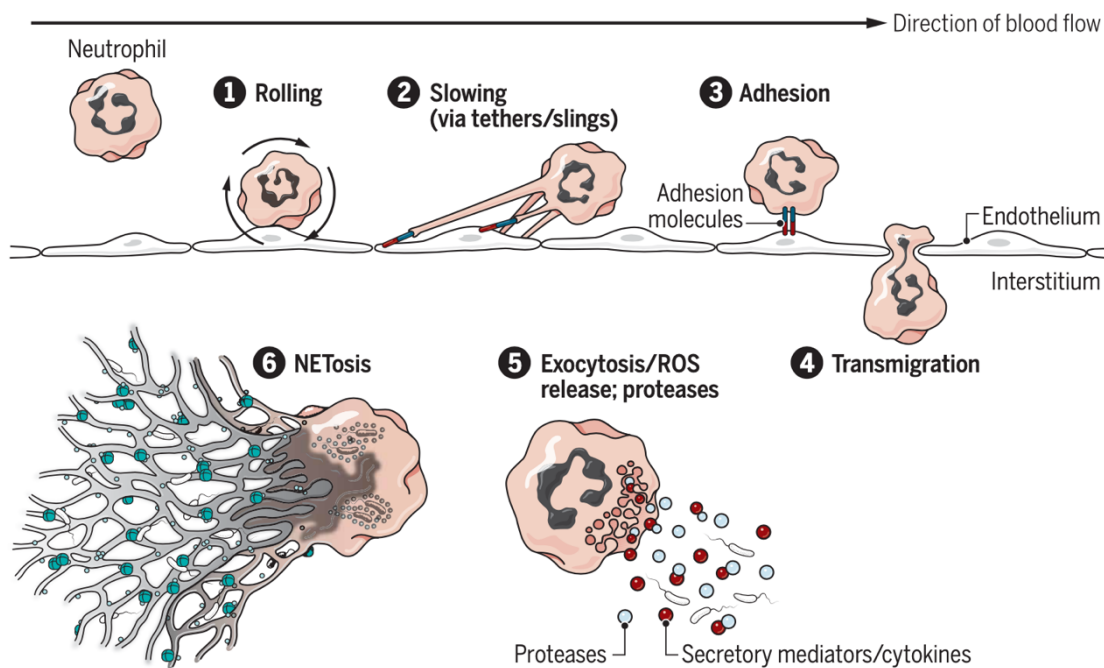


Figure 7. Neutrophil actions in infection and inflammation. Following inflammation or infections, neutrophils are recruited from the blood stream into the inflamed tissue following chemotactic gradients. After upregulating surface molecules, such as L-selectin and PSGL-1, they interact with the activated endothelium in a process called rolling (1). Their motion is then slowed down owing to stronger adhesions with β_2 integrin on the endothelium (2-3). Once they are firmly adhered to the tissue, neutrophils can transmigrate through the endothelium and basal membrane (4). Here, they kill pathogens through exocytosis and degranulation of molecules (such as ROS and proteases) and with the formation of NETs (5-6). (Ley, Klaus, et al. "Neutrophils: New insights and open questions." *Science immunology* 3.30 (2018): eaat4579. License number: 5423520610777).

During inflammation, neutrophils infiltrate inflamed tissues in response to cytokines, pathogen-associated molecular patterns (PAMPs), damage-associated molecular patterns

(DAMPs), and environmental signals that shift their phenotype, reduce apoptosis and increase lifespan⁷⁴. In order to respond quickly and precisely to infections, neutrophils rely on molecules stored in various intracellular granules and secretory vesicles. The proteins contained in granules regulate a variety of processes, including adhesion, transmigration, phagocytosis, and NET formation. Neutrophil secretory organelles are classified as azurophilic (primary), specific (secondary), and gelatinase (tertiary) granules⁸², secretory vesicles⁸³ (Figure 8) and endocytic vesicles multivesicular bodies (MVBs, not shown in the figure)⁸⁴. The composition of granule subsets and their release are strictly regulated depending on the neutrophil maturation stages and their function. Thus, they represent a crucial reservoir for antimicrobial proteins and reactive components of respiratory burst oxidases essential for cytotoxic functions, as well as extracellular matrix (ECM) proteins, adhesion molecules and proteases which are important in diapedesis, cell interaction and migration through the ECM and soluble mediators of inflammation involved in pro- and anti-inflammatory effects in inflamed tissues⁸¹.

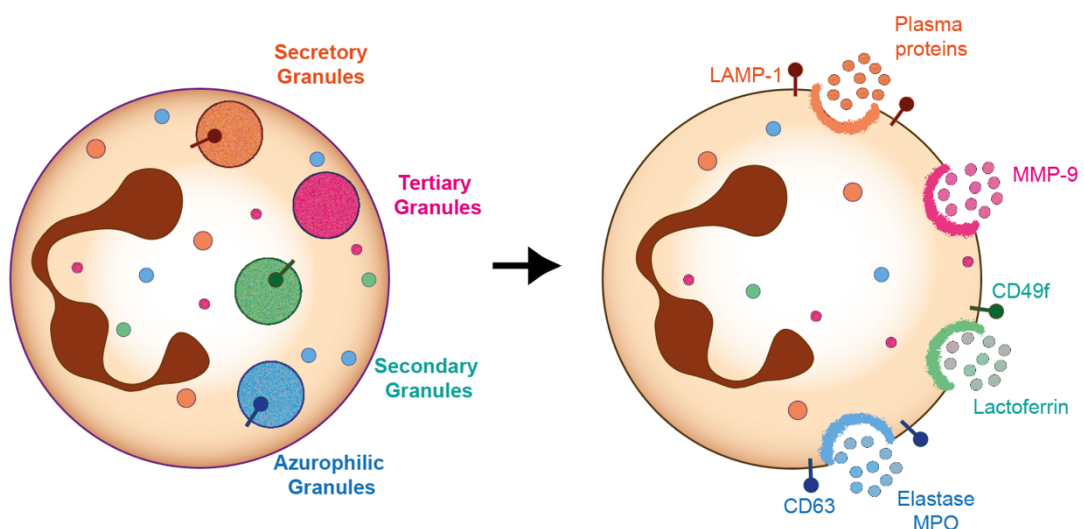


Figure 8. Neutrophils granules and secretory vesicles. After stimulation, neutrophils can release different type of granules, classified as azurophilic, secondary, tertiary, and secretory granules. (Made using Adobe Illustrator 2022). MPO: Myeloperoxidases, MMP-9: Matrix metalloproteinase 9.

III.II Heterogeneity of neutrophils subsets and immunoregulatory functions

Despite long-held beliefs that neutrophils are a homogeneous population, increasing evidence suggests that they have highly plastic characteristics, suggesting the presence of

multiple subsets of neutrophils in both homeostatic and pathological conditions. Heterogeneity in neutrophils can be induced in the bone marrow by specific differentiation programs or in the blood by extracellular signals derived from inflammatory tissues (e.g., cytokines, chemokines or bioactive lipids)⁸⁵. An example of a marked diurnal change in the phenotype of neutrophils is *neutrophils ageing*⁸⁶. Ostuni's et al. recently published a comprehensive study on immunophenotypic and transcriptome analysis, both at bulk and single-cell levels, of neutrophils from healthy donors and patients undergoing stress myelopoiesis, which once again stressed the attention on the plasticity of neutrophils in humans⁸⁷.

The identification of discrete neutrophil populations and the characterization of subsets with immunoregulatory functions have gained exponential popularity in recent decades. Several studies have reported that during systemic inflammation, autoimmune disease, or cancer, distinct cell populations circulating in the blood display neutrophil-like morphology and show either immunosuppressive or pro-inflammatory functions^{80,88-90}. Neutrophils displaying suppressive/regulatory functions have often been defined as polymorphonuclear-myeloid-derived suppressor cells (PMN-MDSCs)⁹⁻¹⁰. In some cases, after density gradient centrifugation, these neutrophils sediment within peripheral blood mononuclear cells (PBMC) and are generally known as low-density neutrophils (LDNs).^{89,90} PMN-MDSCs have also been found in the normal-density neutrophil (NDNs) fraction or within the total leukocytes purified after red cell lysis of whole blood^{91,92}. Fridlender et al. described two different subsets of tumor-associated neutrophils (TANs), namely N1 and N2, which have similar features to the macrophage subsets M1 and M2⁹³. Among the N1 and N2 subsets, cytokine and chemokine production, macrophage activation, and expression of Toll-like receptors and surface antigens differ⁹⁴. More recently, Marini et al. identified CD10 as a phenotypic marker to discriminate between mature and immature regulatory neutrophils present in patients with acute or chronic inflammatory conditions⁹⁵.

A growing body of evidence indicates that neutrophils have both direct and indirect effects on adaptive immunity. Under pathological conditions, neutrophils rapidly migrate in high numbers to the site of inflammation and subsequently to draining lymph nodes. Neutrophils can engage both lymphocytes and antigen-presenting cells⁸⁵. To note, it has been found that neutrophils themselves may act as APCs in terms of presenting antigens

(for examples to memory CD4⁺ T cells) and activating T cells. This might be mediated by the production and release of cytokines and chemokines (GM-CSF, IFN- γ , IL3 and TNF) or through cell-to-cell interactions with T cells that induce the expression of MHC-II and other co-stimulatory molecules on neutrophils. Most studies have shown that neutrophils directly suppress different T-cell responses in various disease models, even though neutrophils can also stimulate T-cell responses, as reviewed by Pillay et al⁸⁰. Neutrophils suppress T-cell functions using similar mechanisms to those displayed in their antimicrobial functions, i.e., they exploit similar mediators (Figure 9).

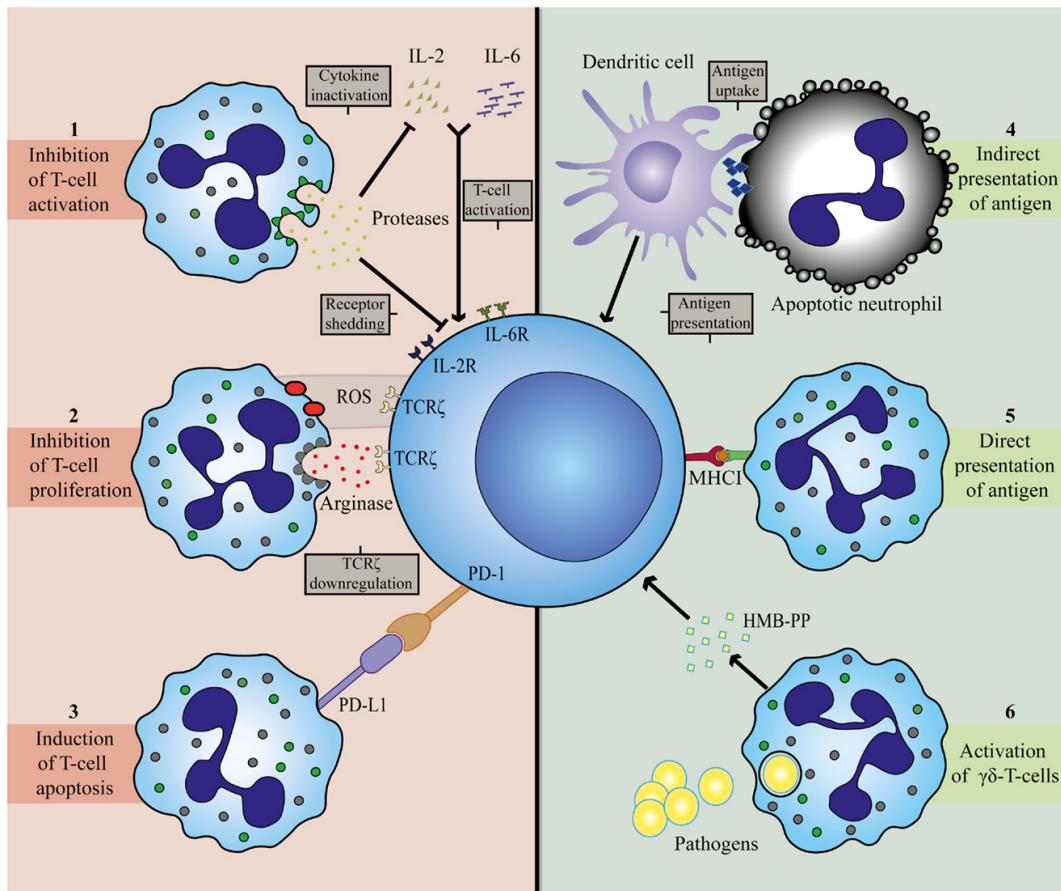


Figure 9. Regulatory or activating neutrophil interactions with T cells and DCs. (Leliefeld, P. H., Koenderman, L., & Pillay, J. (2015). How neutrophils shape adaptive immune responses. *Frontiers in immunology*, 6, 471)

The two most commonly reported suppression mechanisms are the ARG and ROS pathways. Other proposed mechanisms involve the PD-1/PD-L1 axis via IFN- γ stimulation⁹⁶ or degranulation of granular constituents, including neutrophil elastase.

These proteases can cleave and inactivate essential cytokines, such as IL-2, and receptors, such as the IL-2 and IL-6 receptors on T-cells⁹⁷.

III.III Neutrophil in EAE and MS

For many years, the involvement of neutrophils in the pathogenesis of autoimmune diseases has been neglected, mainly because of their perception as terminally differentiated, short-lived immune cells. In recent years, cutting-edge techniques have demonstrated neutrophils' importance in neuroinflammatory disorders, and their role in stroke, MS and AD appears to be undeniable⁹⁸⁻¹⁰¹. In the pathogenesis of MS and EAE, the trafficking of leukocytes to the CNS via the BBB plays an important role causing tissue damage and activating microglia and astrocytes, resulting in myelin sheath disruption and axonal death¹⁰². As neutrophils release ROS, enzymes, NETs, and cytokines in different pathophysiological conditions, they contribute not only to acute inflammation, but also to chronic collateral damage, even in the absence of conspicuous accumulation within the tissue in chronic contexts⁸¹. Different chemokines and mechanisms have been found to recruit neutrophils to the brain and SC¹⁰³. During all stages of autoimmune progression, neutrophils play an important role in antigen presentation, modulation of several cell types, and tissue damage¹⁰². They contribute passively to tissue damage by the deposition of autoantibodies, and actively by producing pro-inflammatory molecules as effector immune cells¹⁰⁴.

In MOG₃₅₋₅₅-induced EAE in C57Bl/6J mice, the percentage of neutrophils infiltrating the CNS fluctuates significantly during the course of the disease: it increases dramatically at the beginning of the disease, remains high until the peak stage, and then drastically decreases¹⁰⁵. Further labeling experiments showed a conspicuous accumulation of neutrophils near demyelinated injured areas and axonal loss sites in the early stages of EAE, suggesting that neutrophils are among the main inflammatory cells involved in demyelination and axonal degeneration¹⁰⁵. The blockade of fundamental cytokines for the recruitment of neutrophils in EAE, namely CXCR2 and GM-CSF, results in reduced disease severity¹⁰⁶. Furthermore, mice immunized with MOG peptide displayed an increase in neutrophils in the BM and consequently circulating neutrophils in the bloodstream during the preclinical phase of EAE¹⁰⁷. Prior to the onset of EAE, neutrophil adhesion to the CNS microvasculature and subpial perivascular infiltration are crucial

mechanisms for allowing an early breakdown of the local BBB and subsequent leukocyte invasion^{107,108}. Notably, neutrophils accumulate exclusively in CNS regions with ongoing injury such as vascular leakage, demyelination, and axonal damage¹⁰⁹. During active EAE, infiltrating neutrophils release TNF- α , IFN- γ , IL-6 and IL-12, in addition to inducing the activation and maturation of CNS-resident APCs. According to the early recruitment of neutrophils into the CNS during preclinical EAE, neutrophil depletion after the onset has no effect on disease severity or incidence. Preclinical neutrophil depletion through a single dose of anti-Ly6G monoclonal antibody delays the onset of the disease, whereas prolonged treatment completely prevents RR and chronic EAE. Simultaneously, the autoreactive myelin-specific T-cell response remains unaffected^{107,110}. However, the involvement of neutrophils in the induction and progression of brain autoimmune diseases is still unclear and the molecular mechanisms controlling their pathogenic activity in the CNS parenchyma remain to be fully elucidated.

Neutrophils were not detected in CNS biopsies derived from patients with conventional MS, where major mononuclear cell infiltration occurs¹¹¹. This was probably because the samples were obtained from biopsy or autopsies, with lesions that used to be sub-acute or chronic. Thus, the idea that neutrophils do not represent a significant leukocyte subpopulation infiltrating the CNS during the disease might have exclusively reflected a technical bias. This misconception has changed from several recent studies that have shown a significant role for neutrophils in MS. Neutrophils have been found in the CSF of patients with MS during disease activity, especially at an early stage of the disease. In particular, IL-17A, G-CSF and CXCLs levels are associated with the neutrophil expansion in the CSF and blood-brain barrier disruption¹¹²⁻¹¹⁴. In contrast, higher plasma levels of CXCL1, CXCL5, neutrophil elastase and integrin CD11b/CD18 occur in MS patients during relapses than in patients in remitting phases, healthy controls and subjects affected by different neurological disorders¹¹⁵. Moreover, the neutrophil-to-lymphocyte ratio in the peripheral blood has been proposed as a marker of disease activity in patients with relapsing-remitting (RR)-MS patients¹¹⁶. In fact, compared to healthy subjects, MS patients present a higher percentage of circulating neutrophils, which are characterized by a primed phenotype¹¹⁷.

On a different note, recent studies have reported that neutrophils can act as a protective agent in neuroinflammatory disorders, slowing down the progression of the disease¹¹⁸. In

fact, neutrophils can release resolving lipidic mediators (for instance, lipoxins, protectins and resolvins) that can potentially affect their infiltration into target tissues and enhance their phagocytosis by macrophages in a process known as *efferocytosis*¹¹⁹. This mechanism consequently induces macrophage polarization toward an M2-like phenotype, leading to a resolving outcome of inflammation¹²⁰. Immunophenotyping of blood specimens from several MS patients revealed that in subjects with an inactive form of RR-MS, there is a peculiar increase in CD15⁺ neutrophils, as well as in classical and non-classical monocytes. This increase inversely correlated with the number of circulating lymphocytes¹²¹. In the context of neuroinflammation, and EAE in particular, Khorrooshi R. et al. have shown that the PD-1 axis could be of primary importance¹²². The identification and characterization of neutrophils with regulatory functions might help in understanding the mechanisms underlying the pathogenesis and resolution of acute inflammation in MS.

IV. PD1/PD-L axis

Disclaimer: Chapter IV was adapted from the review written by our lab, Manenti et al. *PD-1/PD-L Axis in Neuroinflammation: New Insights* published in *Frontiers in Neurology* in June 2022¹.

Immune checkpoints, such as Programmed cell death protein-1 (PD-1) and its ligands are regulatory molecules that are fundamental for suppressing immune responses and promoting self-tolerance. PD-1 has two known ligands: PD-L1 (also called B7 homolog 1, B7-H1) and PD-L2 (or B7-DC). Both ligands have been characterized as powerful inhibitors of the immune system, helping tumors evade suppression mechanisms. Since 2014, six different inhibitors of PD-1 and PD-L1 have been approved for cancer immunotherapy by the US FDA and European Medicines Agency (EMA)¹²³, revolutionizing the treatment of certain cancers. In addition to their desired effects, immune checkpoint inhibitors (ICIs) modify the balance of immune responses and induce specific off-target toxicities called immune-related adverse events (irAEs)¹²⁴. Although rare, neurological adverse effects are reported within irAEs in clinical trials, especially in patients treated with anti-PD-1 antibodies or a combination of both anti-CTLA-4 and PD-1 drugs. The observations obtained from clinical trials suggest that the PD-1 axis plays a significant role in the regulation of neuroinflammation. Studies in preclinical models have suggested that this axis plays an important role in different pathological conditions involving the CNS, such as viral encephalitis, brain tumors, autoimmune disorders, and dementia. In most cases, the authors described an upregulation of PD-1 or PD-Ls during pathological conditions. Under the current understanding of the PD-1/PD-L1 axis in the CNS, its role cannot be uniquely described as protective or pathogenic. However, in most cases, upregulation of PD-L1 or PD-L2 helps to slow down and limit the inflammatory process, suggesting a protective mechanism^{125,126}.

IV.I Biology of the PD-1/PD-L axis

PD-1 is a 288 amino acid protein that belongs to the immunoglobulin superfamily and is a homolog to CD28. PD-1 is expressed in physiological conditions on a subset of thymocytes but can be induced upon activation in many types of immune cells, including T cells, B cells, natural killer (NK) cells, monocytes, and dendritic cells (DCs)¹²⁷. In its

cytoplasmic tail, PD-1 has two tyrosine motifs, an immunoreceptor tyrosine-based switch-motif (ITSM) and an immunoreceptor tyrosine-based inhibitions motif (ITIM)¹²⁸. PD-ligands are members of the B7 family of type 1 transmembrane proteins, which also include CD86 and CD80¹²⁹. They have similar exon organization of the 5' UTR region, a signal sequence, IgV-like, IgC-like and transmembrane domains, cytoplasmic exon 1, and cytoplasmic exon 2 with the 3' untranslated region¹²⁹. However, PD-L2 affinity to PD-1 is 3-time stronger compared with PD-L1 and this is probably due to tryptophan that is unique to PD-L2¹³⁰. PD-1 ligands differ in their expression patterns: PD-L2 expression is restricted to professional APCs¹³¹, while PD-L1 is ubiquitously expressed in inflamed tissues¹³². To date, in physiological conditions PD-L1 mRNA is largely present in various tissues, while PD-L1 protein is barely expressed on the cell surface, suggesting that PD-L1 mRNA is under tight post-transcriptional regulation. An exception is made in the context of human cancers, where PD-L1 protein is highly expressed by the tumoral cells in the attempt to hide neoantigens from immune surveillance¹³³. The engagement of PD-1 by its ligands leads to the formation of PD-1 micro clusters together with the T Cell or B Cell Receptor (TCR o BCR). This leads to the recruitment of the Src Homology Phosphatase (SH)-2 domain-containing tyrosine phosphatase 2 (SHP2) which then causes a decrease in the phosphorylation of the entire spectrum of TCR downstream signaling molecules. PD-1 engagement decreases both the downstream signaling of T and B cell receptors, respectively by decreasing the phosphorylation of CD3z and protein kinase C q (PCK-q), and that of Igb, Syk, and phospholipase Cg2 (PLCg2). Furthermore, PD-1 engagement leads to the blockage of both the phosphatidylinositol-3 kinase and the serine-threonine kinase Akt through the recruitment of SHP2¹³⁴. The downstream effects of PD-1 and PD-L1/L2 interaction comprehensively result in reduced proliferation of autoreactive leukocytes, suppression of effector T and B cells in parenchymal tissues, reduced cytokine production, induced T cell anergy and exhaustion, reduced motility and increased IL-10 production¹³⁵. The absence of PD-1 leads to an alteration of the signaling threshold during the development of T cells in the thymus, resulting in an increased presence of CD4/CD8 double-negative T-cells. Furthermore, in several preclinical models, the blockade of the PD-1 pathway results in the development or exacerbation of autoimmune diseases depending on the genetic background they have^{136,137,138}. For example, C57BL/6 PD-1^{-/-} mice develop lupus-like glomerulonephritis and arthritis

starting at 6 months of age, while BALB/c knockout mice develop a dilated cardiomyopathy starting at 5 weeks of age^{139–141}. Among others, these findings suggest that the PD-1 axis plays an important role in central and peripheral tolerance, as well as a preventive role for several types of autoimmune disorders (Figure 10).

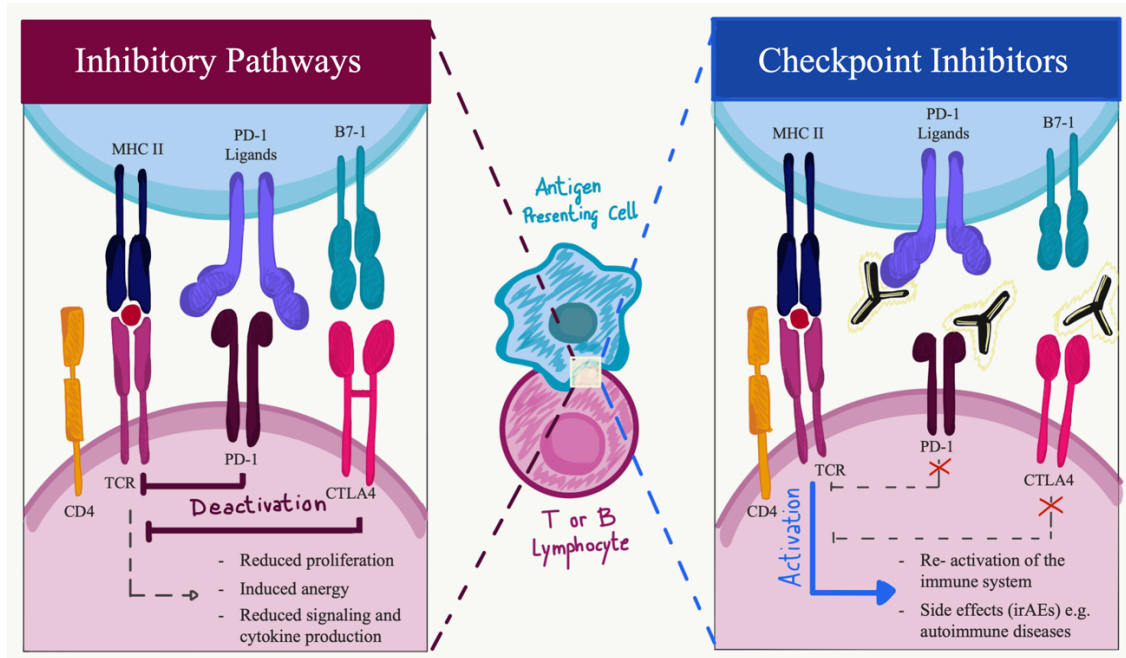


Figure 10. Immune checkpoint function during activation or inhibition pathways. PD-1 and CTLA4 are expressed on activated lymphocytes while PD-Ls and B7-1 are expressed on APCs. The interaction between the inhibitory receptors and their ligands starts an intracellular cascade in the T cells that leads to the inhibition of the TCR, reduced proliferation and signaling and overall anergy of T cells. The usage of PD-Ls axis blocking antibodies inhibits the intracellular cascade and cause the re-activation of the immune system. (Manenti et al. PD-1/PD-L axis in neuroinflammation: new insights. *Frontiers in Neurology*, 2022, 1045.)

IV.II PD-L1 and PD-L2 expression in the CNS of EAE mice

Preliminary evidence of the expression of PD-1 ligands in the CNS comes from experimental autoimmune encephalomyelitis (EAE). In EAE mice PD-L1 is overexpressed on microglial cells, astrocytes, and infiltrating mononuclear cells near the meninges, especially in areas with the highest inflammatory response¹⁴². PD-L1 expression is also increased on the endothelium surrounding the cell infiltrates. Microglial cells, which represent the 5-20% of all glial cells in the murine CNS, constitutively express a low level of PD-L1 and its expression can be up-regulated *in vitro* when exposed

to inflammatory conditions, for example in the presence of IFN- γ or Th1 supernatants. PD-L1 expression by microglia can regulate immune responses by interacting with PD-1. Thus, one of the current hypotheses is that PD-L1, expressed by microglia and infiltrating cells, might be a strong immune inhibitory molecule able to curb T-cell activation and useful to maintain immune homeostasis in the CNS.^{143, 132} PD-L2 functions and distribution are similar but not overlapping to PD-L1 and they are still to be fully elucidated in the CNS. As well as PD-L1, PD-L2 inhibits T cell proliferation by blocking cell cycle progression without increasing cell death. However, PD-L2 seems to be slightly less potent than PD-L1. Moreover, PD-L2 seems to be upregulated on small round cells in the brain, indicative of infiltrating macrophages or B cells¹³². To date, some authors reported that PD-L2 might bind to a second receptor different from PD-1, known as repulsive guidance molecule b (RGMb). RGMb, also called DRAGON, is a part of the RGM family, a group of glycosylphosphatidylinositol-anchored membrane proteins that binds bone morphogenetic proteins (BMPs) and neogenin. RGMb does not directly act as a signaling molecule although it can function as a co-receptor modulating BMP signaling. RGMb is expressed mainly in the CNS and in particular on the surface of macrophages and other immune system cells. There is some evidence that the interaction of PD-L2 with RGMb through the BMPs pathway might be co-stimulatory rather than inhibitory on T cells.¹⁴⁴ This interaction seems to promote the development of respiratory tolerance. The PD-1/PD-L2 axis is here involved in the control of metabolic pathways regulating peripheral T_{reg} Foxp3 stability and suppressive functions¹⁴⁵. However, the potential role of RGMb has just begun to emerge and further studies are needed to clarify its functions.

IV.III Transgenic PD-1^{-/-}, PD-L1^{-/-} and PD-L2^{-/-} in EAE model

Several authors in literature attempted to explain the role of PD-1 and its ligands in autoimmune disease of the CNS with the use of blocking antibodies or transgenic mice, although the results are often contradictory.

- Khoury et al reported that PD-1 and PD-L1 expression was increased over time in the CNS of C57BL/6 EAE mice, with a peak after 3 weeks. PD-1 blockade using anti-PD-1

antibodies resulted in an exacerbation of EAE progression with an increased infiltration of lymphocytes in the CNS. Worsening of disease after PD-1 blockade was associated with an intensified autoimmune response to MOG with antigen-specific T cell expansion, activation, and cytokine production. Interestingly, the blockade of PD-L2 but not PD-L1 in EAE mice resulted in a more severe disease compared to the control group.¹³⁶

- Wiendl and colleagues reported that in the presence of PD-L1 blocking antibody on a C57BL/6 background both the production of inflammatory cytokines (IFN- γ and IL2) and the upregulation of activation markers (inducible costimulatory signal) by T cells were markedly enhanced. Furthermore, once that EAE was induced in WT mice, there was an overexpression of PD-L1 in area with strong inflammatory infiltrates, overlapping with microglia/macrophages as well as T cells.¹⁴³

Afterwards, PD-1^{-/-}, PD-L1^{-/-} and PD-L2^{-/-} knock out mice were generated and then immunized to induce EAE and assess any variation in the disease course.

- Maurisc et al. reported that on the 129svEv background immunized with MOG₃₅₋₅₅ peptide, PD-1^{-/-} and PD-L1^{-/-} mice developed a more severe form of EAE and a general increase in the disease incidence, compared to wild type control. This exacerbation of the EAE is concurrent with an increased production of inflammatory cytokines like IL-6 and IL-17. At the same time, PD-L2^{-/-} knock out mice showed onsets and disease progressions similar to the control group. The inactivation of PD-1 was obtained through the substitution of murine PD-1 exon 1 with human PD-1 cDNA in a targeting construct containing a neo gene flanked by loxP sites. PD-L1^{-/-} and PD-L2^{-/-} knock out mice were generated with a Cre-Lox conditional deletion strategy. These results support a critical role for PD-1/PD-L1 interactions in moderating the severity of EAE. Despite the facts that PD-L2^{-/-} mice showed no exacerbation of the disease progression, PD-L2^{-/-} cells produced an increased amount of IFN- γ and IL-17 in a way similar to the PD-1^{-/-} and PD-L1^{-/-} ones, confirming a coinhibitory function for both PD-1 ligands.¹⁴⁶

IV.IV PD-1/PD-L axis in MS

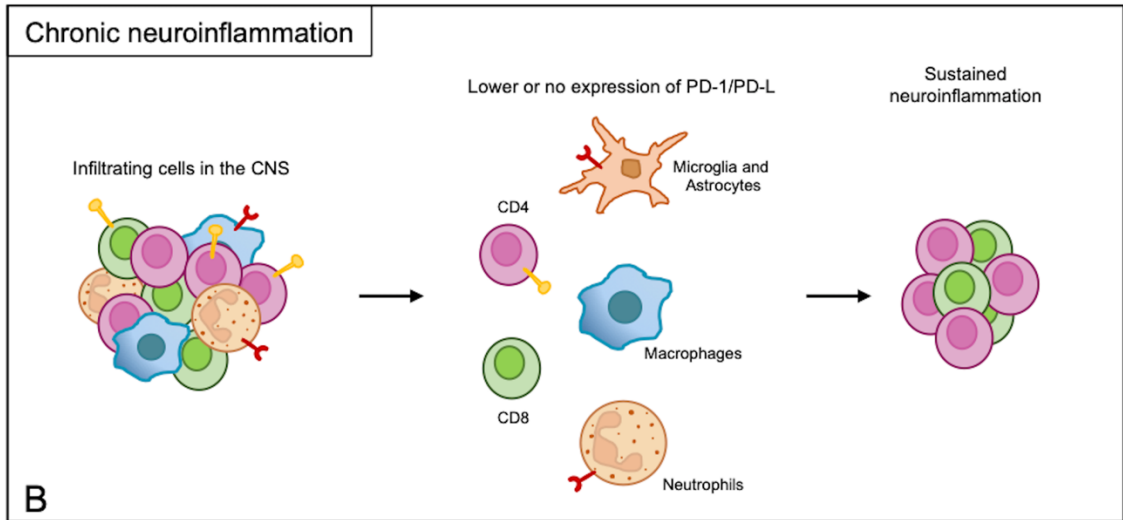
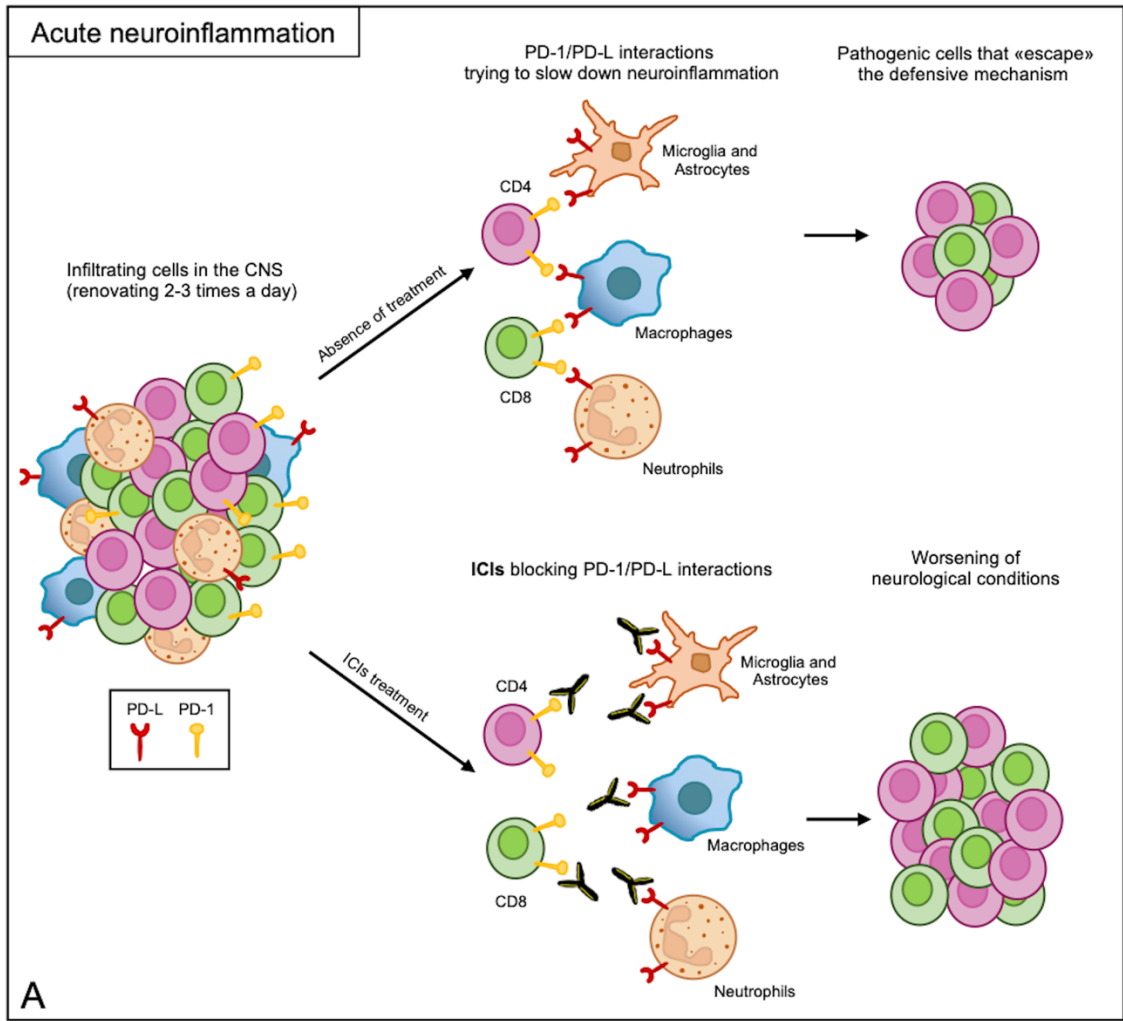
The immune regulatory role of PD-1 in MS is still to be fully elucidated. However, studies have demonstrated the importance of the PD-1 pathway in the development and progression of EAE, suggesting that this pathway may also play a role in human diseases. In people with MS, the PD-1 gene polymorphism (PD-1.3), which is related to reduced PD-1 activity, is associated with a progressive course of the disease, possibly due to a partial defect in PD-1-mediated inhibition of T-cell activation¹⁴⁷. In a population-based and case-control study of 203 patients with MS, Pawlak-Adamska et al., investigated three PD-1 single nucleotide polymorphisms: rs36084323 (PD-1.1), rs11568821 (PD-1.3), rs2227981 (PD-1.5), and rs2227982 (PD-1.9). The study revealed that polymorphic variations could be disease-modifying rather than MS risk factors¹⁴⁸. The relative expression of PD-1 and PD-L1 in the PBMCs of MS patients was significantly lower than that in healthy donors¹⁴⁹. Javan et al. showed a general reduction in the expression of inhibitory receptors such as PD-1, CTLA-4, and TIM-3 in PBMCs of patients with MS, especially PD-1¹⁵⁰. Moreover, after treatment with autologous hematopoietic stem cell transplantation in MS patients, Arruda et al. observed a temporary increase in the number of regulatory T-cells and PD-1-expressing CD8⁺T-cells¹⁵¹. The expansion of CD8⁺PD-1⁺ T and CD19⁺PD-1⁺B cells is associated with better clinical outcomes. Interferon- β , a primary immunomodulatory treatment for MS, enhances PD-L1 expression *in vitro* and *in vivo* in APCs¹⁵². Koto et al. highlighted the differences in the presence of circulating CD8⁺ PD-1⁺ T cells according to disease stage. In fact, in the disease remission state, CD8⁺ PD-1⁺ T cells were decreased in the peripheral blood of patients with MS and resolved in patients treated with IFN- β who showed immune-regulatory cytokine IL-10 expression. In contrast, CD8⁺ PD-1⁺ T cells were enriched in the CSF of patients with MS, which predicted a good response to subsequent IV steroid therapy¹⁵³.

Regarding the neuropathological analysis of post-mortem brain tissues, Pittet et al. showed that PD-L1 is largely expressed in MS lesions compared with controls and that it is colocalized with astrocytes or microglia/macrophage markers. In contrast, PD-L2 expression was notably reduced in the brain endothelial cells of MS brains, while it was easily detectable in controls. In this case, only a small number of infiltrating CD8⁺ T lymphocytes in the lesions expressed PD-1¹⁵⁴. One possible explanation is that, during MS pathogenesis, the inflamed CNS attempts to protect itself against active T

lymphocytes through the expression of PD-L1. However, this process is not effective because the majority of CD8⁺ T-infiltrating lymphocytes lack PD-1 and are insensitive to PD-L1/L2¹⁵⁴. On a different note, van Nierop et al. reported that post-mortem brains of patients with advanced disease contained a high frequency of CD8⁺ T cells that expressed both co-inhibitory (TIM3 and PD-1) and costimulatory (ICOS) T-cell receptors¹⁵⁵.

The clinical use of checkpoint inhibitors (such as Ipilimumab, an anti-CTLA-4 antibody) has been associated with MS development and an increase in MS activity¹⁵⁶. Other checkpoint inhibitors, such as nivolumab, ipilimumab, pembrolizumab, and atezolizumab have been associated with MS relapse^{157,158}. A recent meta-analysis described the rapid progression of MS in 14 patients and concomitant immunotherapy¹⁵⁹. Gerdes et al., using quantitative NGS (Next Generation Sequencing), showed that distinct clonal expansions of CD4⁺ and CD8⁺ T cells in melanoma and CSF were found during ipilimumab treatment, and concomitant MS activity permitted the conversion of RIS to MS¹⁵⁹. These data suggest that the protective antitumor responses could be associated with inadvertent anti-CNS autoimmune response towards different antigens and MS reactivation¹⁵².

It is known that the PD-1/PD-L axis in neuroinflammation appears to regulate the immune response but is not involved in determining the disease or in causing exacerbation. Indeed, inhibition of this axis increases the severity of neuroinflammation, which occurs as a side effect of PD-1 axis inhibition in cancer (Fig. 11A). Most results, however, rely on mouse models of acute inflammation and indicate upregulation of the PD-1/PD-L axis as a counteracting mechanism to re-establish homeostasis. Indeed, anti-migratory therapies that diminish the number of blood-derived CSN-infiltrating cells, are very efficacious in MS. This suggests that inhibitory checkpoints, including the PD-1 axis, can manage the few residual inflammatory cells that still infiltrate the CNS. On the other hand, if the PD-1/PD-L axis fails in the long term, the contribution to chronic CNS inflammation leading to neurodegeneration is not currently known (Fig. 11B). The latter hypothesis, if confirmed, highlights a potential therapeutic strategy for fostering, supporting, and reinforcing this axis to treat chronic neuroinflammation. This underlines the need for further investigation to better understand the role of the PD-1 axis in neuroinflammatory disorders.



AIM OF THE WORK

Over the past two decades, neutrophils have become a critical component of our understanding of autoimmune disorders. Neutrophils play a crucial role in autoimmune progression at all stages, including antigen presentation, modulation of several cell types, and direct tissue damage. Owing to the short half-life of neutrophils and the technical challenges in observing neutrophils near lesions, their role in Multiple Sclerosis (MS) has been overlooked for many years. However, there is increasing evidence in patients and preclinical models of MS that has changed this misconception. Currently, only a few blood-based biomarkers can be used to diagnose MS, assess prognosis, and determine treatment response, highlighting the need for further investigation in this direction.

In my master thesis, while looking for immune checkpoints expressed on leukocytes population in neurological patients, I identified a subpopulation of neutrophils expressing PD-L2. Given these premises, in this study, I will examine whether PD-L2 could be a good marker for identifying a regulatory neutrophil population in both MS and EAE. First, it needs to be clarified whether PD-L2 neutrophils are specific to patients with MS and whether there are any differences in their numbers during different phases of the disease. Next, I aim to characterize this population in terms of the expression of surface markers, release of cytokines and extracellular vesicles. Since the cross-linking of PD-1 with its ligands inhibits TCR signaling, cytokine production and cytolytic function¹³⁴, this suggests that PD-L2 might identify a population of neutrophils with suppressive functions. To prove this, I will perform functional assays using co-cultures of PD-L2⁺ neutrophils with autologous T lymphocytes and determine the outcomes of proliferation and activation of T cells. The second part of my thesis will focus on the murine counterparts. We will dissect the mechanisms of action of PD-L2⁺ neutrophils in EAE by observing their kinetics during the course of the disease in mice. Finally, we aim to explore the relative importance of PD-L2⁺ neutrophils in disease pathogenesis. To do this, we will obtain, characterize, and breed two different transgenic mouse models that will ultimately allow us to conditionally deplete our population of interest at different time points during the disease. Overall, the identification and characterization of neutrophils with regulatory functions may provide new insights into the pathogenesis and resolution of acute inflammation in MS, as well as novel opportunities for noninvasive diagnosis and cell therapy.

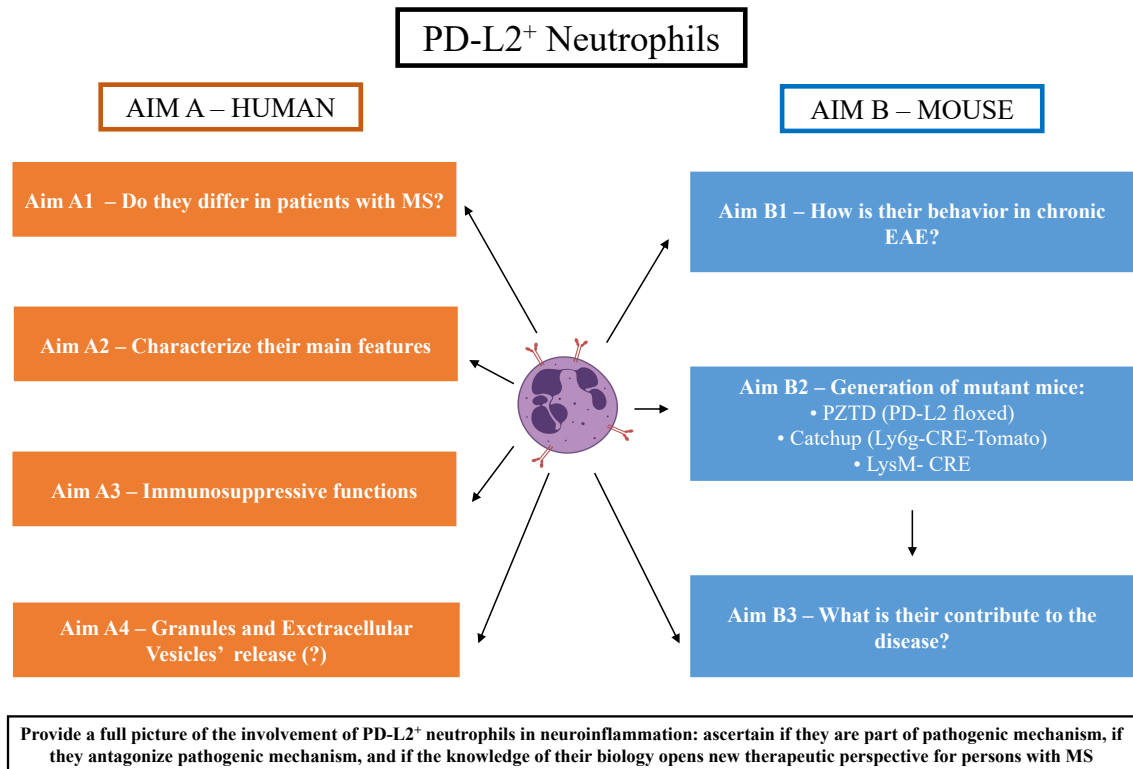


Figure 11. Visual representation of the Aim of Work.

RESULTS

I. Human Results

1.1 PD-L2 expression on circulating immune cells in neurological patients and healthy donors

Growing clinical evidence highlights the association between the PD-1 axis and MS¹²⁷. The PD-1/PD-L axis may play a critical role not only in peripheral immune imbalance, but also in the regulation of neuroinflammation. Thus, I designed a 17 color-panel (described in materials and methods, Table 2.) and analyzed the expression of PD-L1 and PD-L2 on different populations of leukocytes by multiparametric flow cytometry in a cohort of MS patients, patients with other neurological disorders and healthy controls (Table 1).

Variable	Category	MS (n=25)	OIND (n=3)	PN (n=4)	Encephalitis (n=3)	CI (n=16)
Age	-	32.4 (24.3-29.4)	35.2 (23.8-48.2)	43.1 (29.2-55.4)	74.3 (69.4-81.2)	72.03 (64.3-81.7)
Sex	F	16 (64.0%)	2 (66.6%)	2 (33.3%)	8 (80.0%)	9 (56.3%)
OCB	Positive	19 (77.0%)	0	1 (16.6%)	-	-
GD+ Lesions	Positive	13 (52.0%)	1 (33.3%)	-	0	-
EDSS	-	2.0 (1.0-3.5)	-	-	-	-

Table 1. Demographic and clinical characteristics of the study cohort. General features of the patients and controls included in the study. MS= Multiple Sclerosis; OIND= Other Inflammatory Neurological Disorders; PN= Peripheral Neuropathies; CI= Cognitive Impairments; OCB= Oligoclonal bands in CSF; Gd+= gadolinium enhancing lesions; EDSS= Expanded Disability Status Scale.

Through the gating strategy showed in figure 13A, I investigated the following immune cell populations:

- **CD4⁺ T cells** (CD45⁺ CD20⁻ CD3⁺ CD4⁺ CD8⁻)
- **CD8⁺ T cells** (CD45⁺ CD20⁻ CD3⁺ CD8⁺ CD4⁻)
- **B cells** (CD45⁺ CD3⁻ CD20⁺ CD27^{+/-})
- **Classic Monocytes** (CD45⁺ CD3⁻ CD20⁻ CD14⁺ CD16⁺)
- **Non-Classic Monocytes** (CD45⁺ CD3⁻ CD20⁻ CD16⁻ CD14⁺)
- **Neutrophils** (CD45⁺ CD3⁻ CD20⁻ CD16⁺ CD66b⁺)

- Myeloid Dendritic Cells (CD45⁺ CD3⁻ CD20⁻ CD14⁻ CD16⁻ CD11c⁺ CD123⁻)
- Plasmacytoid Dendritic Cells (CD45⁺CD3⁻ CD20⁻ CD14⁻ CD16⁻CD11c⁻ CD123^{high})

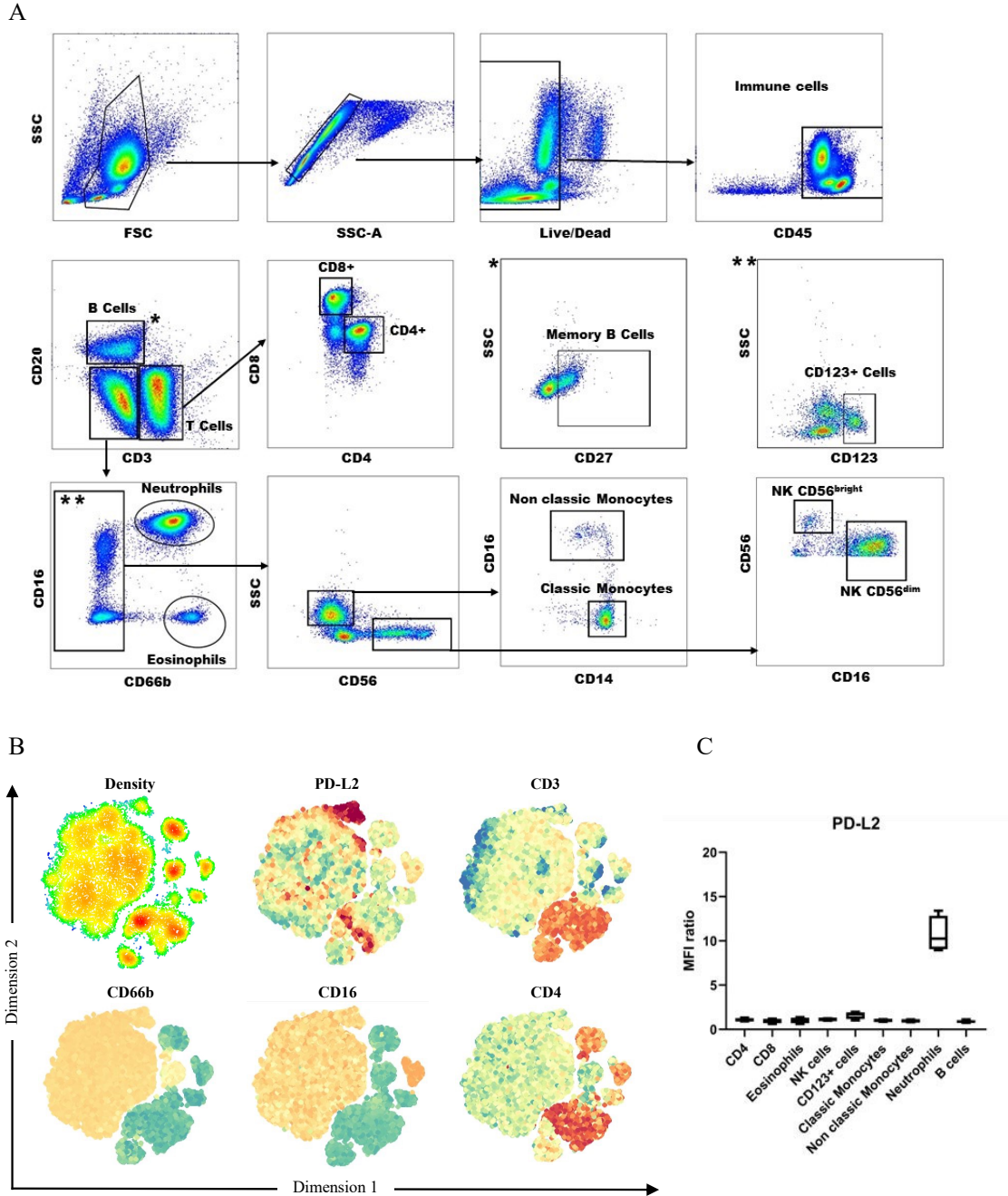


Figure 12. PD-L2 expression on circulating immune cells. A) Gating strategy used to analyze different populations of circulating immune cells. B) tSNE graphs of CD45⁺ cells. PD-L2 is over-expressed in neutrophils, identified by CD16 and CD66b expression, and in a small percentage of CD4⁺ lymphocytes. C) MFI ratio of PD-L2 expression in different leukocyte populations. PD-

L2 expression is only visible in neutrophils, and in a small percentage of DCs (CD123⁺). The analysis was made using FlowJo Software (BD Biosciences).

In patients and controls, PD-L2 expression was detectable at a significant percentage in neutrophils, as shown in Figure 13B where a small cloud of PD-L2^{high} expressing neutrophils is visible within the CD16⁺CD66b⁺ population. PD-L2 was also detectable at lower levels a small population of activated CD4⁺ T cells and in CD123⁺ Dendritic Cells (DCs) (Figure 13B-C). PD-L1 expression was also detected in both myeloid and lymphoid cells, but at very low levels (data not shown). This population of CD16⁺CD66b⁺PD-L2⁺ neutrophils (from now on referred to as PD-L2⁺ neutrophils) had never been described in the literature when I first observed it (2018). However, in the last few years, other groups have observed PD-L2⁺ neutrophils in different contexts, such as early pregnancy¹⁶⁰ (2020) and gastric cancer¹⁶¹ (2021). In early pregnancy, decidual factors stimulate neutrophils to acquire PMN-MDSC-like phenotypes and function via phosphorylated STAT5/PD-L2 signaling after stimulation with decidual GM-CSF. Decidual PMN-MDSCs suppress T-cell proliferation via PD-1 signaling, suggesting a new and important function in inducing tolerance to the growing fetus during early pregnancy¹⁶⁰. In contrast, neutrophils overexpressing PD-L2 and FasL in human gastric cancer have been described as pro-tumorigenic. In this context, they acquired an immunosuppressive function on tumor-specific CD8⁺ T cells and promoted the growth and progression of tumors *in vitro* and *in vivo*¹⁶¹. However, their role in neuroinflammation remains unclear.

1.II PD-L2⁺ neutrophils are increased in patients with an active form of MS, but not in other autoimmune diseases

PD-L2⁺ neutrophils were detectable in both healthy controls and MS patients but were significantly increased in the latter group. The difference was even more evident when the patient group was divided by disease activity, generally corresponding to the relapse (active) or remission (non-active) phases. Patients with an active form of the disease and with no treatment had a higher percentage (between 5 and 18%) of PD-L2⁺ neutrophils on total neutrophils, compared to patients in the non-active phase (Figure 14).

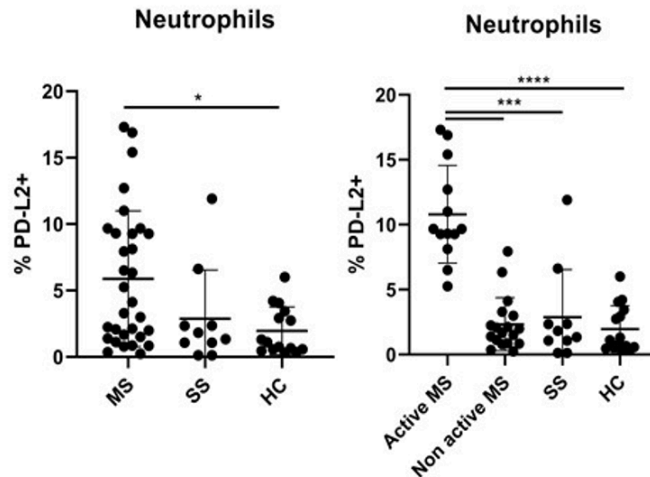


Figure 13. Percentage of PD-L2 neutrophils on total CD16 CD66b neutrophils in patients and healthy controls. In the graph on the left, all patients with MS are grouped together, while in the graph on the right patients are divided by disease activity. MS = Multiple Sclerosis, HC= Healthy Controls, SS = Systemic Sclerosis. The analysis was made using FlowJo Software (BD Biosciences).

We tested whether this population was specific to people with MS or whether it was also common in other autoimmune diseases by testing blood samples from patients with systemic sclerosis. We identified patients with systemic sclerosis as good controls since all patients were at their first diagnosis or were not undergoing treatment. PD-L2⁺ neutrophils were detected in percentages similar to those found in healthy controls but were more correlated with MS activity phases. Since PD-L2 is an immunosuppressive molecule, we speculated that in this case, it might identify a population of neutrophils with regulatory functions. Starting from what is known in the literature, I characterized this population of human neutrophils to prove my point.

1.III PD-L2⁺ neutrophils are a group of mature cells sedimenting in the ND

First, the maturation stage of the PD-L2⁺ neutrophils was identified. The expression of CD16 is known to be acquired at the band cell stage during neutrophil differentiation and is further upregulated in mature neutrophils¹⁶². From the flow cytometry data, PD-L2⁺ neutrophils seemed to be characterized by high levels of CD16 antigen (CD16^{high}) and high levels of CD62L, indicative of a late maturational stage. The May Grunwald Giemsa staining performed on sorted neutrophils also confirmed this hypothesis. PD-L2⁺ neutrophils showed a segmented nucleus, typical of mature neutrophils (Figure 15).

Neutrophils can also be classified on the basis of their density. Following density gradient centrifugation of the blood, some of the previously described regulatory neutrophil subsets settle within the peripheral blood mononuclear cell (PBMC) layer. Thus, they are generally defined as LDNs^{88,90}. However, PD-L2⁺ neutrophils were found in the normal density layer (NDL) but not in the low-density layer (Fig. 16). These results suggest that PD-L2⁺ neutrophils possess an advanced maturational stage, which distinguishes them from other populations described in the literature.

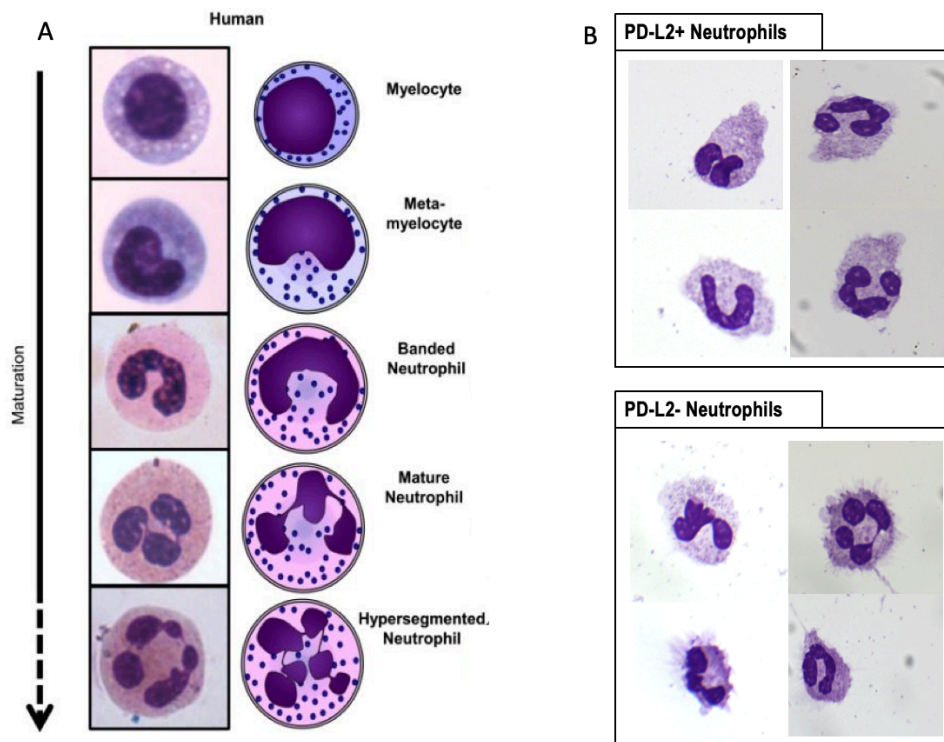


Figure 14. Neutrophils maturation stages. A) Different maturation stages of human neutrophils with May-Grünwald Giemsa staining (Pillay, J., Tak, T., Kamp, V. M., & Koenderman, L. (2013). *Immune suppression by neutrophils and granulocytic myeloid-derived suppressor cells: similarities and differences*. Cellular and molecular life sciences, 70(20), 3813-3827.) B) Representative images of PD-L2 positive and negative neutrophils acquired with light microscopy at 100X magnification.

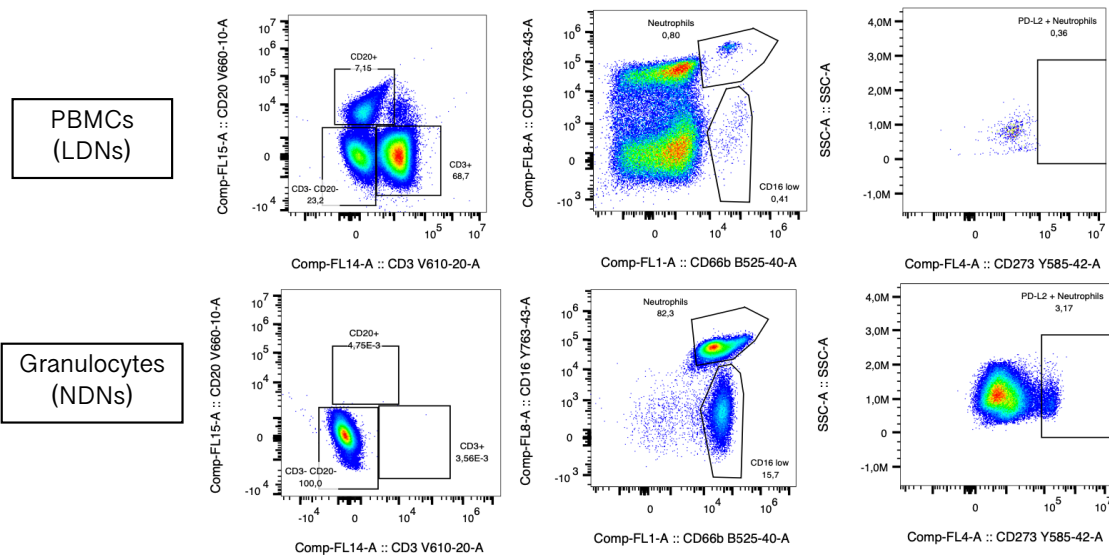


Figure 15. PD-L2 neutrophils in different centrifugation layers. $CD3^- CD20^+ CD66b^+ CD16^+$ PD-L2⁺ neutrophils are only found within the NDN layer (graphs below) and not in the LDN layer (graphs above). The analysis was made using FlowJo Software (BD Biosciences).

I.IV PD-L2 neutrophils express markers typically associated with regulatory functions

To further characterize this new population, I designed a second panel for multiparametric flow cytometry detecting antigens typically associated with regulatory functions (shown in materials and methods, Table 3). As expected, PD-L2⁺ neutrophils from the whole blood of patients with MS displayed increased expression of CD10, previously described as a marker for mature suppressive neutrophils⁹⁵. CD54 (ICAM), CD35 (complement receptor type I) and CD11c (associated with PMN-MDSCs) were also upregulated in PD-L2⁺ neutrophils. CD62L has a higher expression on PD-L2⁻ neutrophils compared to the PD-L2⁺ ones, although remaining at high level of expression (Figure 17B).

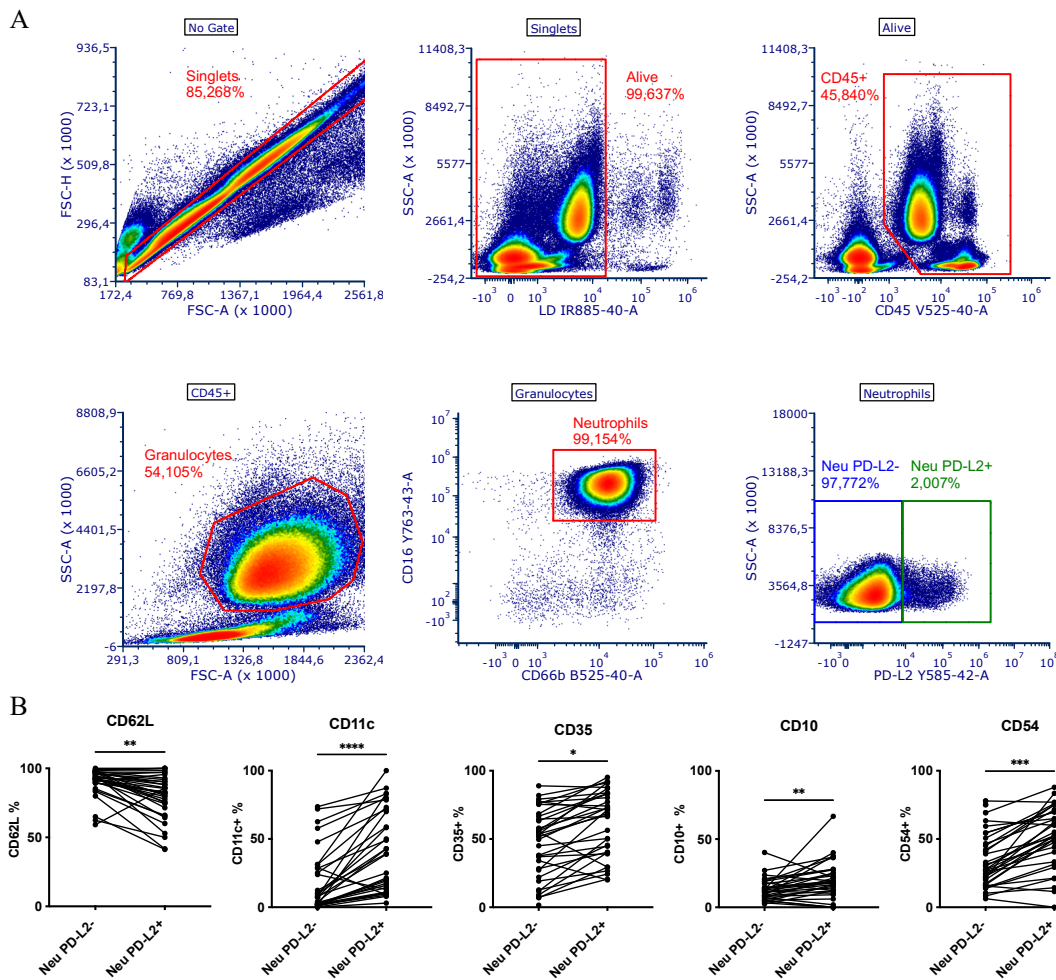


Figure 16. Percentage of expression of regulatory markers on PD-L2⁺ neutrophils compared to PD-L2⁻ neutrophils. The expression of regulatory markers was compared between PD-L2⁺ neutrophils and other neutrophils (PD-L2⁻). A) Gating Strategy for the identification of PD-L2⁺ or PD-L2⁻ neutrophils. Respectively, singlets, Alive cells, CD45⁺, morphological gate, CD16⁺CD66b⁺. B) Quantification of the percentage of expression of surface markers in PD-L2⁺ or PD-L2⁻ neutrophils. Each dot represents a different donor. The analysis was made using FCS Express Software (De Novo Software). Statistical analysis: Mann-Whitney test. * $p < 0.05$; ** $p < 0.01$; *** $p < 0.001$.

IV Anti-inflammatory cytokines are detectable in the supernatants of PD-L2 neutrophils co-cultured with T lymphocytes

Since PD-L2 is an immune checkpoint, I hypothesized that neutrophils expressing this marker have a regulatory function on other immune cells in MS, especially T

lymphocytes. To test this, PD-L2⁺ neutrophils were sorted and co-cultured with CD3⁺ T lymphocytes. After three days of co-culture, the cytokines released in the supernatant were measured. Interestingly, IL-4 and IL-10 were detectable only in co-cultures with PD-L2⁺ neutrophils. On the other hand, proinflammatory cytokines, such as IL-1 β and IL-12p70, were detectable only in the co-culture with neutrophils not expressing PD-L2 (here PD-L2⁻) (Fig. 18).

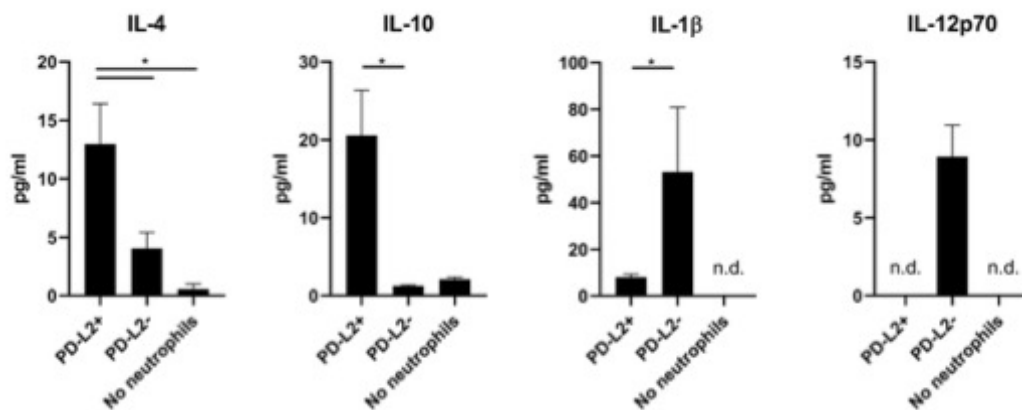


Figure 17. Cytokines released in the supernatant of co-culture between sorted neutrophils and T lymphocytes. PD-L2⁺= cocultures of CD3⁺ T cells and sorted neutrophils that express PD-L2; PD-L2⁻= cocultures of CD3⁺ T cells with sorted neutrophils that don't express PD-L2, No neutrophils = only CD3⁺ cells without neutrophils. Samples were analyzed using MesoScale Discovery Electrochemiluminescence (AcroBiosystem). n=5 independent donors. Statistical analysis: Ordinary One-way ANOVA. * $p < 0.05$; ** $p < 0.01$; *** $p < 0.001$.

To understand where the IL-4 in supernatants came from, I asked whether PD-L2⁺ neutrophils were able to produce and release IL-4. Intracellular staining (ICS) was performed on neutrophils isolated from whole blood samples from patients with MS. Again, IL-4 levels were detectable only in the PD-L2⁺ neutrophils (Fig.19). Overall, these observations suggested that PD-L2⁺ neutrophils have regulatory functions.

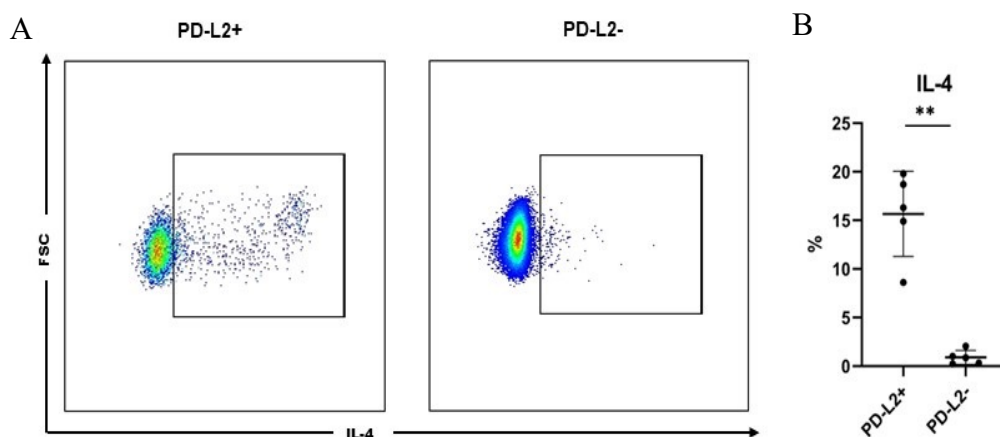


Figure 18. ICS of IL4 in PD-L2⁺ and PD-L2 negative neutrophils. Whole blood from patients with MS was analyzed through flow cytometry. Cells were permeabilized with brefeldin for 3h to quantify the production of cytokines inside neutrophils. A) Representative gating of IL-4 staining in PD-L2⁺ and PD-L2- neutrophils. B) Quantification of IL-4 percentage from flow cytometry data. The analysis was made using FlowJo Software (BD Biosciences). n=5 independent donors. Statistical analysis: Mann-Whitney test * $p < 0.05$; ** $p < 0.01$; *** $p < 0.001$.

1.VI PD-L2⁺ neutrophils are inducible ex vivo after stimulation with cytokines

To further characterize PD-L2⁺ neutrophils, I examined possible stimuli that could induce PD-L2 expression on neutrophils *ex vivo*. Since IL-4 is already known in literature to upregulate PD-L2 levels in myeloid cells such as macrophages¹⁶³, I stimulated purified neutrophils from healthy donors with different concentrations of IL-4, from 0 to 150 ng/ml. Samples were then analyzed using multiparametric flow cytometry with a specific panel of antibodies (Table 4). Even at low concentrations (starting from 0.1 ng/ml), IL-4 could upregulate PD-L2 on 20-40% of neutrophils, depending on the donor (Figure 20 A and B). We also characterized the kinetics of PD-L2 expression following IL4 stimulation. An increase in PD-L2 expression was visible starting from 0,1 ng/ml and the maximum expression was reached between 10 and 20 ng/ml (Figure 20 C). From now on, 20 ng/ml is the chosen concentration used for the stimulation of neutrophils with IL-4. Moreover, because neutrophils usually have a short half-life *in vitro*, we also measured the viability of neutrophils at the same time points used to study the kinetics of PD-L2 expression (Figure 20D). Neutrophils stimulated with IL-4 showed a good viability (approximately 90% of live cells) up to 16 hours of stimulation. After 24 hours, the

neutrophil death rate was approximately 20% of the total cells, which increased dramatically after 48 hours, reaching over 60%.

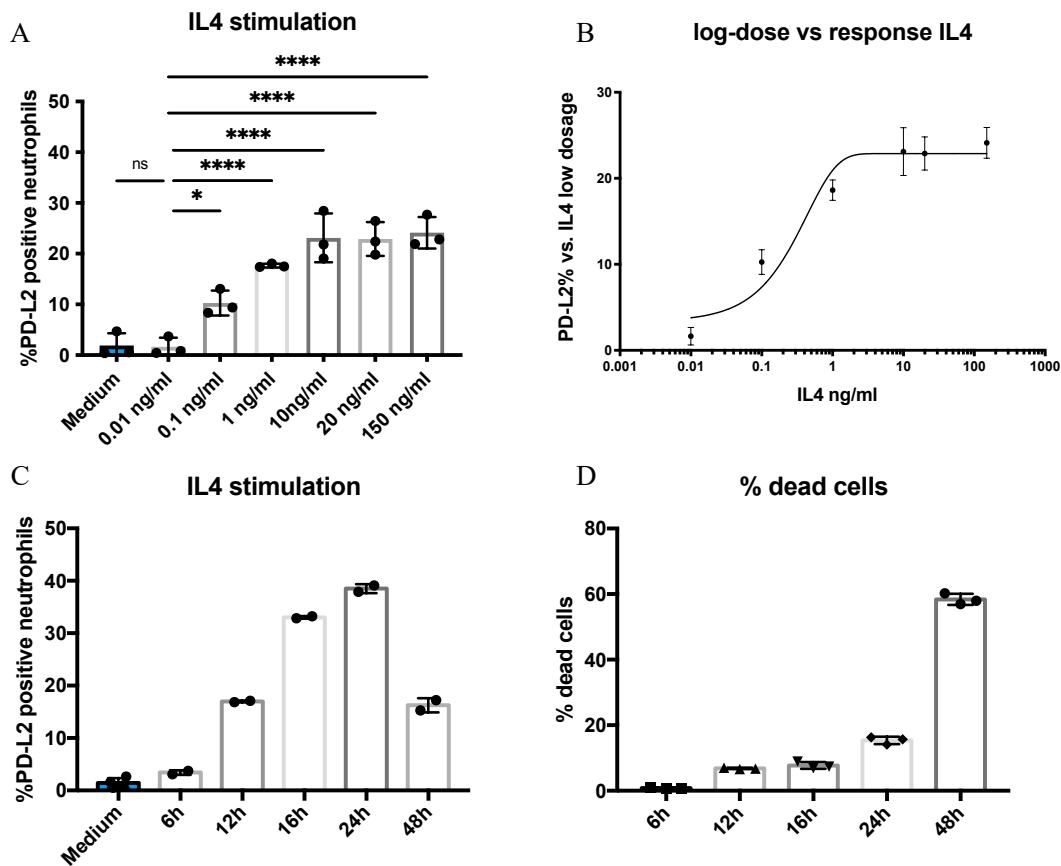


Figure 19. Dose response and Kinetics of neutrophils response to IL-4 ex vivo stimulation.

A) Quantification of the percentages of PD-L2+ neutrophils after stimulation with different IL4 concentrations (0.01, 0.1, 1, 10, 20 and 150ng/ml). B) Log-dose response curve of the percentage of PD-L2 neutrophils after IL4 stimulation. C) Quantification of the percentages of PD-L2+ neutrophils after IL4 stimulation (20ng/ml) at different time points. D) Quantification of the percentages of dead cells at different time points. The analysis was made using FCS Express Software (De Novo Software). n=3 independent donors. Statistical analysis: Ordinary One-way ANOVA. * $p < 0.05$; ** $p < 0.01$; *** $p < 0.001$.

PD-L2 *in vitro* expression after IL-4 stimulation, in addition to the data we collected in patients with MS that PD-L2 neutrophils can release IL-4, led us to hypothesize an autocrine loop between IL-4 production and release and PD-L2 upregulation. IL-4 upregulates PD-L2 on neutrophils, leading to increased production of IL-4 (as observed with ICS staining), which maintains the expression of PD-L2.

I also verified that IL-4 stimulation did not affect neutrophil morphology or maturation stage. After 16-18 hours of stimulation with IL-4, neutrophils maintained the same morphological characteristics as non-stimulated neutrophils (Figure 21).

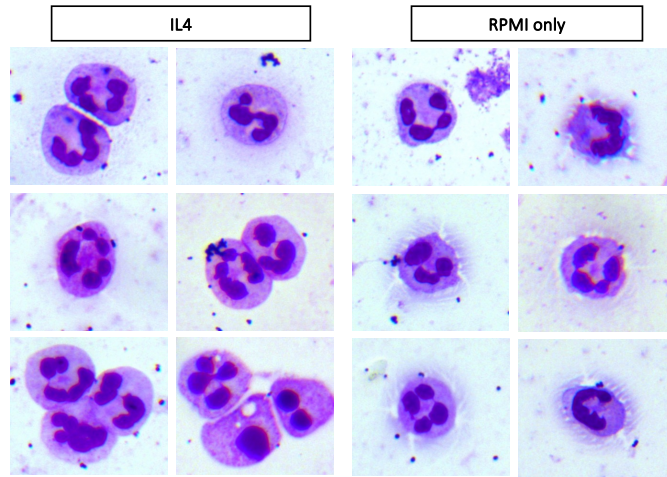


Figure 20. May-Grunwald Giemsa staining of neutrophils isolated from healthy donors, stimulated with IL-4 for 18 hours, or not stimulated (RPMI only). Images were acquired at a 100X magnification on a Leica inverted microscope.

Next, I tested other cytokines already described in the literature to upregulate PD-L2 (such as IFN- γ alone or in combination with GM-CSF), interleukins that bind to the same receptor (such as IL-13) and other cytokines usually present in the plasma of pwMS (TNF- α , IL-1 β and IL-8)¹⁶⁴.

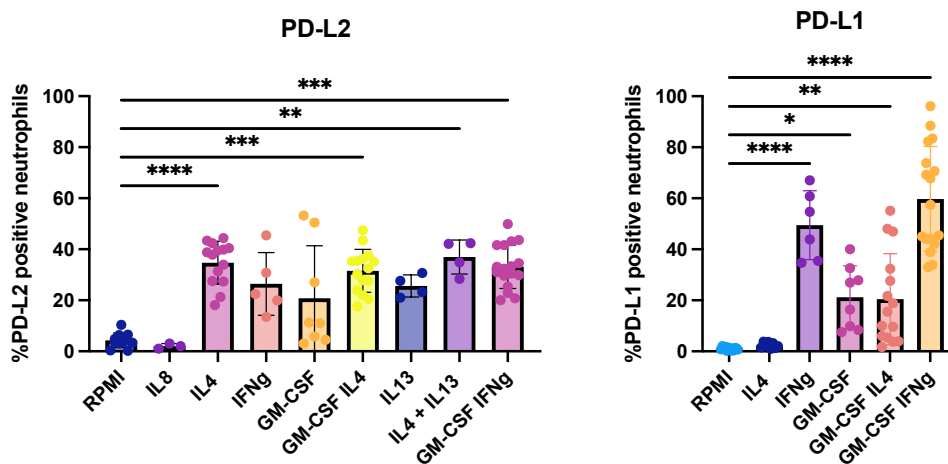


Figure 21. Percentage of neutrophils expressing PD-L2 after ex vivo stimulation for 18h, alone or in combination. Neutrophils were isolated from the NDJ after Ficoll centrifugation and plated for 18 hours at 37°C. Different cytokines alone or in combination were tested. The percentage of expression of PD-L2 or PD-L1 was measured using flow cytometry. The analysis was made using

*FCS Express Software (De Novo Software). Each dot represents a different donor. Statistical analysis: Ordinary One-way ANOVA. * $p < 0.05$; ** $p < 0.01$; *** $p < 0.001$.*

Other than IL-4, IL-13, GM-CSF and IFN- γ were able to upregulate PD-L2 neutrophils from healthy donors. Interestingly, GM-CSF and IFN- γ (alone or in combination) increased the expression of both PD-L2 and PD-L1, while IL-4 seemed to be highly specific only for PD-L2 upregulation (Fig. 22).

I then characterized the kinetics of the second most effective stimulation, IFN- γ in combination with GM-CSF. In this case, the kinetics was slightly slower than that with IL4 stimulation, reaching a peak between approximately 18 and 20 hours of stimulation (Figure 23). Although the maximum percentage of PD-L2⁺ neutrophils was observed after 48 hours, we could not use this time point because the majority of neutrophils were dead. When neutrophils undergo apoptosis, they downregulate CD16 expression. Thus, we only considered PD-L2 and PD-L1 expression in the CD16^{high} group. We also measured PD-L1 expression, which has a kinetics similar to those of PD-L2, but it has even higher levels of expression.

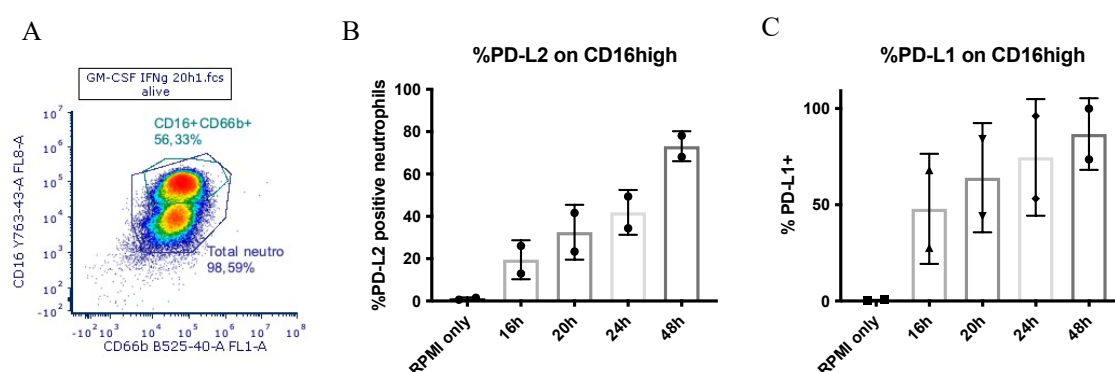


Figure 22. Kinetics of neutrophils response to GM-CSF and IFN- γ ex vivo stimulation. A) Gating strategy for the identification of total CD16⁺ CD66b⁺ neutrophils and CD16^{high} CD66b⁺ neutrophils. B-C) Percentage of PD-L2 and PD-L1 expression on CD16^{high} neutrophils. The analysis was made using FCS Express Software (De Novo Software).

I also confirmed the increased expression of PD-L2 (and PD-L1) after stimulation with IL-4 or GM-CSF + IFN- γ using immunofluorescence (Figure 24). As expected, PD-L2 mean intensity is significantly increased after 18 hours of incubation with both stimulations, while PD-L1 mean intensity is only increased after stimulation with GM-CSF + IFN- γ (Figure 24). I also measure MPO (Myeloperoxidases) expression, as a

marker of neutrophils activation. Following both stimulations, MPO levels are significantly increased compared to the untreated control (UT).

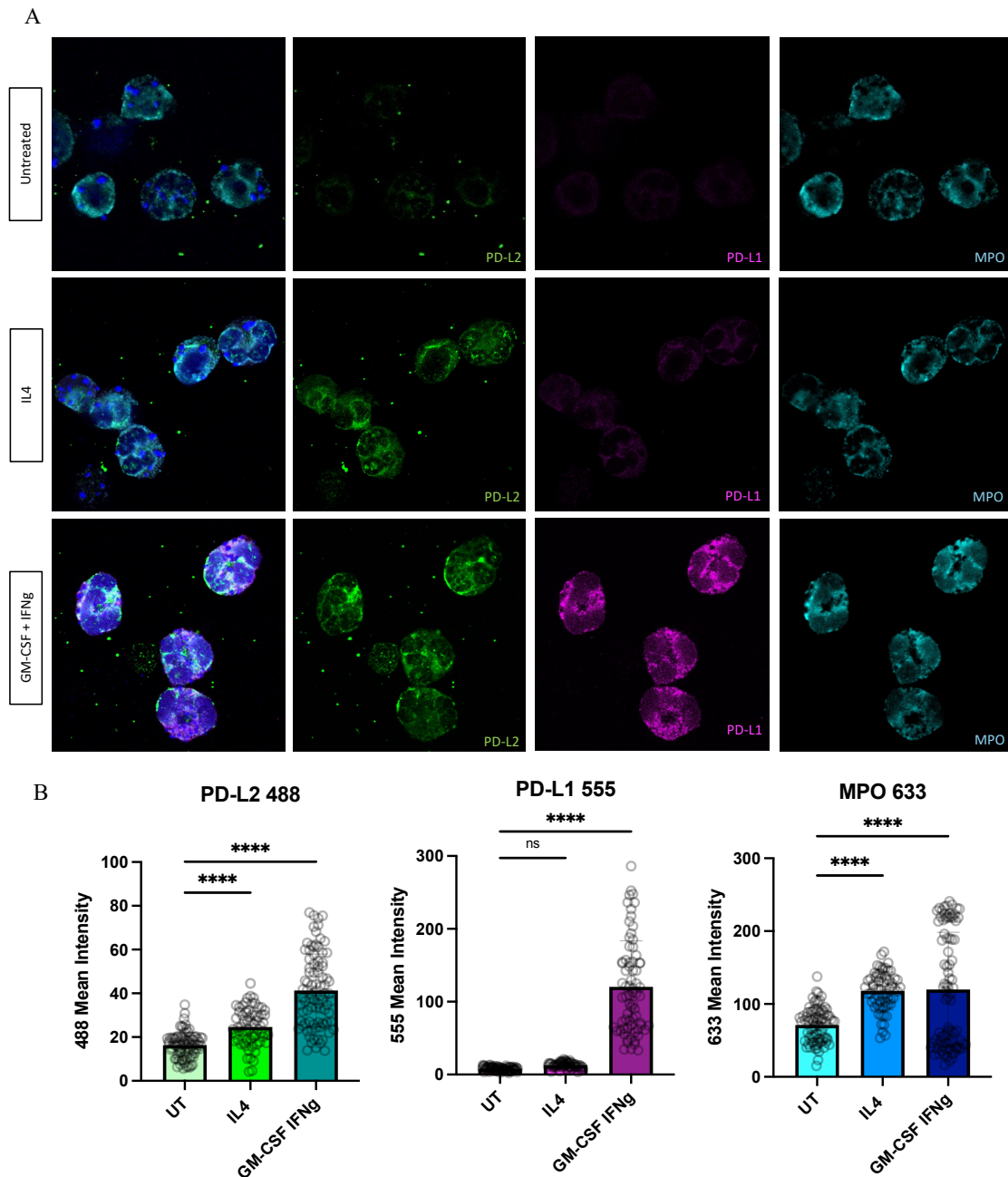


Figure 23. Human neutrophils with or without stimulation. A) Representative images of UT=untreated or stimulated neutrophils at 63X magnification. All images were acquired with a Sp5 Leica confocal microscope and analyzed with Fiji/ImageJ Software. Hoechst staining (blue) was used to identify neutrophil nuclei, primary antibodies were used to identify PD-L2 (green), PD-L1 (magenta), MPO (cyan). B) Quantification of the mean grey intensity of PD-L2, PD-L1 and MPO signals. Fiji Software (NIH) was used for the analysis. An average of 20 cells/images were considered for the analysis. Ordinary One-way ANOVA was used to determine statistical

significance followed by Holm-Šídák's multiple comparisons test. * $p \leq 0.05$, ** $p \leq 0.005$, *** $p \leq 0.0005$; n.s., not significant.

I.VII CyTOF mass spectrometry confirms that PD-L2⁺ neutrophils express markers typically associated with regulatory features

We then exploited a cutting-edge technique such as mass cytometry, also called cytometry by time-of-flight (CyTOF), to obtain a powerful single-cell proteomic analysis of PD-L2⁺ neutrophils. CyTOF utilizes rare metal isotopes instead of fluorophores for antibody labeling, which allows to overcome the limitations of the multiplexing capability of flow cytometry¹⁶⁵⁻¹⁶⁷. We designed a comprehensive panel of ~40 markers (Shown in Material and Methods, table 5) and analyzed purified neutrophils stimulated overnight with IL-4 (Figure 25, population N4).

PD-L2⁺ neutrophils expressed the same markers as those seen in patients with MS, such as high expression of CD16, CD11a, CD54, and CD62L. This observation allowed us to confirm similarities between the two populations. Interestingly, Arg1 was upregulated in populations expressing PD-L2. Arg1 is associated with the capacity of myeloid-derived suppressor cells to slow T cell proliferation and chemokine release, suggesting a regulatory phenotype for PD-L2⁺ neutrophils. On the same note, KLF4, a potent tumor suppressor and inhibitor of cellular proliferation¹⁶⁸, is also increased on PD-L2 neutrophils compared to controls as well as CD39, a nucleotide metabolizing enzyme that regulates immunity and inflammation. Notably, we observed no expression of Lox1 protein which has been described in polymorphonuclear myeloid-derived suppressor cells in cancer patients¹⁶⁹ and it is used to discriminate immature neutrophils.

Overall, mass cytometry analysis showed that PD-L2⁺ neutrophils have a clear regulatory phenotype and identify a newly discovered subgroup, different from those already described in the literature.

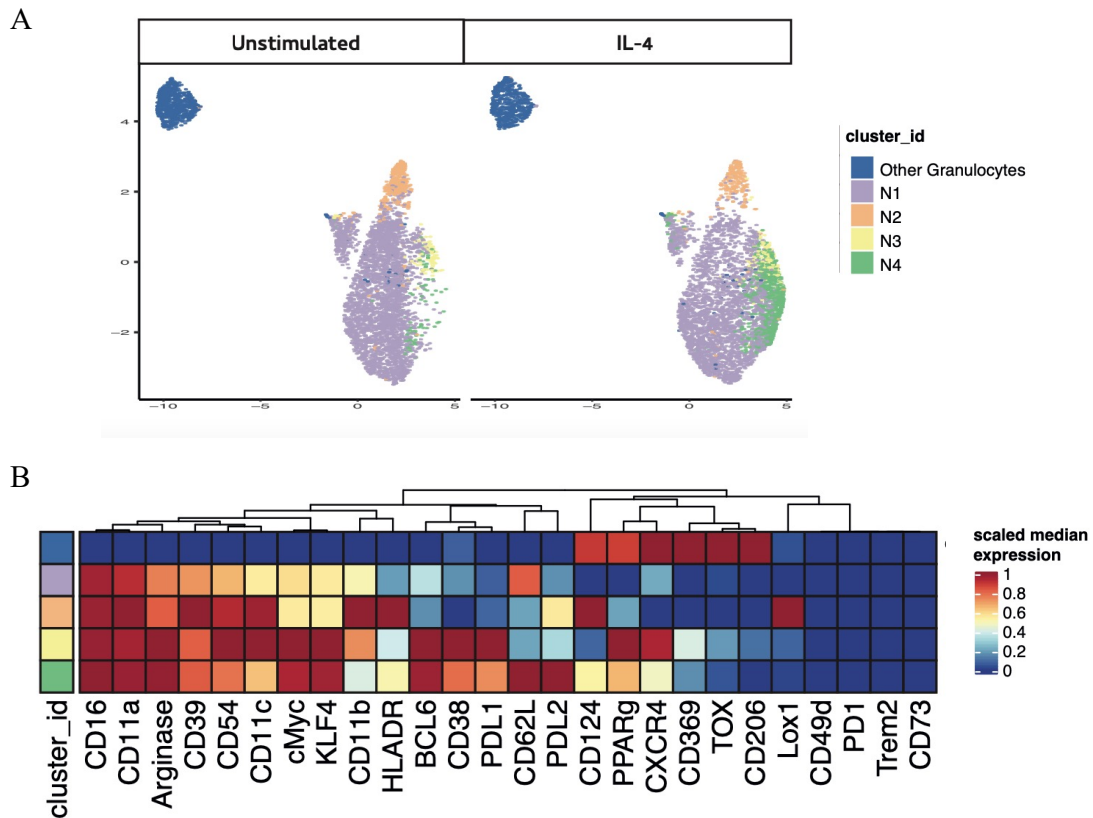


Figure 24. CyTOF results. Neutrophils from healthy donors were stimulated with IL-4 to induce PD-L2 expression. We then analyzed the different populations using multiparametric mass cytometry. N4 is a PD-L2-expressing neutrophil population. A) tSNE graph. B) Heatmap of the relative antigen expression. $n=3$ independent donors.

I.VIII PD-L2 neutrophils inhibit T cell proliferation and IFN- γ release in the supernatant of coculture

To provide functional evidence that PD-L2⁺ neutrophils have immunosuppressive capacity, neutrophils were co-cultured with activated PBMCs from healthy donors. Neutrophils were isolated using the Ficoll protocol, stimulated for 18 hours with IL-4 or GM-CSF + IFN- γ , examined for their capacity to affect T lymphocyte proliferation after 4 days (approximately 96 h). PD-L2⁺ neutrophils suppressed CD3/CD28-induced proliferation, compared with untreated neutrophils (Figure 26). The release of IFN- γ in the supernatant of the same co-cultures was also measured using ELISA. When neutrophils express PD-L2, there is a decrease in the production of IFN- γ (Figure 26C), indicating a suppressive action.

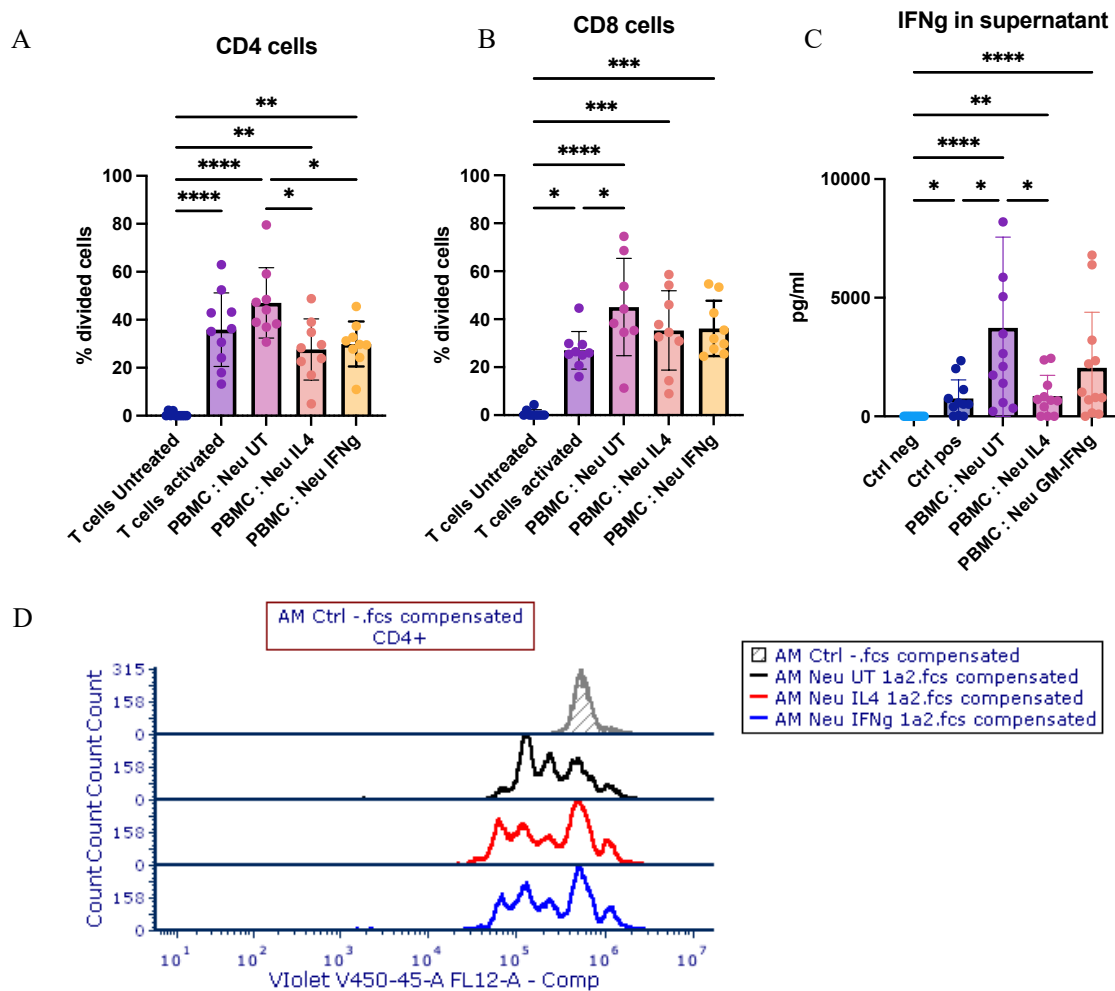


Figure 25. Immunosuppressive assays: co-culture between neutrophils and activated T cells. A-B) Quantification of CD4 and CD8 T cell proliferation by flow cytometry. PD-L2 neutrophils have a stronger effect on CD4 T cells proliferation in comparison with CD8 T cells. C) Quantification of the IFN- γ released in the supernatant of co-culture after 3.5 days. D) Representative histograms of T cell proliferation by dilution of the Violet Cell Tracer dye. The analysis was made using FCS Express Software (De Novo Software). Statistical analysis: Friedman test. * $p < 0.05$; ** $p < 0.01$; *** $p < 0.001$.

I.IX Blocking PD-1 axis, the inhibitory effect of PD-L2 neutrophils is partially restored

To verify that the immunosuppressive capacity was attributed to PD-L2 interaction with the PD-1 receptor (expressed on activated lymphocytes), I repeated the co-culture experiment in the presence of a blocking PD-1 antibody. The PD-1 blocking antibody

partially reversed the inhibitory effect of PD-L2 neutrophils, confirming that the suppressive action was due to the PD-1 axis (Figure 27). This effect was more consistent when neutrophils were stimulated overnight with IL-4.

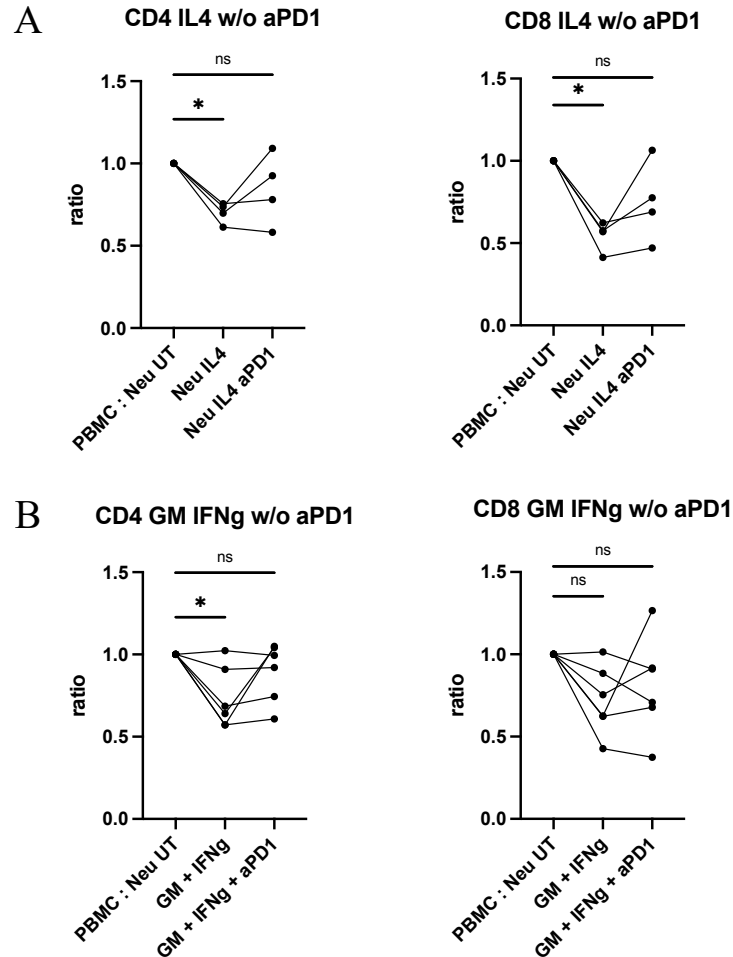


Figure 26. The suppressive function of PD-L2 neutrophils is partially reverted in the presence of PD-1 blocking antibody. A) Quantification of the proliferation of CD4 and CD8 T cells after coculture with untreated (UT) or IL4-stimulated neutrophils and with α PD1 blocking antibody. B) Quantification of the proliferation of CD4 and CD8 T cells after coculture with untreated (UT) or IFN- γ + GM-CSF-stimulated neutrophils and with α PD1 blocking antibody. The analysis was made using FCS Express Software (De Novo Software). Statistical analysis: Friedman test. * $p < 0.05$; ** $p < 0.01$; *** $p < 0.001$.

However, the activation status of T cells (measured by the expression of CD69 and PD-1), did not change significantly in the presence of neutrophils or according to the neutrophil stimulation and phenotype (Figure 28).

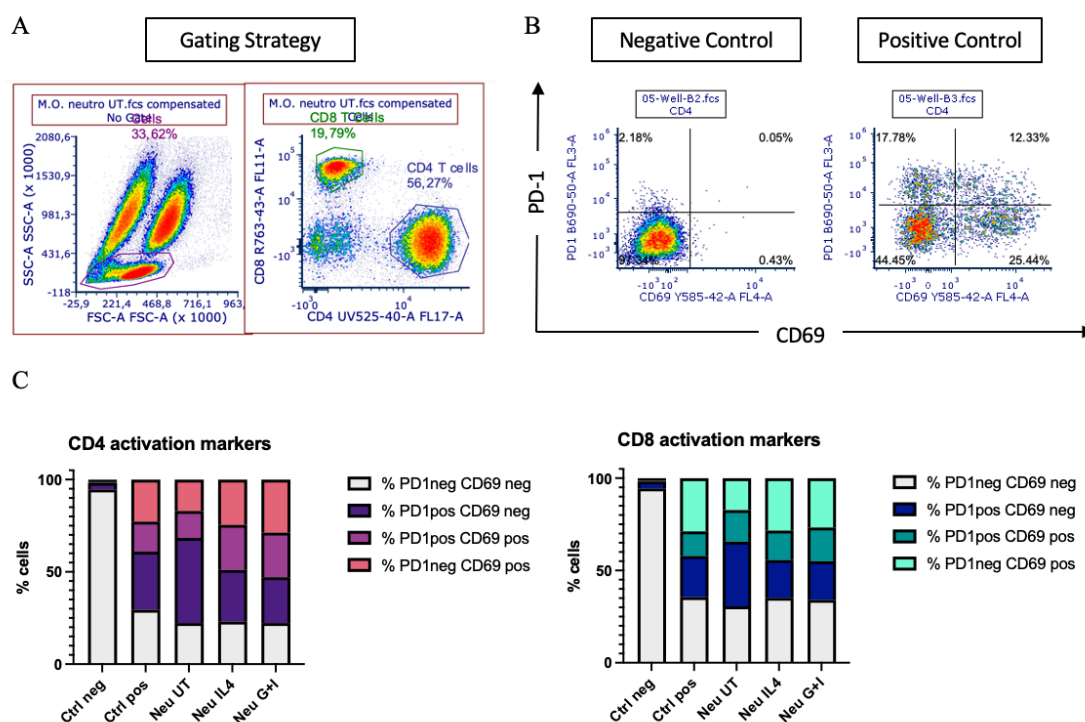


Figure 27. Activation status of T lymphocytes in co-cultures with or without neutrophils.
 A) Gating strategy for analysis of CD4 and CD8 T cells co-cultured with neutrophils.
 B) Representative images of negative (unstimulated) and positive (CD3⁺ T cells) controls.
 C) Quantification of activation markers, PD-1^{+/−} and CD69^{+/−}, on CD4 and CD8 T cells. The analysis was made using FCS Express Software (De Novo Software).

LX Neutrophils and CD3 cells form conjugates in vitro

To characterize the interface between PD-L2 neutrophils and CD3 cells, I compared the ability of PD-L2 neutrophils to form conjugates with activated CD3 cells, compared to untreated neutrophils. Neutrophils and CD3 cells were cocultured for 2 hours directly on a microscope slide to allow the formation of immune synapses. Cocultures were then carefully fixed, permeabilized, and stained with α CD3 and α CD16 antibodies. Images of Neutrophils/CD3 cell conjugates were captured using epifluorescence microscope (Figure 29) or confocal laser scanning microscope. Using 3-dimensional imaging (x-y-z plane), I visualized the immune synapses between neutrophils and CD3 cells (Figure 30). Interestingly, in most of the acquired images of the stimulated and the untreated conditions, neutrophils seemed to interact with lymphocytes in a 3 to 1 ratio.

Then, the number of conjugates was measured and compared. PD-L2⁺ neutrophils formed more conjugates than unstimulated neutrophils and the area of the conjugates was larger in the PD-L2⁺ neutrophils/CD3 cells co-cultures (Figure 31 A-D). Moreover, the colocalization of the CD3 signal with the CD16 signal was analyzed. Because these are preliminary data and the number of replicates at that moment is too small, the colocalization coefficient (*R coloc*) between the two conditions is not different. However, there is a trend suggesting that colocalization increases in PD-L2⁺ neutrophils/CD3 cells co-cultures (Figure 31C).

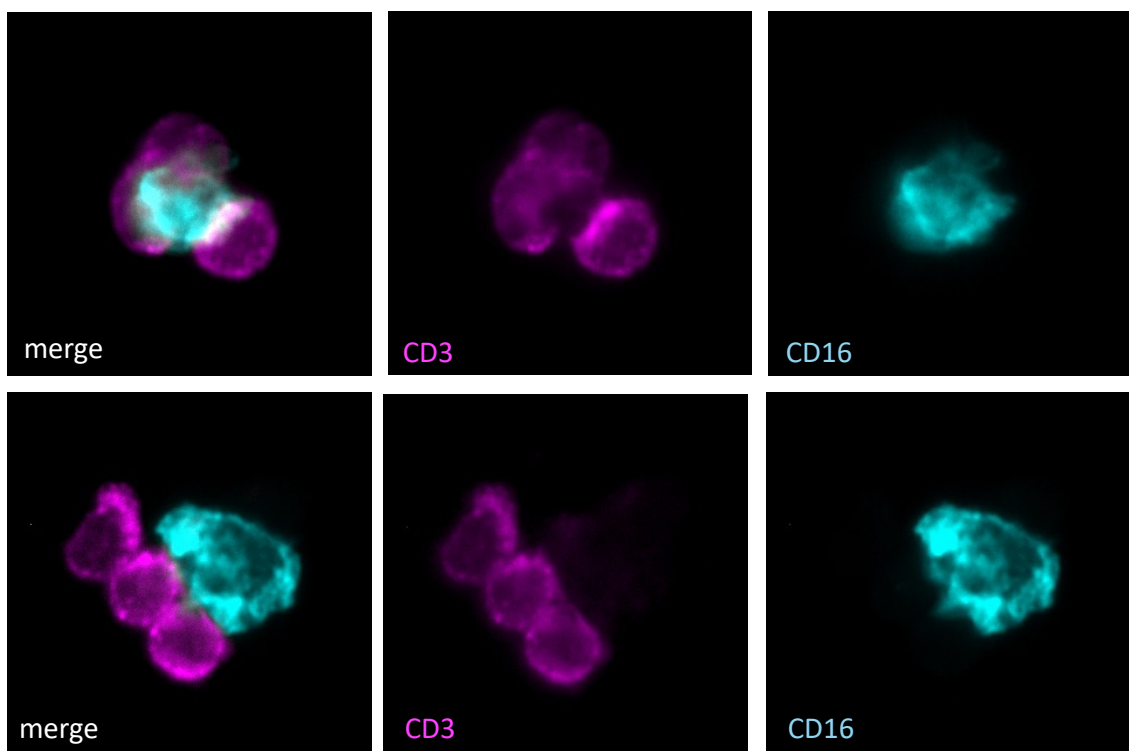


Figure 28. Neutrophil/CD3 conjugates. Representative images of Neutrophils/CD3 conjugate using epifluorescence microscope at 100X magnification. Stimulated (IL-4) human neutrophils and activated CD3 cells were cocultured at a 2:1 ratio on a microscope slide. CD3 (magenta) and CD16 (cyan) primary antibodies were used to identify cells. Hoechst was used for nuclei counterstaining (not shown here).

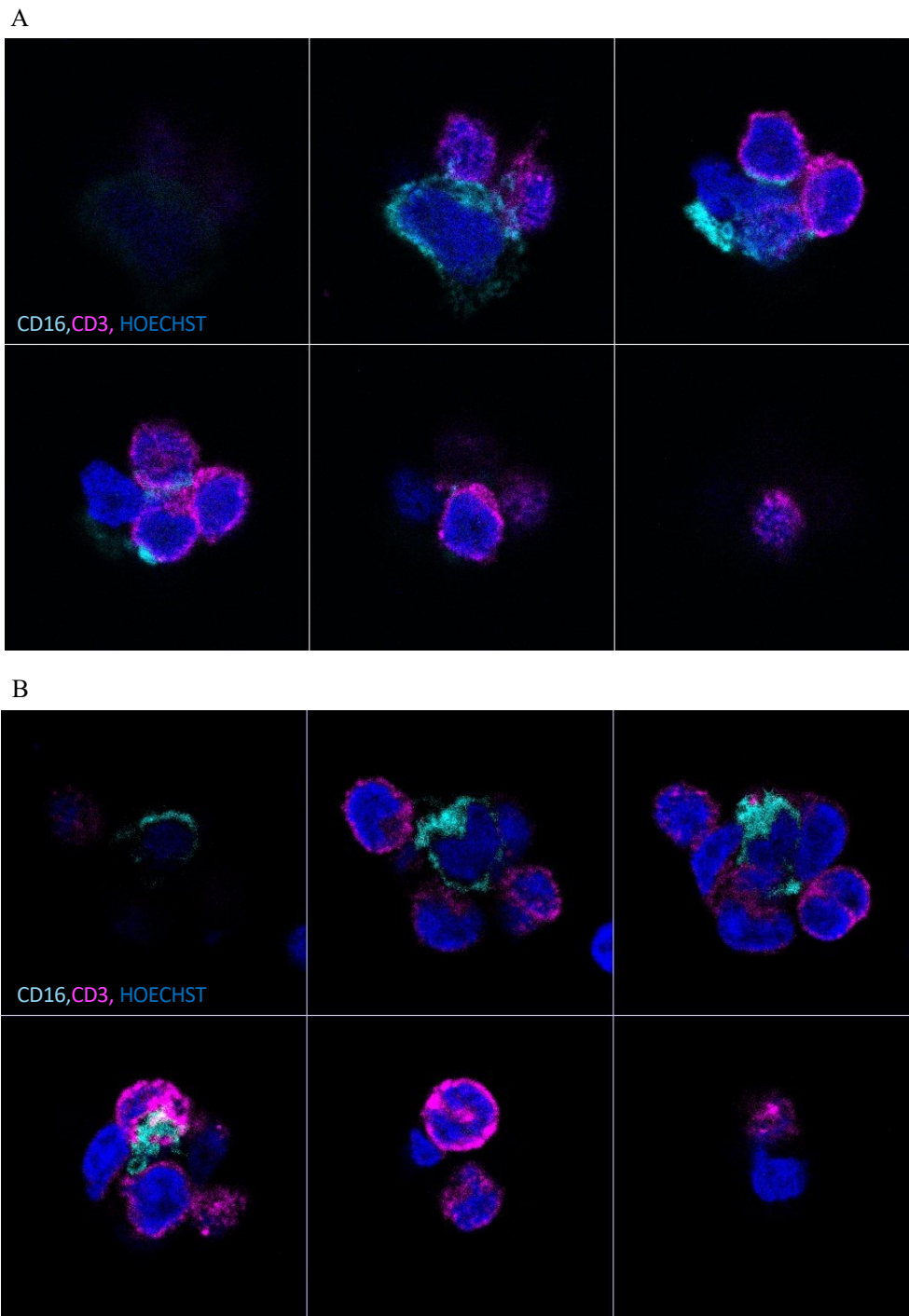


Figure 29. Stacks of Neutrophil/CD3 conjugates. Representative images of Neutrophils/CD3 conjugates at 63X magnification, 3x digital zoom-in. A-B) Each image is a z-stack every 2 μ m. A) Stimulated (IL-4 20 ng/ml) and B) unstimulated human neutrophils were cocultured with activated CD3 cells at a 2:1 ratio on microscope slides and stained with CD3 (magenta), CD16 (cyan) and Hoechst (blue) for nuclei counterstaining. Images were acquired using Sp5 confocal microscope and analyzed using Fiji Software (NIH).

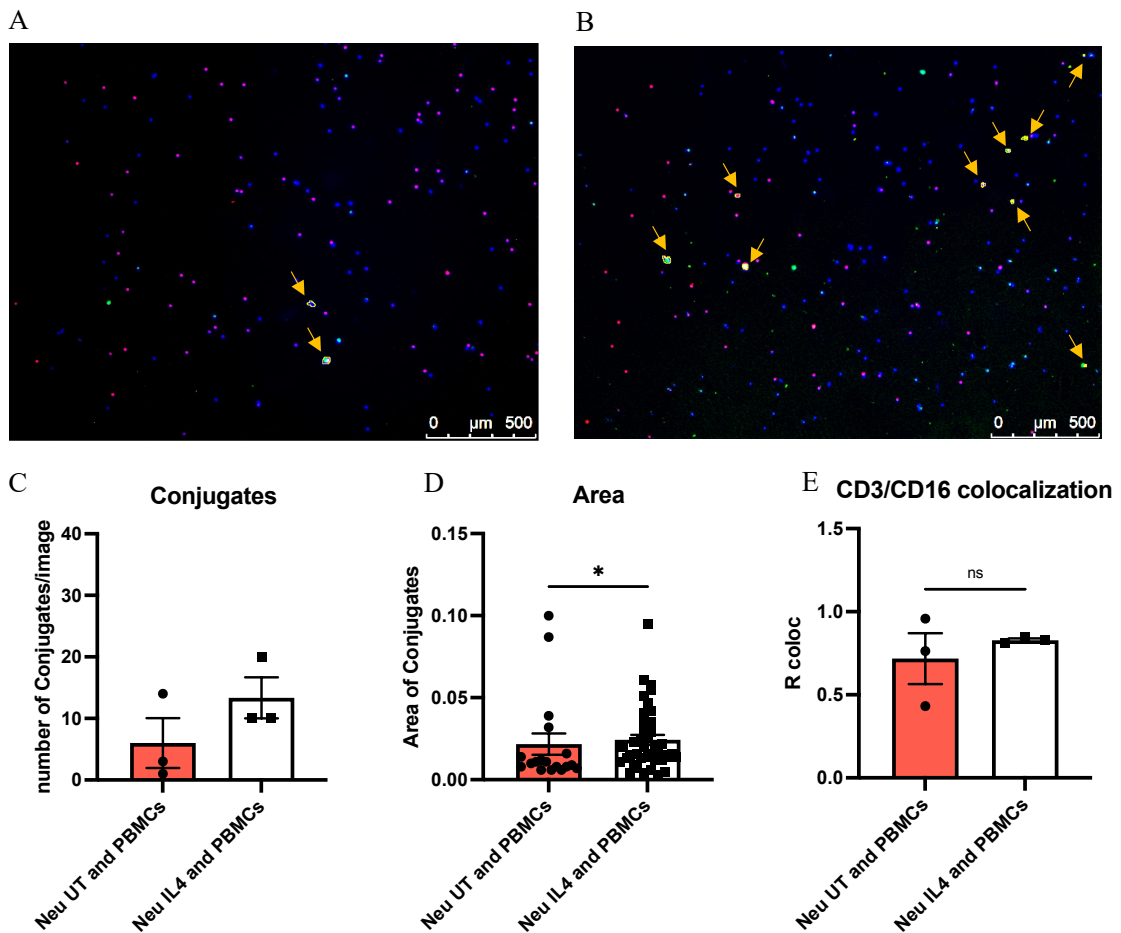


Figure 30. Analyses of Neutrophils/lymphocytes conjugates. A-B) Representative images of neutrophil/lymphocyte conjugates at low magnification (4X). The conjugates are surrounded by yellow and identified by yellow arrows. A. Unstimulated neutrophil/lymphocyte conjugates. B. PD-L2/lymphocyte conjugates. C) Quantification of the number of conjugates. D) Quantification of the conjugate area. E) Analysis of colocalization of CD3 and CD16 signals in unstimulated and PD-L2 neutrophils. The analysis was made using Fiji Software (NIH). Statistical analysis: Kolmogorov-Smirnov test. * $p < 0.05$; ** $p < 0.01$; *** $p < 0.001$.

LXI Quantification of soluble hPD-L2 in plasma and CSF of patients with MS

Finally, we observed and quantified the presence of soluble PD-L2 in the plasma of patients with MS versus healthy controls (Figure 32). Few recent works were published about the potential predictive and prognostic role of sPD-L1/L2 as biomarkers in renal¹⁷⁰, epithelial ovarian¹⁷¹ and lung¹⁷² malignancies. However, there is no literature about soluble PD-Ls in neurological disorders. From the data we collected, soluble PD-L2 seems to be reduced in patients with MS and this difference becomes even more evident when patients are divided according to disease activity.

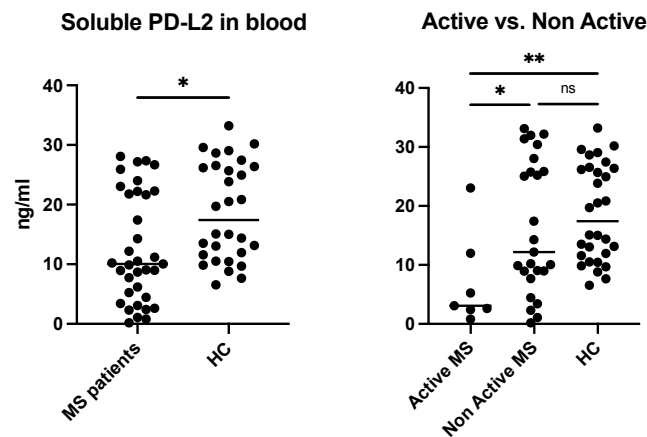


Figure 31. Soluble PD-L2 found in the serum. Soluble PD-L2 was measured using ELISA in the serum of MS patients (total or divided by disease activity) and healthy controls. Samples were analyzed with ELISA (R&D System). Statistical analysis: Kolmogorov-Smirnov test. * $p < 0.05$; ** $p < 0.01$; *** $p < 0.001$.

In addition, soluble PD-L2 has been found in the CSF of patients with MS and patients with other neurological disorders, such as hydrocephalus. PD-L2 levels appeared to be reduced in patients with MS (both active and non-active) compared to those with other diseases, suggesting an absorption mechanism. However, the cohort of analyzed samples was too small to draw definitive conclusions. Currently, no studies have been published on soluble PD-L2 in neurological disorders. Therefore, future experiments and clinical trials will help to shed light on this unknown marker and its potential usefulness in MS.

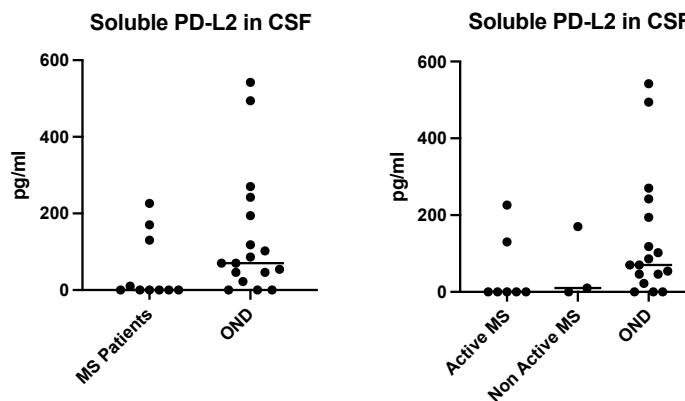


Figure 32. Soluble PD-L2 found in the CSF. Soluble PD-L2 was measured using ELISA in the CSF of patients with MS total or divided by disease activity and patients with other neurological disorders (OND). Statistical analysis: Kolmogorov-Smirnov test.

II.I Mouse Results - Wild type mice

II.I.I PD-L1 and PD-L2 expression on immune cells during EAE

To study the contribution of regulatory neutrophils in the preclinical model of MS, we induced EAE in C57/B16 mice. We analyzed CNS-infiltrating neutrophils at four different time points after the induction of the disease, corresponding to the phase before the onset of symptoms (7 d.p.i), logarithmic phase of the disease (14 d.p.i), the peak of the disease (21 d.p.i), and remission phase (28 d.p.i), as summarized in Fig. 34A. The clinical scores and the weights of the mice were measured every day for 28 days, as described in Material and Methods. As a control, we immunized mice with CFA without the MOG₃₅₋₅₅ antigen. This type of immunization induces systemic inflammation, without being specific to myelin. The CFA group of mice did not develop motor symptoms or weight loss, as opposed to the EAE group (Figure 34 B).

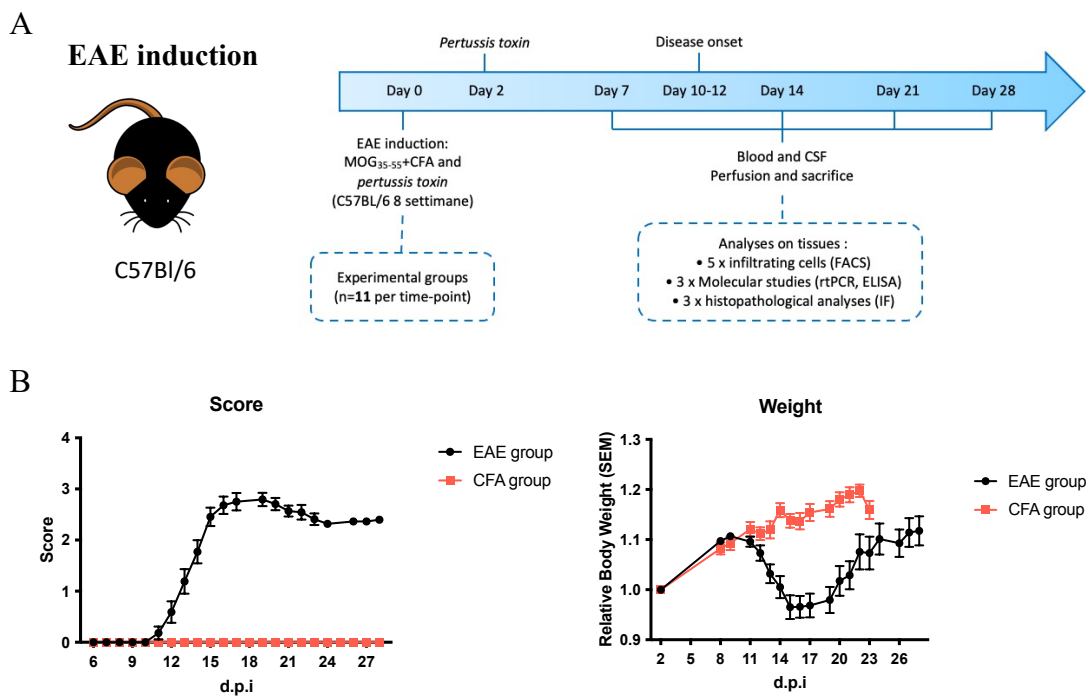


Figure 33. EAE. A) Timeline of EAE groups and sacrifices. B) Score and weight of C57/B16 EAE mice and CFA controls from day 5 to day 28 d.p.i. n=44 mice, 11 mice per group.

Using flow cytometry, I analyzed the expression of PD-L2 and PD-L1 on different immune populations of infiltrating cells in the CNS (neutrophils and monocytes) or resident cells (microglia cells) (Table 8). I detected CD11b⁺Ly6g⁺ neutrophils infiltrating

in the CNS. A significant percentage of these neutrophils (up to 30%) expressed PD-L2. Ly6g⁺PD-L2⁺ neutrophils increased after the onset of symptoms, peaking in the CNS at 14 d.p.i when inflammation was maximum. As the disease entered the remission phase, the number of PD-L2⁺ neutrophils decreased, returning to physiological percentages at 28 d.p.i. (Figure 35A).

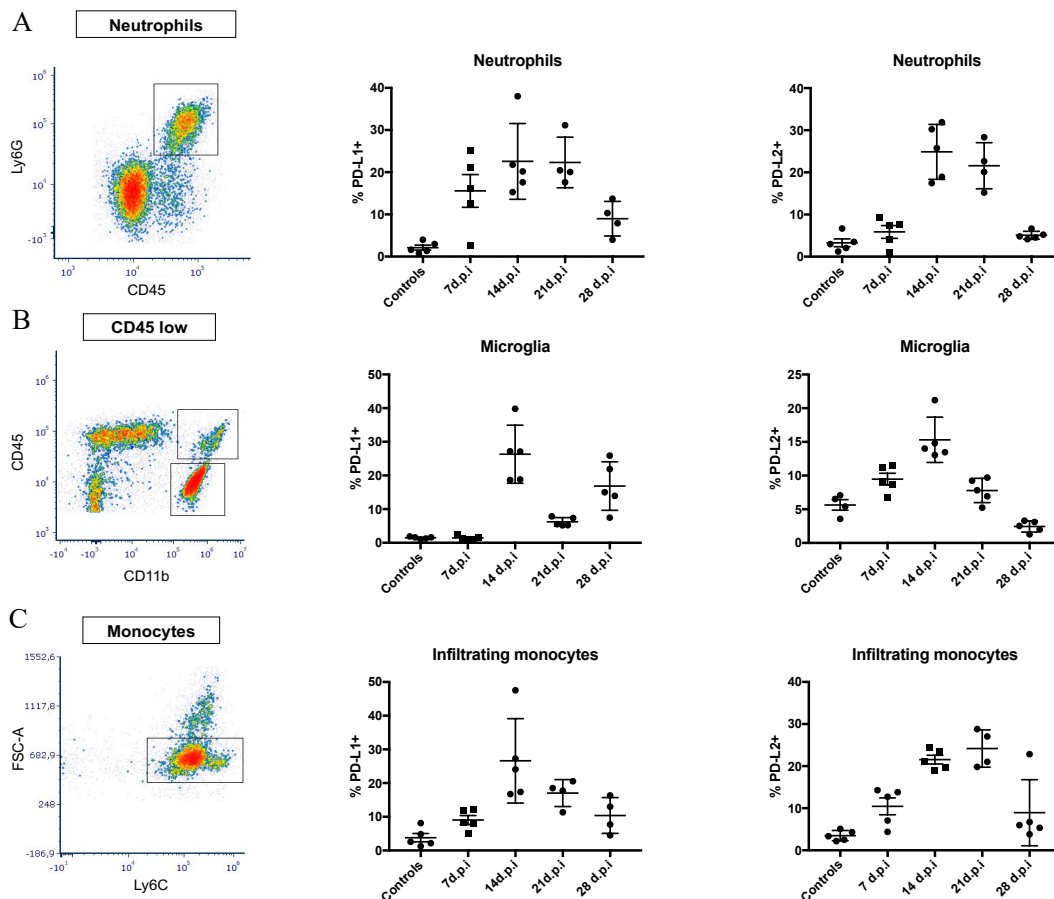


Figure 34. Infiltrating and resident cells in the CNS expressing PD-L1 or PD-L2 in EAE. Representative staining and percentages of PD-L1⁺ and PD-L2⁺ cells at different time points of the disease. A) Neutrophils were identified as CD45⁺ Ly6G⁺ cells. B) Microglial cells were identified as CD45^{low} CD11b⁺ cells. C) Monocytes were identified as Ly6C⁺. The analysis was made using FCS Express Software (De Novo Software). n=5 mice per timepoint.

Next, we analyzed the presence of PD-L2⁺ (and PD-L1⁺) neutrophils in other lymphoid compartments. In both the spleen and lymph nodes, PD-L2⁺ neutrophils showed delayed kinetics, increasing in number at 21 d.p.i. (Fig. 36).

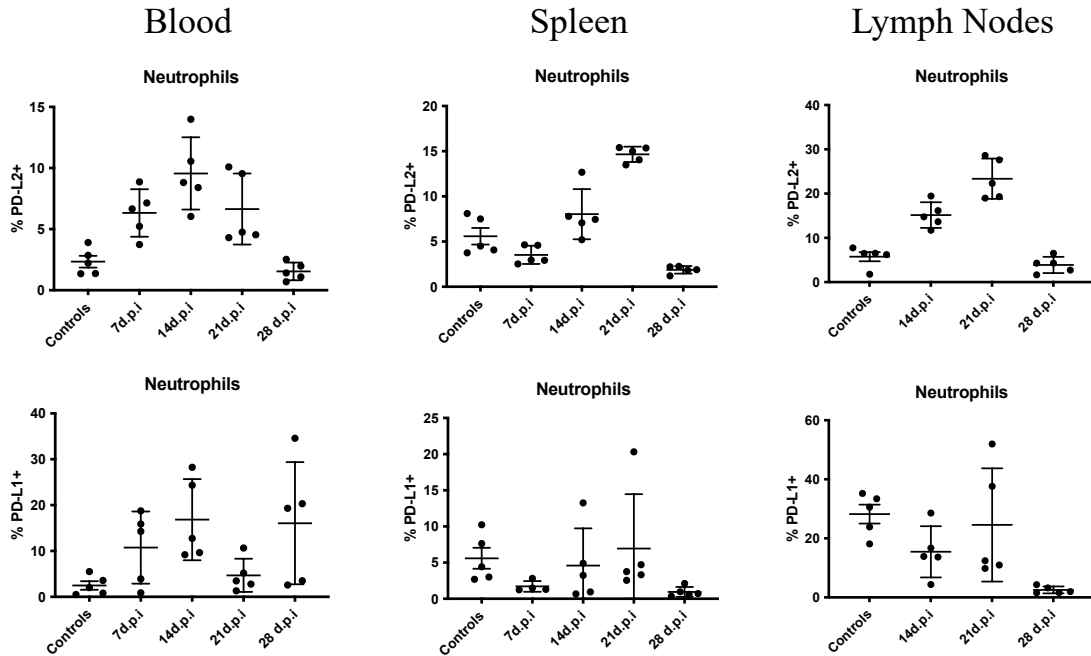


Figure 35. PD-L2 and PD-L1 neutrophils in blood and lymphoid organs. Samples from blood, spleen and lymph nodes were stained and analyzed using flow cytometry at 7, 14, 21 and 28 d.p.i in EAE mice, as well as in the CFA control group. The percentage of expression of both PD-L2 (upper graphs) and PD-L1 (lower graphs) were quantified on Ly6g⁺ neutrophils. The analysis was made using FCS Express Software (De Novo Software). n=5 mice per timepoint.

This led us to consider that this subpopulation of neutrophils is recruited to the CNS in the initial phase of the disease and then released into circulation as inflammation resolves. Fluorescence microscopy confirmed the presence of Ly6g⁺PD-L2⁺ cells in spinal cord sections of EAE mice at 14 d.p.i. Interestingly, Ly6g⁺PD-L2⁺ neutrophils were localized in the proximity of the meninges and blood vessels and were usually found in small groups, in accordance with the behavior of already described regulatory leukocytes in the CNS (Fig. 37C). This phenomenon of migrating in groups is well known for neutrophils and it is called *collective swarming*⁸¹.

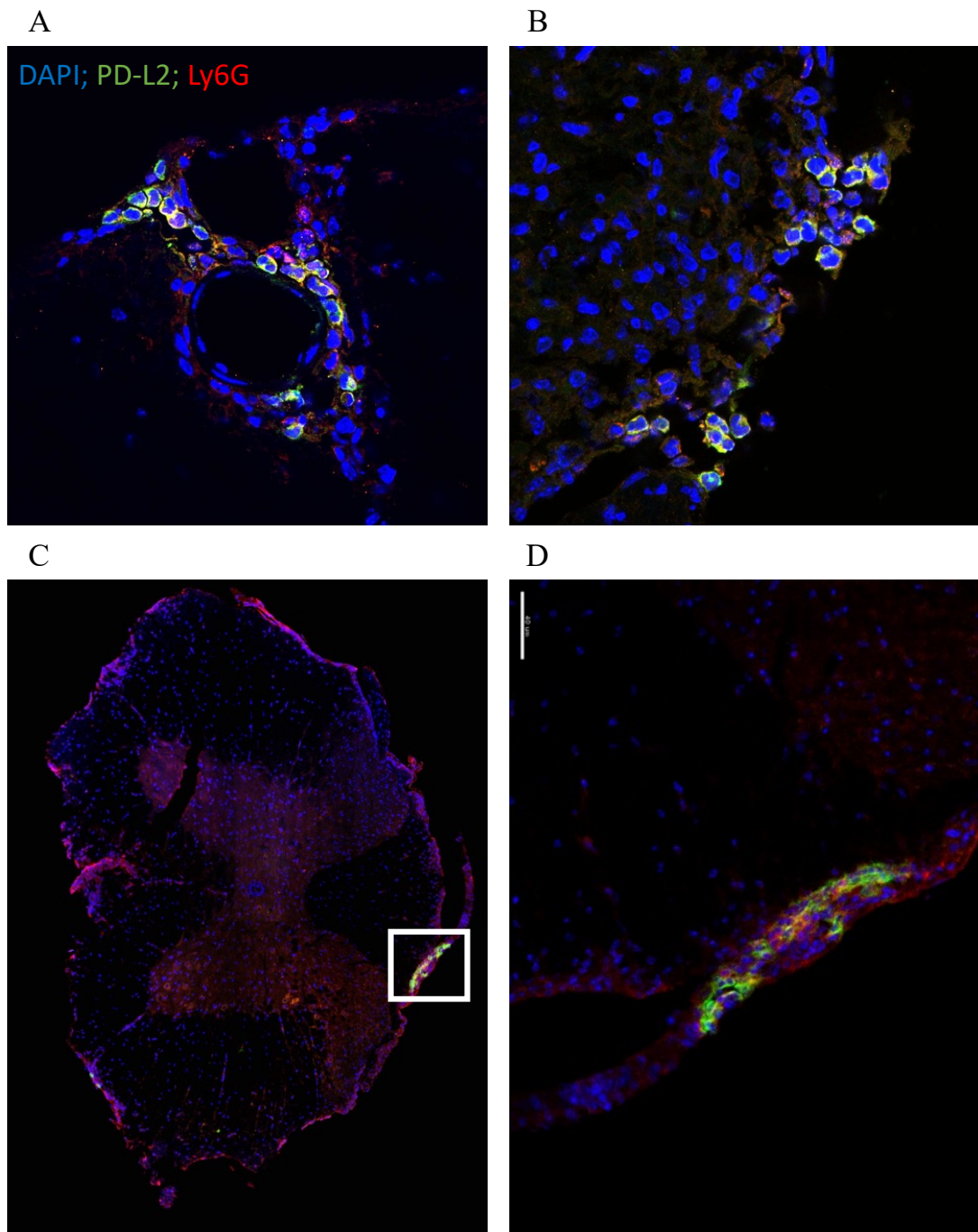


Figure 36. Representative images of PD-L2 neutrophils infiltrating the CNS of EAE mice at 14 d.p.i. 15 μ M-thick SC slices. Ly6G (red) identifies neutrophils, PD-L2 (green) and HOECHST (blue). A-B) Images acquired with a confocal Sp5 Leica microscope at 63X magnification. C) Sections acquired with confocal MAVIG microscope at 40X magnification. D) Zoom-in of image C, Small group of PD-L2 neutrophils localized in the meninges of the spinal cord. n=3 mice per timepoint.

II.I.II CXCR2 seems to be fundamental for the recruitment of PD-L2⁺ neutrophils

EAE is characterized by a specific intrinsic inflammatory program in the CNS. This assumption was confirmed by the increased levels of inflammatory cytokines, such as IFN- γ , IL-1 β , IL-6, measured by qPCR after the onset of the disease (14 d.p.i). Next, we measured the mRNA levels of SELP and ICAM, typical adhesion molecules expressed by endothelial cells, and CXCL1, CXCL2, CXCL10 neutrophil-recruiting chemokines. All these chemokines were significantly increased at 14 d.p.i in the spinal cord, confirming the major recruitment of leukocytes, and in particular neutrophils, in the days after the onset of symptoms (Fig 38).

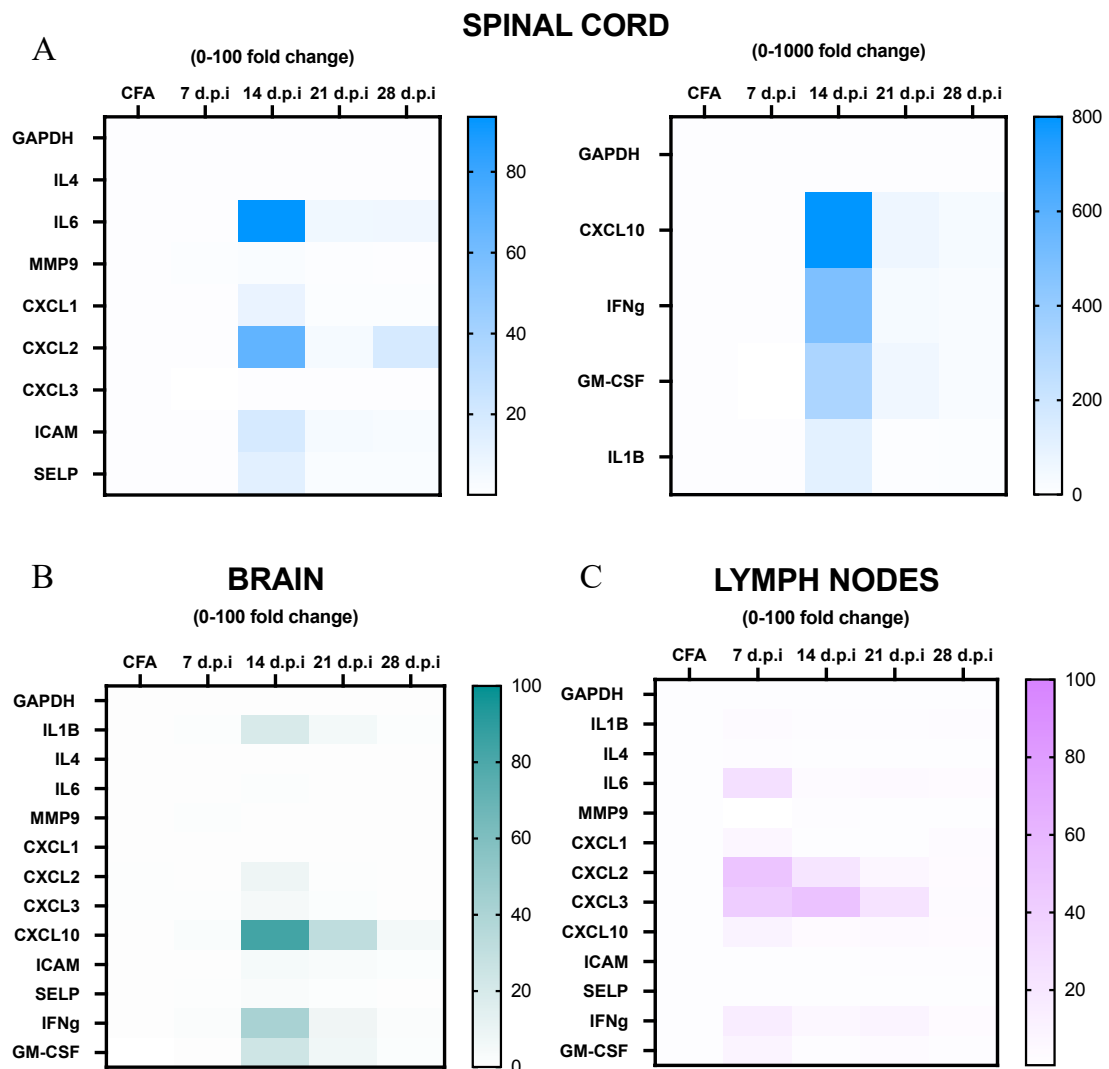


Figure 37. Heatmaps of transcript expression in brains, spinal cords, and lymph nodes in EAE mice at different time points. RT-PCR were performed on tissues isolated from EAE mice and CFA controls at different timepoints. A) Spinal cord. Transcripts were divided by the fold change

0-100 or 0-1000 to improve the visualization of each gene. B) Brain. C) Lymph Nodes. $n=3$ mice per timepoint.

This led us to investigate whether $\text{Ly6g}^+\text{PD-L2}^+$ neutrophils were preferentially recruited to the CNS through CXCR2. To test this, we measured CXCR2 fluorescence in $\text{CD11b}^+\text{Ly6g}^+$ cells by flow cytometry in both blood and cells infiltrating the CNS (Table 9). The fluorescence intensity of CXCR2 on PD-L2^+ neutrophils in the blood was remarkably higher than that on PD-L2^- cells, suggesting that $\text{Ly6g}^+\text{PD-L2}^+$ neutrophils are preferentially recruited to the CNS after the onset of the disease (Fig 39).

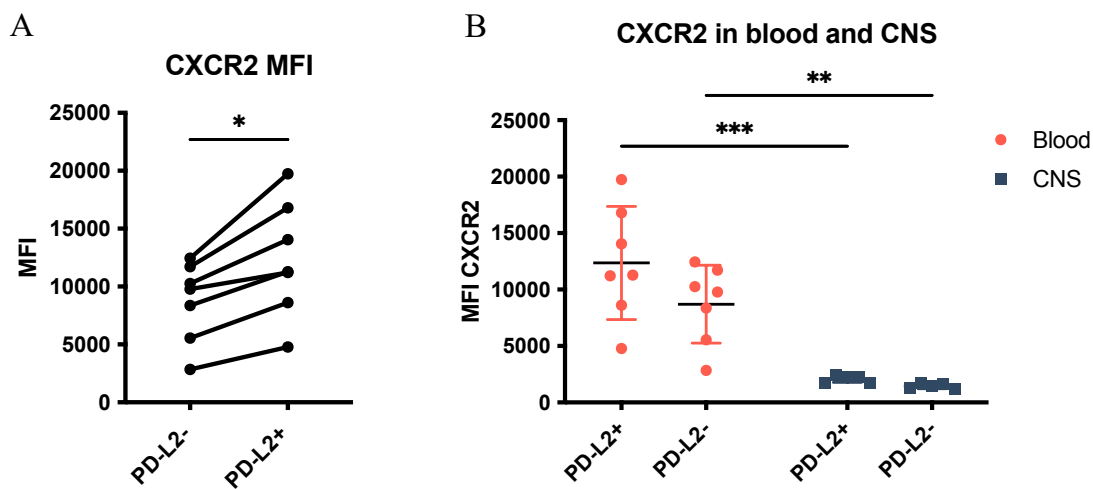


Figure 38. PD-L2⁺ neutrophils in the CNS and circulating in the blood. A) Quantification of the MFI of CXCR2 in $\text{Ly6g}^+\text{PD-L2}^+$ and $\text{Ly6g}^+\text{PD-L2}^-$ neutrophils isolated from blood of EAE mice at 14 d.p.i. B) Comparison of the CXCR2 expression on $\text{Ly6g}^+\text{PD-L2}^+$ and $\text{Ly6g}^+\text{PD-L2}^-$ neutrophils in the blood at 14 d.p.i. (red dots) and infiltrating neutrophils the CNS at 21 d.p.i. (grey squares). The analysis was made using FCS Express Software (De Novo Software). $n=7$ mice for blood isolation and $n=5$ mice for infiltrating cells in the CNS. Statistical analysis: Wilcoxon test. * $p < 0.05$; ** $p < 0.01$; *** $p < 0.001$.

II.I.III PD-L2 expression cannot be induced in murine neutrophils after ex vivo stimulation

To verify whether murine neutrophils could express PD-L2 ex vivo after stimulation, we stimulated neutrophils isolated from the bone marrow with the same cytokines used in humans such as IL-4, GM-CSF and IFN- γ . If this were the case, it would have been very helpful in studying the role of PD-L2^+ neutrophils during EAE. If PD-L2^+

neutrophils were protective during the disease, we could have studied their function with a passive transfer of stimulated neutrophils in mice with EAE. Unfortunately, mouse neutrophils did not significantly upregulate PD-L2 in any of the stimulation tested (Figure 40).

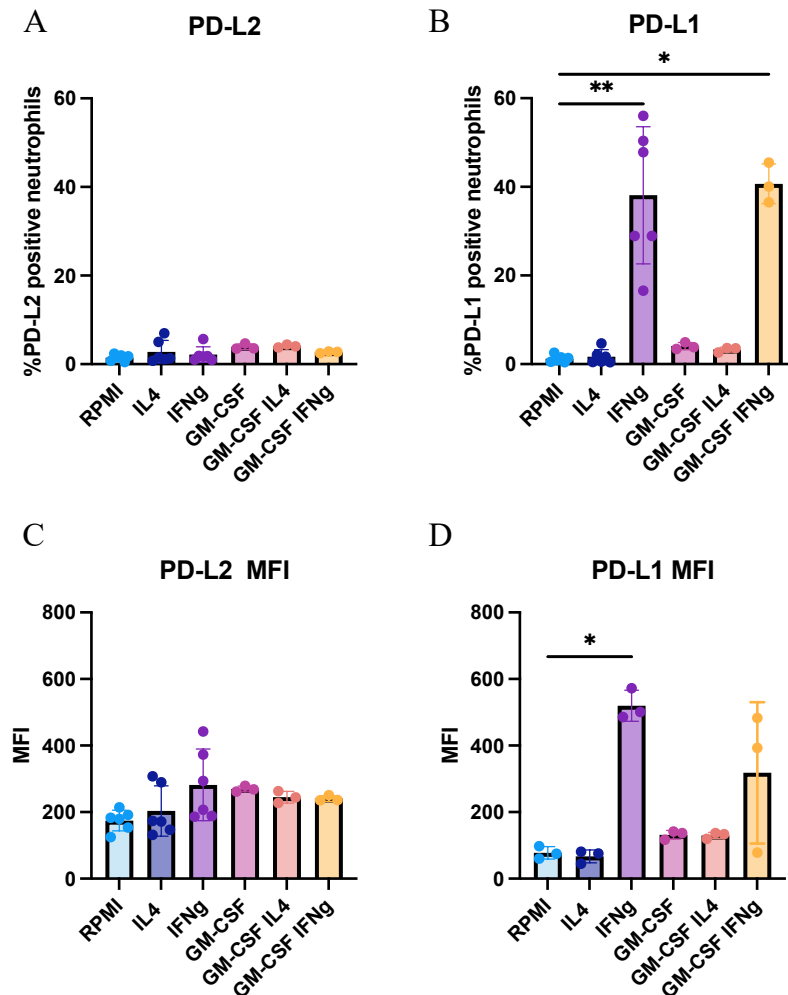


Figure 39. Ex vivo stimulation of mouse neutrophils. Neutrophils were isolated from the bone marrow of healthy mice, stimulated ex vivo overnight with different cytokines, stained and analyzed using flow cytometry. A-B) Percentages of Ly6g⁺ neutrophils expressing PD-L2 (A) or PD-L1 (B) after overnight stimulation. C-D) MFI quantification of PD-L2 and PD-L1 in Ly6g⁺ neutrophils. The analysis was made using FCS Express Software (De Novo Software). Statistical analysis: Kruskal-Wallis test. * $p < 0.05$; ** $p < 0.01$; *** $p < 0.001$.

II.I.IV DT toxicity

Thus, we decided to use transgenic mice model to deplete PD-L2⁺ Ly6g neutrophils. Since DT administration was fundamental for depleting cells in the models we aimed to use, we first had to test its toxicity in concomitance with MOG immunization. Some contradictory data have been published in the literature regarding the toxicity of DT in EAE^{173,174}. To assess whether in the MOG₃₅₋₅₅ EAE model the administration of DT for 3 days was lethal to the mice, we induced the disease and performed three i.p. injections of DT at 7, 10 and 13 d.p.i. (Figure 41). We didn't consider earlier timepoints since PD-L2 neutrophils are absent till after 7 dpi. We then weighed the mice and estimated their clinical score every day for approximately 28 days and compared them to the clinical scores of a previous EAE performed in the lab on C57/Bl6 mice ("EAE old" in the graph). DT did not result in toxicity in mice in terms of weight reduction or in terms of increasing clinical scores.

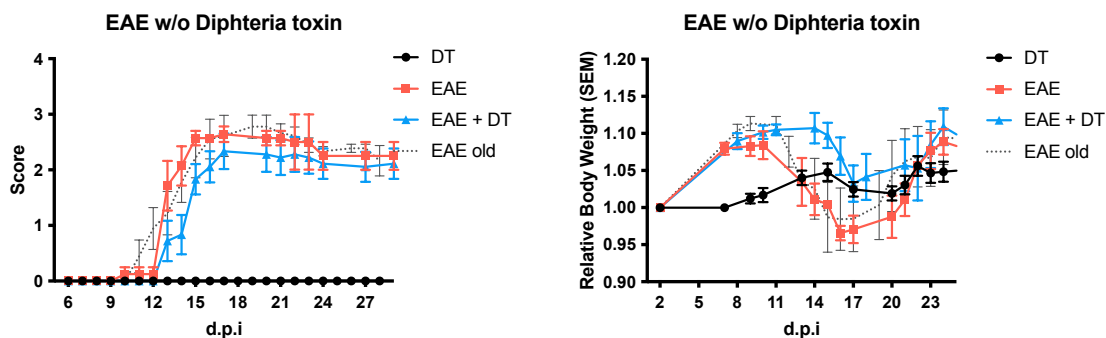


Figure 40. EAE course with or without DT administration. DT was administered through i.p. injections on days 7, 10 and 13 after disease induction. Mice were weighed and their clinical scores were checked daily for approximately four weeks. DT: mice treated with DT at day 7,10 and 13 without immunization; EAE: control EAE; EAE + DT: mice with EAE and 3 i.p. injections of DT at day 7, 10 and 13; EAE old: previous EAE performed in the lab on C57/Bl6 mice.

II.II Mouse Results – Transgenic mouse models

II.II.1 PZTD mouse model

In the PZTD mouse model, as described in detail in the Methods section, a human diphtheria toxin receptor (DTR) gene was inserted into a duplicated exon of the gene coding for PD-L2 (*Pdcd1lg2*). First, I set the PCR protocol for genotyping using our in-house reagents and verified that the mice that were sent to us were homozygous for the knocked-in mutation. The data published in literature were confirmed by performing peritoneal washout on heterozygous mice¹⁷³ and analyzing the isolated cells using flow cytometry. PD-L2 is expressed in physiological conditions on a specific population of B cells found in the peritoneum ($CD45^+$, $B220^+$ $CD3^-$) (Figure 42).

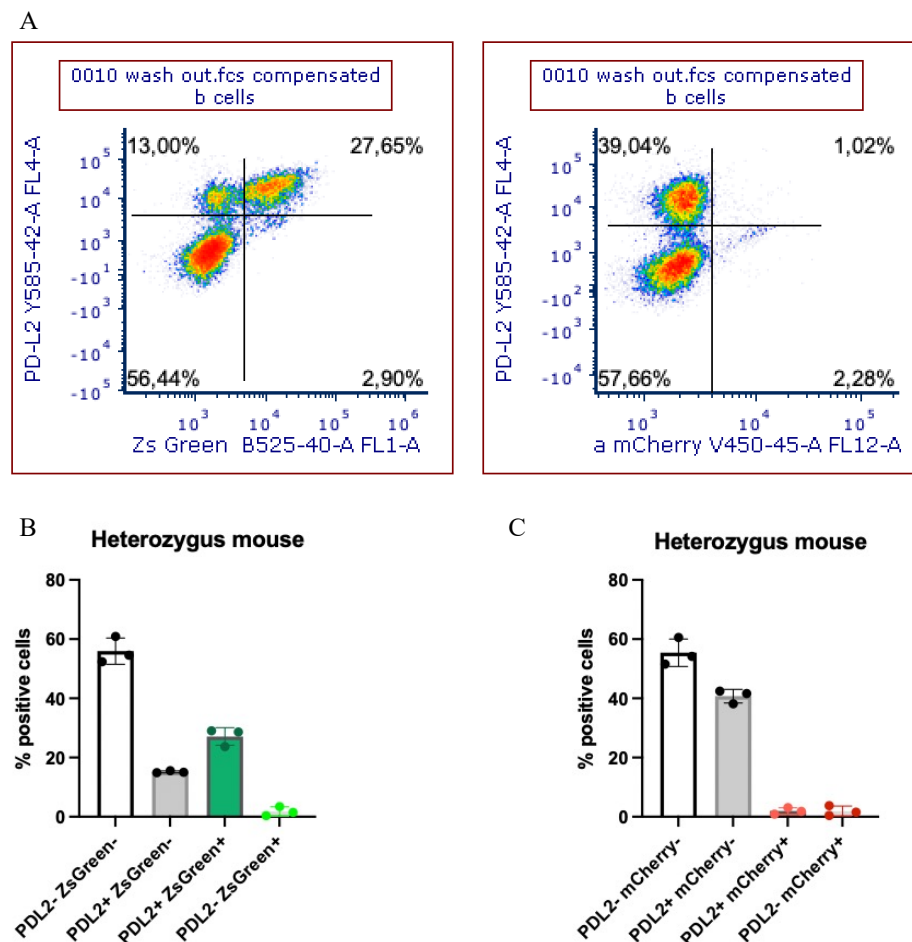


Figure 41. Peritoneal washout of PZTD heterozygous mice. The cells were isolated from the peritoneum of PZTD-heterozygous mice (F1) and stained for flow cytometric analysis. A) Representative gating strategy of the PD-L2/ZsGreen signal on the left and the PD-L2/mCherry

signal on the right. B-C) Quantification of the percentage of cells in the four quadrants in A. The analysis was made using FCS Express Software (De Novo Software). $n=3$ mice.

We then induced EAE in PZTD homozygous and heterozygous mice, males and females, to confirm that they were susceptible to the disease and that the clinical scores were comparable with those of WT controls. We measured the clinical scores and weighed the mice for 28 days (Figure 43).

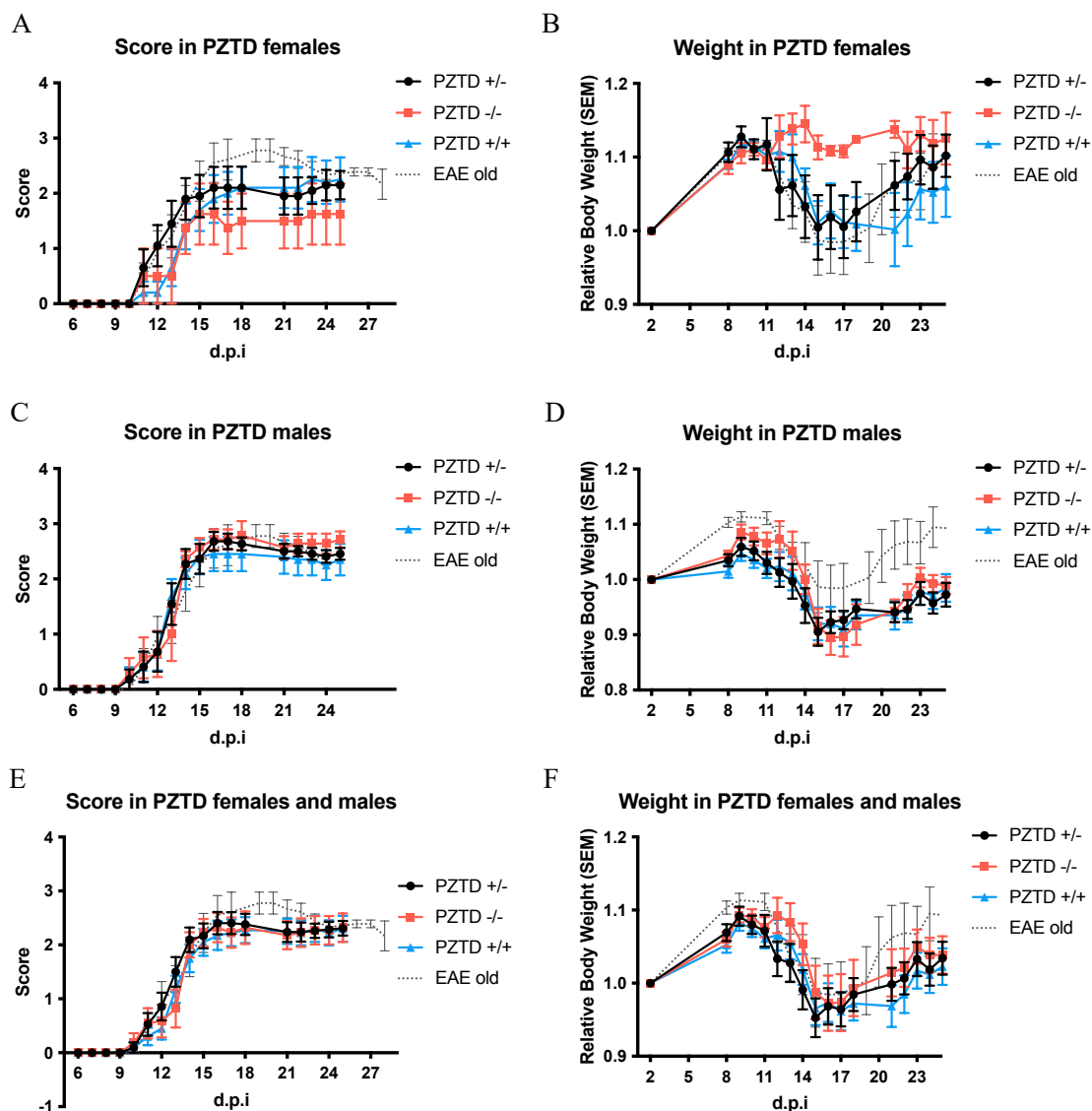


Figure 42. EAE in PZTD transgenic mice. Clinical score and weight were measured daily from day 0 to day 28. A-B) Female mice. C-D) Male mice. E-F) female and male mice plotted together. $n=8$ mice per group. $n=8$ mice per group.

To confirm that the expression of PD-L2 was consistent with that observed in WT mice, I analyzed the expression of the ZsGreen in infiltrating and resident cells of the CNS in a small sample (n=3) of PZTD^{+/-} mice at 14 d.p.i. (Figure 44, Table 11). Zs green was visible on microglia, neutrophils, monocytes, and lymphocytes, although the expression on neutrophils was slightly lower than the one observed in the WT mice. This might be because we analyzed samples from heterozygous mice and not from PZTD homozygous mice. Moreover, the percentage of infiltrating neutrophils in this experiment was slightly lower than the one observed in the WT experiment, maybe due to a milder disease.

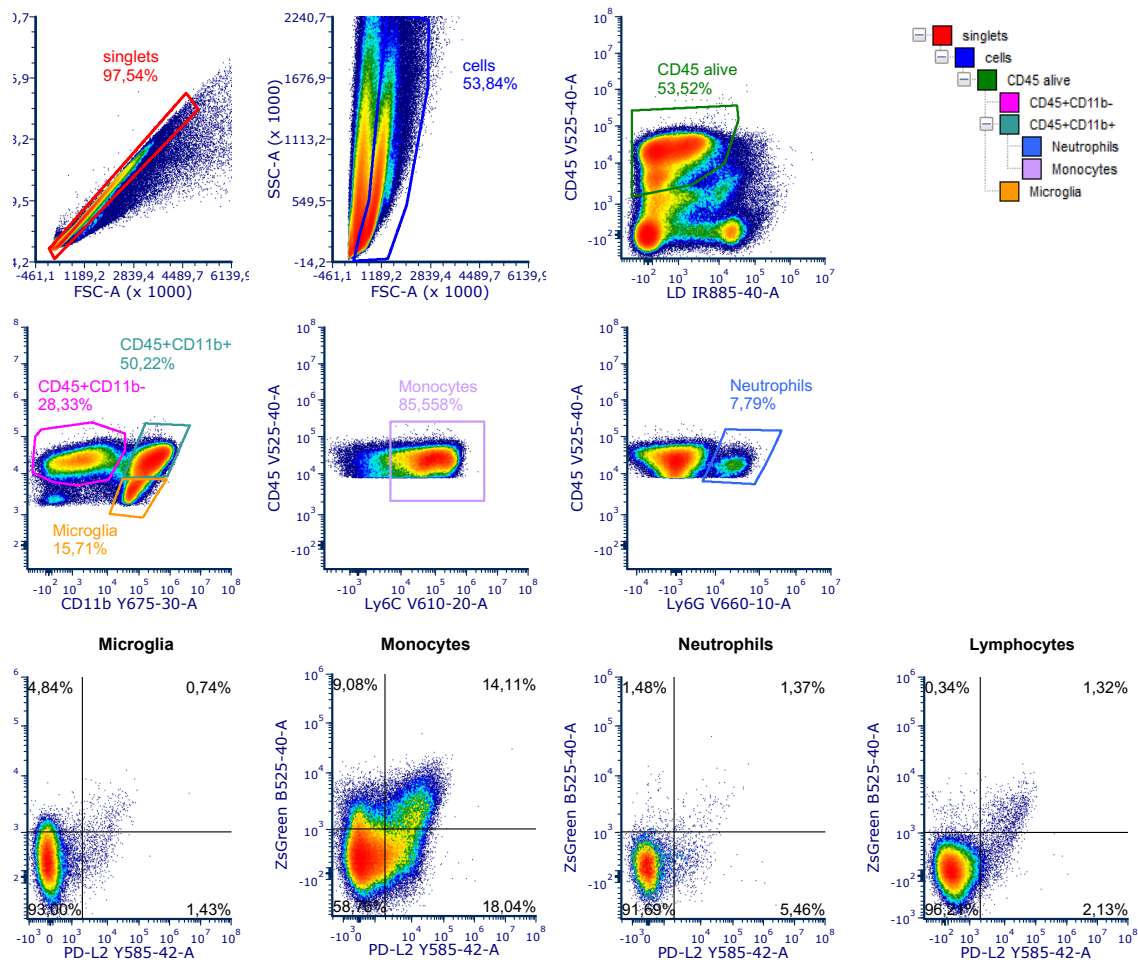


Figure 43. Gating strategy of immune cells in the CNS of PZTD mice with EAE. CNS infiltrating cells were isolated from the brain and the SC of PZTD^{+/-} mice with EAE at 14 d.p.i. (n=3). Samples were then stained and analyzed using multiparametric flow cytometry. Representative gating strategy used to quantify PD-L2 and Zs-green expression on different subpopulation of infiltrating or resident cells of the CNS. The analysis was made using FCS Express Software (De Novo Software). n=5 mice.

I then confirmed the same observations using IHC. I observed the colocalization of the ZsGreen signal with markers for different cell populations. PD-L2/ZsGreen was visible in neurons, microglia, and neutrophils (Fig. 45), but not in CD3+ cells.

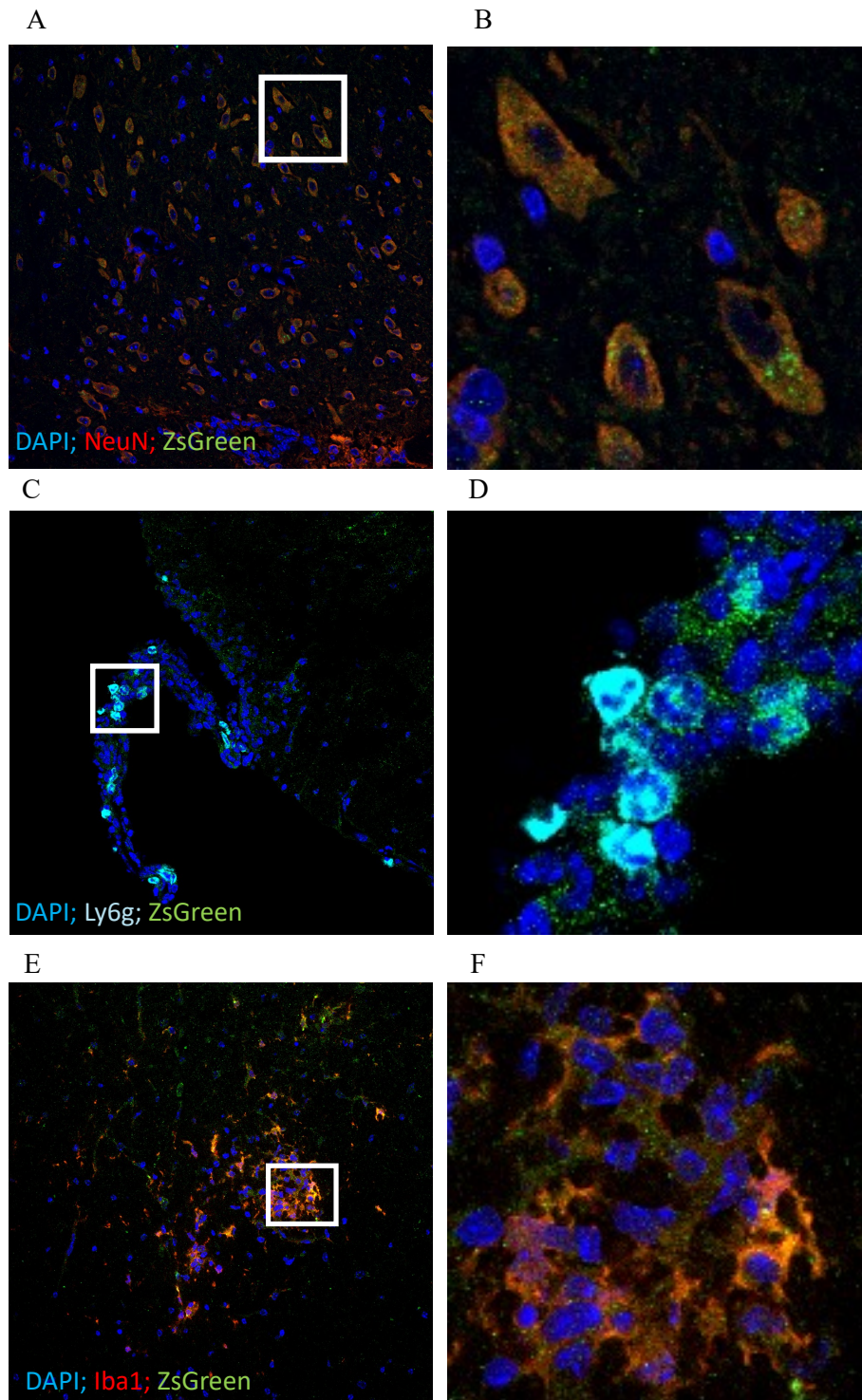


Figure 44. Co-localization of ZsGreen with different cell population markers in PZTD mice with EAE at 14 d.p.i. 15 μM-thick SC slices. HOECHST (blue) stains all the nuclei. A-B)

Colocalization of Zs Green with neurons, as identified by NeuN (red). C-D) Colocalization of Zs Green with neutrophils, identified by Ly6G (cyan); E-F) Colocalization of Zs Green with microglia, identified by Iba1 (red).

II.II.II Catchup mouse model (CRE specific for Ly6G locus)

In the “Catchup” mouse model, the Cre recombinase and the fluorescent protein tdTomato are expressed in the Ly6G locus, thus strongly restricted to neutrophils¹⁷⁵. First, I analyzed blood samples from wild-type, heterozygous and homozygous Catchup mice to assess TdTomato reporter expression in neutrophils (Figure 46).

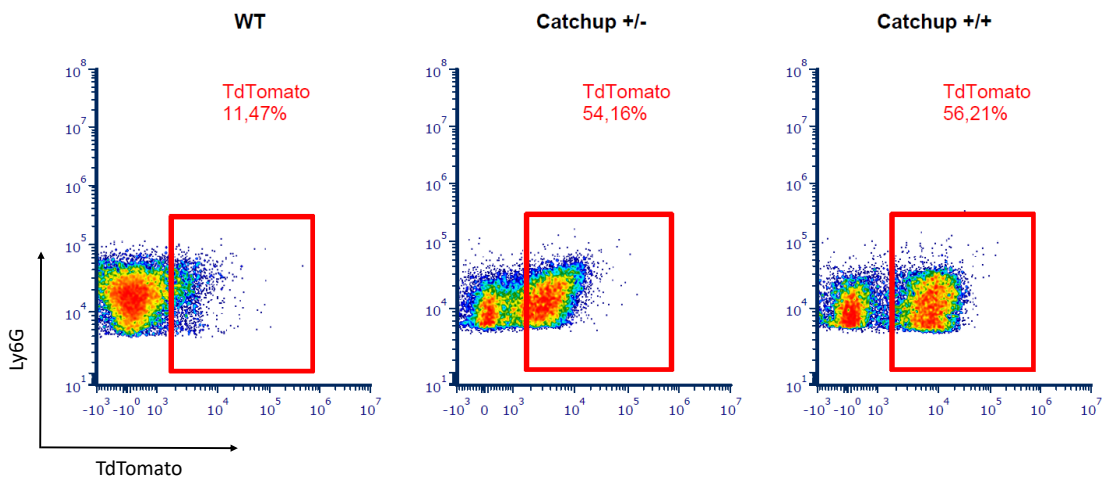


Figure 45. Blood analysis of Catchup mice. TD Tomato expression was measured on $CD45^+CD3^-B220^-CD11b^+Ly6g^+$ cells on samples from a WT mouse, a heterozygous Catchup mouse and a homozygous Catchup mouse. The analysis was made using FCS Express Software (De Novo Software). $n=3$ mice.

I then induced the EAE in Catchup homozygous and heterozygous mice, both males and females, to confirm that they were susceptible to the disease and that the clinical scores were comparable with those of WT controls. We measured the clinical score and weighted the mice for 28 days. However, the homozygous group of females had a significantly milder disease.

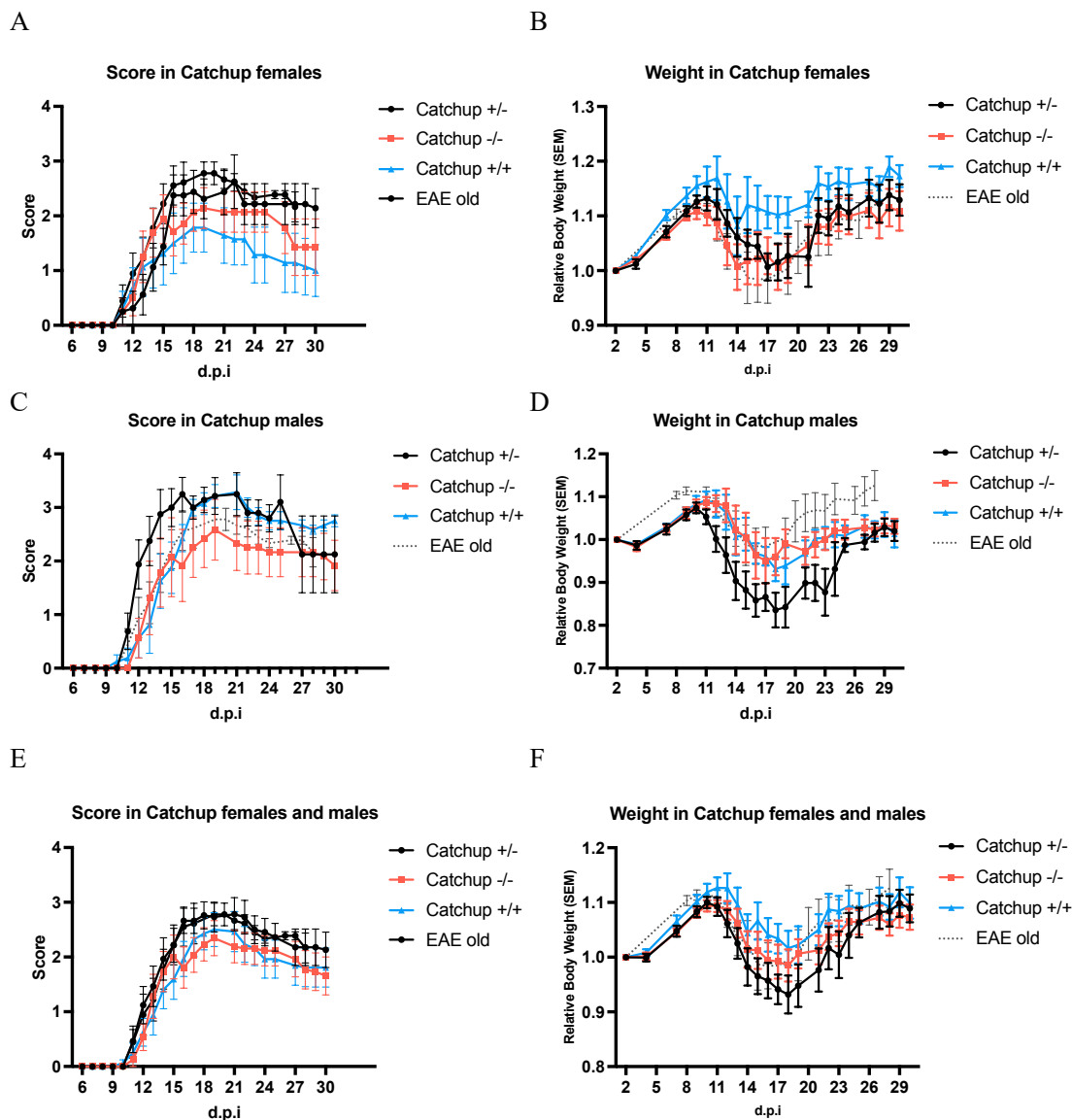


Figure 46. EAE in Catchup mice. Clinical score and weight were measured daily from day 0 to day 28. A-B) Female mice. C-D) Male mice. E-F) female and male mice plotted together. $n=8$ mice per group. $n=8$ mice per group.

Then, I confirmed the same observation through immune histochemistry (IHC). I observed infiltrating neutrophils in the SC of mice with EAE at 14 d.p.i. The reporter protein TdTomato was visible alone or with a primary antibody against mCherry or RFP (which have already been used in the literature to recognize and amplify the TdTomato reporter expression), as shown in figure 48. As expected, the endogenous Ly6g signal was overlapping with the TdTomato signal (not shown).

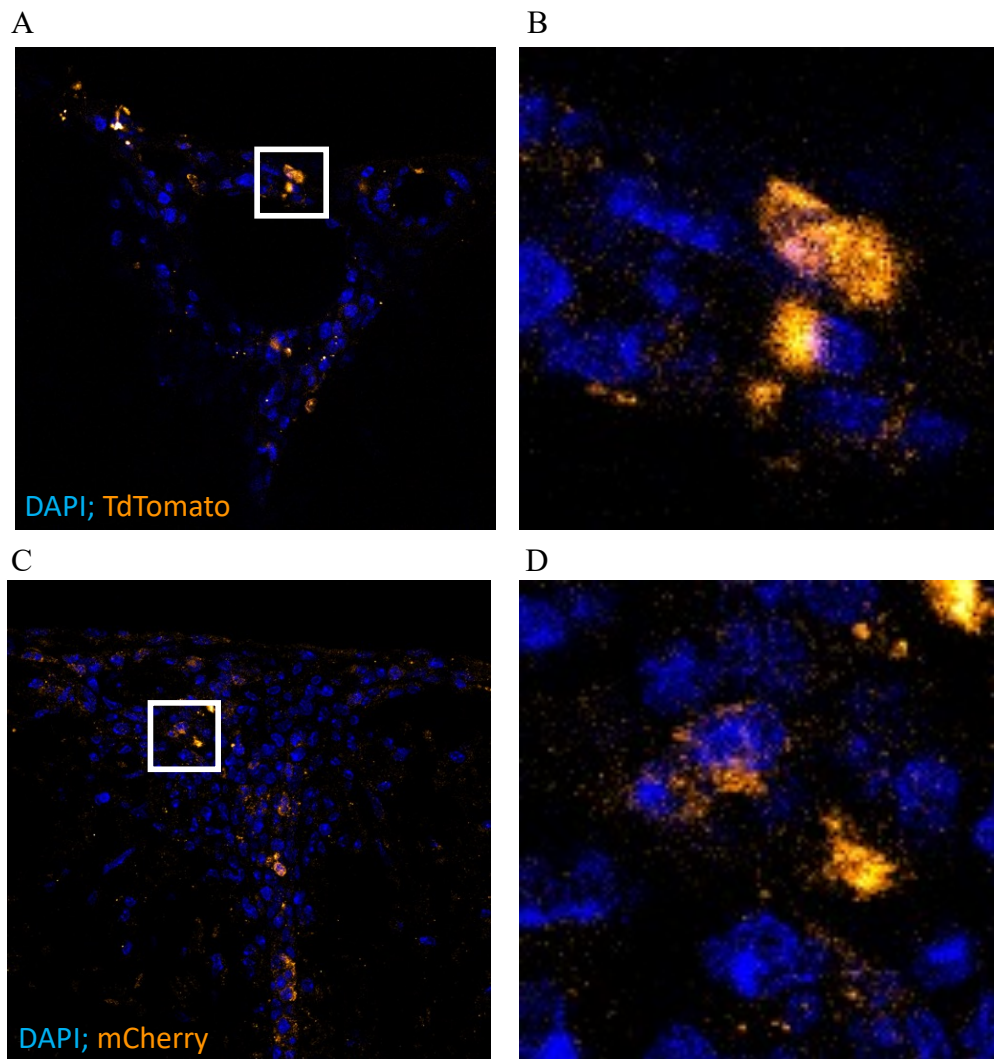


Figure 47. Infiltrating neutrophils in Catchup mice with EAE at 14 d.p.i. 15 μ M-thick SC slices. Hoechst (blue) stains all the nuclei. A-B) Representative image and zoomed-in of the TdTomato reporter signal without amplifying antibodies in infiltrating cells. C-D) Representative image and zoomed-in of mCherry antibody against TdTomato amplified by a secondary antibody in 546. Images were acquired using a Leica Sp8 confocal microscope at 40X magnification.

II.II.III Depletion of PD-L2⁺ myeloid cells (LysM⁺) during EAE

Considering that the Catchup mice were never used in EAE, and that the homozygous female group had a significantly milder disease compared to the wt and the heterozygous ones, we switched to a different CRE recombinase mouse model, LysM-CRE. This latter model was suggested by an expert in EAE on transgenic mice models, Prof. Ari Waisman,

for the purpose of this thesis. This model is commonly used to study the contribution of neutrophils and myeloid cells in general during EAE and in other diseases. LysM is widely expressed in innate myeloid cells, namely neutrophils and infiltrating monocytes, and in small percentages in neurons and microglia. Of course, in this case, the observed effect might not only be attributed to the depletion of PD-L2⁺ neutrophils, but also to other cells expressing both PD-L2 and LysM.

We crossed and genotyped mice to obtain the following experimental groups:

- PZTD^{+/+} LysM-CRE^{-/-} 10 males and 10 females
- PZTD^{+/+} LysM-CRE^{+/-} 10 males and 10 females
- PZTD^{+/+} LysM-CRE^{+/+} 10 males and 10 females

In each group, five mice were intraperitoneally injected with DT (25ng/mice) every three days starting from day 7 after the induction of disease (as summarized in Figure 49A) to deplete PD-L2⁺ LysM⁺ cells. Once again, DT should not be toxic or influence the course of disease in mice that do not have the LysM-CRE knock-in allele (PZTD^{+/+} LysM-CRE^{-/-}). At the same time, mice that did have the knock-in, but were not treated with DT, should undergo a normal disease course. Clinical scores and weights were measured daily by an operator blinded to genotype and treatment. The mice were sacrificed on day 16 d.p.i., when significant differences in the clinical scores between the groups were observed. Mice were then perfused with 4% PFA and their brains and SCs were collected for histological analyses to confirm clinical observations (the latter analyses are still ongoing and will not be part of this thesis).

Mice that were depleted of PD-L2⁺ myeloid cells (PZTD^{+/+} LysM-CRE^{+/+} and PZTD^{+/+} LysM-CRE^{+/-} mice injected with DT) had worse disease and an increased incidence of EAE (Figure 49 B-C). In females, 100% of depleted mice developed the disease 16 d.p.i., compared to approximately 60% of control mice. The difference between depleted and control mice was less evident in males. In fact, most of the mice from both groups developed the disease on day 16 d.p.i.. I analyzed the clinical scores of depleted and control mice of both sexes (Figure 49 D-F) and found that the clinical score was significantly worse in mice depleted of PD-L2⁺ LysM⁺ cells. We then divided the mice by genotype to test whether DT was toxic or influenced their scores (Figure 49 E-G). DT injections had no effect on PZTD^{+/+} LysM-CRE^{-/-} female mice (Figure 49 E, grey curve), compared to the other groups that had the LysM-CRE knock-in. However, contrary to

what was expected, the PZTD^{+/+} LysM-CRE^{-/-} male group treated with DT showed a disease worse than the ones of the heterozygous group (Figure 84 G).

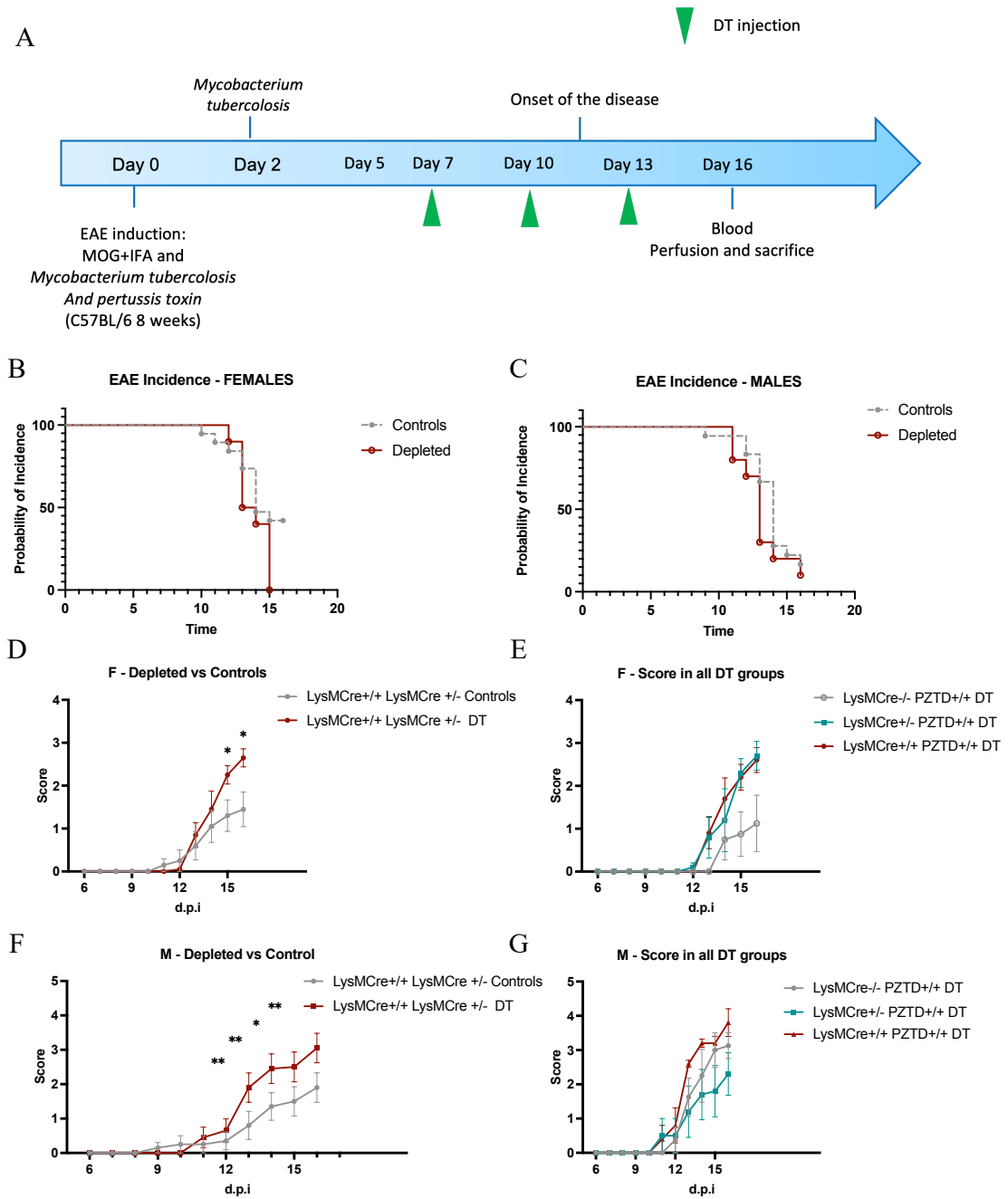


Figure 48. EAE in PZTD x LysM mice. A) Timeline of EAE induction and DT injections (green triangles). B-C) Incidence curves in depleted vs control mice in B) females and C) males. D-G) Clinical scores measured daily from day 0 to day 16 by an operator blinded to treatment and genotype. D-E) Female mice divided by depletion (D) or divided by genotype in all groups treated with DT (E). F-G) Female mice divided by depletion (F) or divided by genotype in all groups treated with DT (G). $n=10$ mice per sex per genotype, of which 5 treated with DT. $n=10$ mice per

*genotype group per sex. Statistical analysis: 2way ANOVA test. * $p < 0.05$; ** $p < 0.01$; *** $p < 0.001$.*

The results observed here cannot be traced back to PD-L2⁺ neutrophils, but the contribution of other myeloid cells expressing LysM (monocytes, macrophages and microglia) must be taken into consideration. Moreover, further studies are necessary to verify whether the effect on the clinical score observed in depleted mice is due to an actual depletion of PD-L2⁺ LysM⁺ cells infiltrating the CNS and other lymphoid organs compared to the controls with different genotypes or without DT injections.

Finally, we will repeat the same EAE experiments crossing PZTD mice with the Catchup mouse model, even with its limitations, to assess whether the absence of PD-L2⁺ neutrophils can lead to worsening of the EAE course.

DISCUSSION

In addition to the proinflammatory functions of neutrophils that might contribute to the onset and progression of MS, a few recent studies have revealed the existence of neutrophils with an immunosuppressive and protective role in EAE mice. However, the identification and characterization of neutrophils with regulatory functions in patients with MS are still lacking.

In this study, we analyzed blood samples from neurological patients to determine the expression of immune checkpoints, namely the PD-1 receptor and its ligands, in different leukocyte populations. We detected a subpopulation of neutrophils expressing CD16⁺CD66b⁺PD-L2⁺, which, to the best of our knowledge, had not been described in the literature at that time. As PD-L2 is an immune checkpoint, we wondered whether PD-L2⁺ neutrophils could be a novel population of PMN-MDSCs. A few observations have led us in this direction. First, PD-L2⁺ neutrophils are mature neutrophils with segmented nuclei that are found in the NDL after differential centrifugation, whereas known regulatory neutrophils are often described as immature and have lower granularity⁹⁰. Moreover, PD-L2⁺ neutrophils do not express Lox1 (low-density lipoprotein receptor-1), which was used to distinguish PMN-MDSCs in cancer patients¹⁶⁹. However, PD-L2⁺ neutrophils express other markers that are typically associated with regulatory functions such as CD10, CD124, CD54, and KLF2. For instance, Marini et al. identified CD10 as a marker for distinguishing mature neutrophils with regulatory functions in G-CSF-treated donors⁹⁵. Although there is some functional evidence of PD-1/PD-L interaction in the suppressive function, we still cannot determine whether PD-L2 identifies a new homogeneous population of neutrophils with a specific function or is a new marker that regulatory neutrophils can express. Interestingly, in the last two years at least two more groups have identified this population in different contexts in humans, namely in early pregnancy¹⁶⁰ and gastric cancer patients¹⁶¹.

Our data showed that the PD-L2⁺ neutrophil population was significantly more frequent in blood from patients with MS than in healthy controls. However, our study has some limitations that must be considered. We detected an increase in PD-L2⁺ neutrophils mainly in patients at the first diagnosis of MS or in those without any ongoing treatment. It is likely that both first- and second-line treatments for MS negatively affect the presence and percentage of PD-L2⁺ neutrophils. In this case, the observed role of PD-L2

neutrophils in humans might be limited to the initial phases of the disease and not to the subsequent relapsing phases. Moreover, to confirm that this population was specific to patients with MS and not to those with other autoimmune disorders, we analyzed blood samples from patients with systemic sclerosis. Although patients with SS were not undergoing treatment and most of them were at their first diagnosis, we cannot be sure that it is the best possible control group. SS is an immune-mediated rheumatic disease that does not involve the CNS and whose patients are usually 20 years older than MS patients. Moreover, the presence of PD-L2⁺ neutrophils should be explored in other autoimmune and chronic inflammatory diseases to better understand the specificity of their increase.

We then identified specific cytokines that could induce PD-L2 expression in neutrophils *ex vivo*, starting with blood samples from healthy donors. This *escamotage* helped us to perform subsequent experiments since during the Covid-19 pandemic it was challenging to obtain samples from neurological patients. Moreover, neutrophils are a very delicate cell population, and isolating and sorting neutrophils from patients may alter their activation status and viability, resulting in misleading outcomes. The most effective stimulations were IL-4 and IFN- γ , alone or in combination with GM-CSF. The IL4 stimulation might seem counterintuitive because the serum and CSF levels of patients with MS are usually enriched with pro-inflammatory cytokines (such as IFN- γ) rather than IL-4. However, IL4 has been used to upregulate PD-L2 *in vitro* in other myeloid cell population, such as macrophages and microglia^{125,176}. Although the markers expressed in neutrophils analyzed from the fresh blood of patients are, for the most part, similar to those expressed by stimulated neutrophils from healthy donors, we cannot be sure that these are the same exact population. This may be another major limitation of this study at the present time. Performing RNA bulk sequencing or single-cell RNA sequencing might help overcome this issue, as well as identify the major pathways that are involved in PD-L2⁺ neutrophils biology. We are currently collecting samples for RNA bulk sequencing and will soon be able to answer some of these questions.

We performed phenotypic and functional characterization of PD-L2⁺ neutrophils. When co-cultured with CD3⁺ lymphocytes, PD-L2⁺ neutrophils isolated from patients released anti-inflammatory cytokines such as IL-4 and IL-10 and reduced the production of pro-inflammatory molecules. Since we detected these cytokines in the supernatant of

co-cultures, we cannot be sure that they were released by neutrophils and not by T lymphocytes. Although we confirmed IL4 production in PD-L2⁺ neutrophils with ICS using flow cytometry, these results are still surprising in the neutrophil community. Moreover, cytokines in the supernatant were detectable at very low concentrations. It must be taken into consideration that these results might be a technical artifact and further experiments such as RT-PCR or western blotting, as well as the RNA sequencing mentioned above, might help to clarify this issue.

Moreover, the only functional proof of PD-L2⁺ neutrophil action in humans, is that they can reduce CD4⁺ T cell proliferation and decrease the release of IFN- γ in the supernatant. We also observed a trend of decreasing CD8⁺ T cells proliferation, although this was not statistically significant. Cells infiltrating the CNS do not proliferate *in situ*, suggesting that PD-L2⁺ neutrophils act mainly in secondary lymphoid organs, such as the lymph nodes, rather than in the CNS parenchyma. Contrary to our expectations, we did not observe an alteration in the activation status of CD4⁺ or CD8⁺ T cells. However, it must also be considered that T cells are very likely not the only population that interacts with PD-L2⁺ neutrophils, and the same experiments should be repeated with different cell types such as monocytes, B cells, or CNS resident cell populations.

We established a new protocol for imagining the co-culture of neutrophils and lymphocytes *ex vivo*. We were able to observe the formation of immune conjugates and appreciate the cell-to-cell interactions between neutrophils and lymphocytes. No similar data have been reported in the literature. Interestingly, our preliminary results suggest that neutrophils can interact with more than one lymphocyte at time, with a ratio of 1:3 which has not been previously reported.

We also wondered whether the regulatory action of neutrophils could be mediated by extracellular vesicles carrying PD-L2. PD-L2, however, was not associated to extracellular vesicles. Iodixanol gradient centrifugation of extracellular vesicles isolated from a murine myeloid cell line displayed the PD-L2 signal in the non-vesicular fractions (data not shown). Therefore, considering the shedding mechanism, we analyzed soluble PD-L2 in the blood and CSF of patients with MS to test this hypothesis. Contrary to our expectations, PD-L2 was reduced in both the blood and CSF of patients with MS (especially in those with disease activity) compared to controls. We hypothesized a

consumption mechanism by inflamed tissues, however there is no literature on the biological function of soluble PD-L2 in body fluids in neurological disorders.

Next, we examined the murine counterpart in a preclinical MS model. As expected, PD-L2⁺ neutrophils were visible in small groups near the meninges and blood vessels at the peak of the disease. Cells with regulatory functions are generally found in these locations rather than infiltrating tissues. We hypothesized that PD-L2⁺ neutrophils are preferentially recruited to the CNS because of the increased expression of CXCR2 when circulating in the blood. CXCR2 is a fundamental receptor for the recruitment of immune cells and neutrophils into the CNS during neuroinflammation^{177,178}. Moreover, the percentage of PD-L2⁺ neutrophils among the total neutrophils increased in infiltrating cells in the CNS compared to neutrophils circulating in the blood. However, these assumptions may not be sufficient, and further studies are required to prove that PD-L2⁺ neutrophils are preferentially recruited to the CNS. In this regard, we are about to start collaborating with Prof. Gabriela Constantin to use live intra-vital microscopy on the spinal cord of mice with EAE.

An important difference that we have found between the human and mouse neutrophils, that must be taken into consideration, is that murine neutrophils do not respond to *ex vivo* stimulation. We were unable to identify any cytokines or molecules that could upregulate PD-L2 expression in purified mouse neutrophils. These considerations highlight the fact that the molecular mechanisms leading to the polarization and expression of PD-L2 in neutrophils still require further investigation.

Finally, we aimed to deplete PD-L2⁺ neutrophils in transgenic mice. We were unable to find an available constitutive model for the depletion of PD-L2. The PZTD model (PD-L2 – ZsGreen – TdTomato – DT receptor), which allows the depletion of PD-L2 populations following DT administration, was the only option that we were able to find. Since this model has never been used in the context of EAE, we ensured that the mice were effectively immunized using our EAE protocol. The same was true for the Catchup model (Ly6g-CRE), which has never been published in an EAE study. When we immunized Catchup mice, the homozygous group of females had a significantly milder disease. Following the suggestions of an expert in EAE on transgenic mouse models, Prof. Ari Waisman, we switched to a different CRE recombinase mouse model for the

purpose of this thesis. In this case, using the LysM-CRE model, the observed effect might not only be attributed to the depletion of PD-L2⁺ neutrophils, but also to other cells expressing both PD-L2 and LysM. Another limitation is the use of DT itself. We decided to administer DT three times every three days, starting from day 7. Using this setup, DT was found to be non-toxic to mice and did not interfere with the course of the disease, contrary to the findings of a study in literature¹⁷⁴. However, with this timeline, we cannot be entirely sure that we are effectively depleting all PD-L2⁺ neutrophils, especially considering the high turnover of this leukocyte population.

The final EAE helped in clarifying the relative importance of PD-L2⁺ neutrophils in the context of EAE. We speculated that PD-L2⁺ neutrophils are regulatory and have a protective function. In fact, the depletion of PD-L2⁺ LysM⁺ cells worsened the disease course. This allows us to support the theory that PD-L2⁺ neutrophils are firemen recruited in the CNS to limit and contain ongoing inflammation. However, using the LysM-CRE model the observed effect cannot be traced back to PD-L2⁺ neutrophils, but the contribution of other myeloid cells expressing LysM (monocytes, macrophages, and microglia) must be considered. Of course, these are preliminary results that only allow us to obtain a proof of concept. Further studies are necessary to verify the actual depletion of PD-L2⁺ LysM⁺ cells after DT administration and to confirm that these data are reproducible.

Moreover, we aim to repeat the EAE on PZTD mice crossed with Catchup mice, even considering the milder disease that we observed in homozygous females in the first EAE. The effects that we will observe in this model, if successful, will only be due to PD-L2⁺ neutrophils and not myeloid cells in general.

In summary, our study demonstrates that PD-L2 is a suitable candidate for identifying regulatory neutrophils in both MS and preclinical models. We speculate that a better understanding of PD-L2⁺ neutrophils, could lead to innovative approaches for noninvasive diagnosis and, eventually, new ideas for cell therapies.

In this regard, our work encourages prospective studies aimed at carefully investigating the mechanisms that lead to upregulation of PD-L2 in the peripheral blood of both humans and mice. Moreover, the depletion of PD-L2 neutrophils using genetic mouse paved the way for a better understanding of the functions and the importance of

this population in EAE. Finally, our work adds to the puzzle of a better understanding of the involvement of the PD-1 axis in neuroinflammation, which is still far from finding its final picture.

MATERIALS AND METHODS

I. Human samples

1.1 Whole blood analysis with multiparametric flow cytometry

Blood samples were collected from patients in the neurology department and from healthy controls. Blood samples were collected in ethylenediaminetetraacetic acid (EDTA)-treated tubes via venipuncture and processed within one hour. In-house lysis buffer was used to lyse RBCs for 5 min. All samples were then incubated in Stain Buffer (BD). TruStain FcX Fc receptor blocking reagent (BioLegend) was used for all staining to prevent nonspecific signals. The cells were then labeled with fluorophore-conjugated antibodies for FACS analysis or sorting.

- For multiparametric flow cytometry analyses, the panels of antibodies used for this staining are presented in Tables 2 and 3. All samples were analyzed using a CytoFlex LX cytometer.

- To sort neutrophils, cells were stained for CD45⁺CD16⁺CD66b⁺PD-L2⁺ or PD-L2⁻. Cells were sorted using a FACS Melody Sorter (BD).

This study was approved by the Human Research Ethics Committee of the San Raffaele Hospital. All participants agreed to participate and signed an informed consent form. Disability was determined by a specially trained and certified neurologist using the Expanded Disability Status Scale (EDSS), a 10-point disease severity score derived from nine ratings for individual neurological domains.¹⁷⁹ Cerebral and, in selected cases, spinal MRI scans were performed at the time of diagnosis and at least every six months. Further scans were performed as required.

Human Panel – Immune checkpoint on whole blood				
Antibody	Fluorochrome	Company	Cat number	Dilution
PD-L1	APC	BioLegend	393610	1:50
PD-L2	PE	BioLegend	329606	1:50
CD45	BV510	BioLegend	304036	1:100
CD66b	BB515	BD Biosciences	564679	1:50
CD16	PE-Cy7	Beckman Coulter	6607118	1:50
CD20	BV650	BioLegend	302335	1:100
CD3	BV605	BioLegend	300460	1:100
CD4	BUV495	BD Biosciences	103239	1:100
CD8	APC eFluor 780	Invitrogen	1951528	1:100
CD27	BV421	BD Biosciences	562513	1:30
CD14	BUV395	BD Biosciences	563561	1:50
CD11c	PE/ Cy5	BioLegend	301610	1:100
CD56	APC aFluor 700	Beckman Coulter	B10822	1:100
CD123	BUV737	BD Biosciences	741769	1:50
CD161	PE Dazzle 594	BioLegend	339940	1:50
PD-1	PerCP-Cy5.5	BD Biosciences	561273	1:100

Table 2. Immune checkpoint analysis on whole blood from neurological patients.

Human Panel – Regulatory Markers				
Antigen	Fluorochrome	Company	Cat number	Dilution
CD45	BV510	BioLegend	304036	1:100
CD16	PE-Cy7	Beckman Couture	6607118	1:100
CD66b	BB515	BD Bioscience	564679	1:100
CD10	APC eFluor780	Thermofisher	47-0108-42	1:100
PD-L2	PE	BioLegend	329606	1:50
CD11c	PE-Cy5	BioLegend	301610	1:100
CD62L	BV605	BioLegend	304833	1:100
CD54	PE Dazzle 594	BIolegend	353117	1:100
CD18	AlexaFluor 700	Biolegend	363421	1:200
CD124	BV421	BioLegend	355013	1:100
CXCR4	BV650	BD Bioscience	740599	1:100
CD35	APC	Thermofisher	17-0359-42	1:50
L/D	IR	Backman Coulter	C36628	1:500

Table 3. Regulatory markers in circulating neutrophils on whole blood from patients with MS and healthy donors.

I.II Neutrophils and PBMCs isolation

Peripheral blood mononuclear cells (PBMCs) and neutrophils were isolated by density gradient centrifugation using a Ficoll-Paque Plus (GE Healthcare, USA). PBMCs were harvested from the interface, and neutrophils were obtained from the bottom half of the tube after red blood cell lysis. Cells were used immediately after isolation for characterization and functional experiments. The purity of the isolated cells (>90%) was confirmed using flow cytometry. In some experiments, neutrophils from healthy donors were stimulated with recombinant human GM-CSF (20 ng/ml, R&D Systems, USA), IL-4 (20 ng/ml, PeproTech, USA), or IFN- γ (20ng/ml, R&D Systems, USA) alone or in combinations for 16-18 hours. After stimulation, the cells were harvested for flow cytometry or functional analysis.

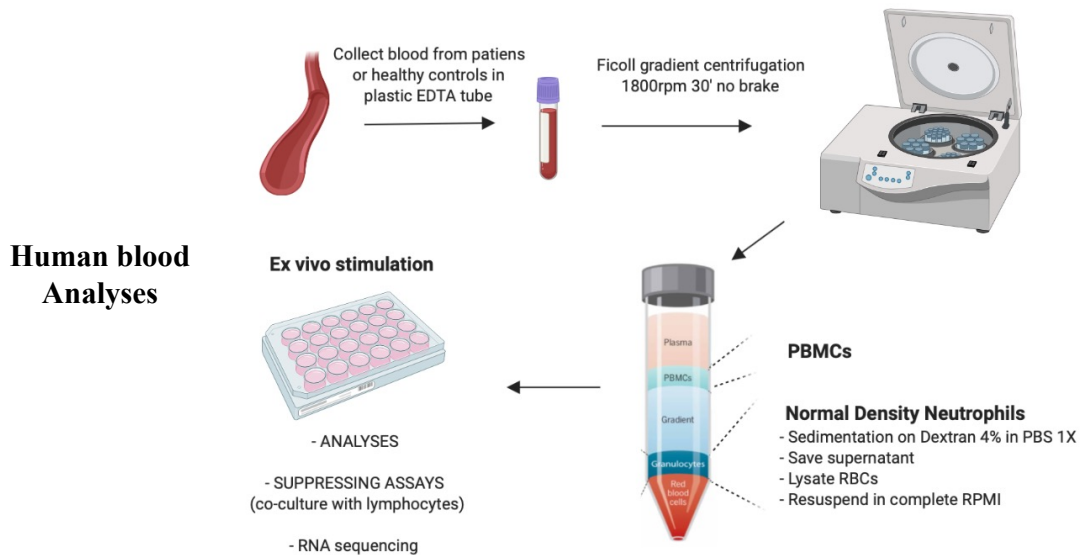


Figure 49. Schematic protocol for the isolation of neutrophils and PBMCs from whole blood.
Made using Biorender.com.

I.III Ex-vivo neutrophil stimulation

Human neutrophils (1×10^6) isolated from the blood of healthy donors were resuspended in RPMI and either treated with one of the following stimulations (20ng/ml or otherwise specified) or left untreated for 16-18 hours at 37°C:

- IL4 (PeproTech #200-04)
- GM-CSF (R&D #215-GM)
- IFN γ (R&D #285-IF)

- IL13 (PeproTech #200-13)
- IL8 (PeproTech, #200-08M-5µg)

To evaluate the plasma membrane expression of PD-L2 or PD-L1, cells were washed and resuspended with TruStain FcX Fc receptor blocking reagent (BioLegend), to prevent nonspecific staining signals. The cells were then labeled with fluorophore-conjugated antibodies diluted in Stain Buffer (BD). A table of antibodies used for this staining is presented in Table 4.

Human Panel – Ex vivo neutrophil stimulation				
Antigen	Fluorochrome	Company	Cat number	Dilution
CD45	BV510	BioLegend	304036	1:100
CD16	PE-Cy7	Beckman Couture	6607118	1:100
CD66b	BB515	BD Bioscience	564679	1:100
PD-L2	PE	BioLegend	329606	1:50
PD-L1	BV605	BioLegend	329723	1:100
L/D	IR	Backman Coulter	C36628	1:500

Table 4. Panel used for the quantification of PD-L2 and PD-L1 expression on neutrophils after overnight ex vivo stimulation.

I.IV CyTOF Mass Spectrometry analysis

• **Panel design and heavy-metal conjugation of antibodies** | For the characterization of neutrophils by single-cell mass cytometry (CyTOF), we designed a panel of 36 antibodies (Suppl. Tab 03). Most antibodies were pre-conjugated from Fluidigm®. Targets were allocated to specific heavy-metal isotopes based on the sensitivity of the mass cytometer (e.g., placing lower abundance targets on higher sensitivity channels), and to avoid problems with potential spectral overlap, as outlined previously¹⁸⁰. Where needed, in-house conjugations were performed using the MIBItag conjugation kit (IonPath®), following the latest published protocol (Cust-0001_C). Each antibody clone and lot were titrated to optimal staining concentrations using human PBMCs from healthy volunteers, with all appropriate positive and negative controls.

• **Mass-tag cellular barcoding** | Mass-tag cellular barcoding was performed using six different CD-labeled CD45 antibodies from Fluidigm®. Briefly, after 18h of incubation with the appropriate stimuli, 2×10^6 cells from each condition were washed with 10ml of

RPMI +10%FBS and centrifuged at 250g for 10 min. Cells were resuspended in residual volume (50:1) (PBS with 0.5% BSA and 0.02% NaN₃), and 5:1 of TruStain FcX™ antibodies (BioLegend) were added to each sample for 10 min at RT to block Fc receptors. Without washing, the cells were stained with distinct combinations of stable Cd-labeled CD45 antibodies for 30' at 4' and washed twice with 5ml of MaxPar Cell Staining Buffer. Samples from any given biological replicate were then barcoded together. After data collection, each condition was deconvoluted using a single-cell debarcoding algorithm¹⁸¹.

• **Mass cytometry staining and measurement** | Surface marker antibodies were then added to the composite sample, yielding a final reaction volume of 200 µl, and stained for 30 min at RT with gentle vortexing after 15 min. Following staining, cells were washed 2 times with MaxPar cell staining buffer, and cisplatin viability stain was used before fixation of samples with 1.6% PFA for 10 min at RT and permeabilized with ice-cold absolute methanol for 10 min on ice. Cells were then washed twice in MaxPar cell staining buffer to remove the remaining methanol and stained with intracellular antibodies in 200 µl for one hour at RT with gentle vortexing every 15'. Cells were washed twice in cell staining medium and then stained with 1mL of 1.25nM 191/193Ir DNA intercalator (Fluidigm®) diluted in PBS with 4% PFA overnight. Cells were then washed twice with cell staining medium and twice with Cell Acquisition Solution (Fluidigm®). Mass cytometry samples were diluted in Cell Acquisition Solution containing bead standards (Fluidigm®) to approximately 0.56cells per mL and then analyzed on a Helios mass cytometer (Fluidigm®) equilibrated with Cell Acquisition Solution. We analyzed 1-5x10⁵cells per condition, which is consistent with generally accepted practices in the field.

• **Mass cytometry bead standard data normalization and analysis** | Mass cytometry data were normalized and debarcoded using the Fluidigm CyTOF software version 6.7. The composite sample was manually gated using FlowJo software (Tree Star, Inc.) to exclude normalization beads, cell debris, and dead cells. Only CD45⁺ CD11b⁺ CD66b⁺ (PMN) cells were used for downstream analysis. All analyses of the CyTOF data were performed after arcsinh (with cofactor=5) transformation of marker expression. Clustering, data visualization and dimension reduction (UMAP, Uniform Manifold Approximation and Projection for Dimension Reduction), were performed using the

CyTOF workflow package [PMID: 28663787].

Human Panel - CyTOF		
Surface Markers	Metal	Availability
CD45	89Y	HIM Kit
TREM2	106Cd	Purified
Lyve-1	110Cd	Purified
MSR1	111Cd	Purified
CD206	112Cd	Purified
Siglec-1	114Cd	Purified
CD115	116Cd	Purified
CCR2	139La	Purified
CCR6	141Pr	HIM Kit
CD11a (LFA-1)	142Nd	Order Fluidigm
II-3R	143Nd	Order Fluidigm
CD163	145Nd	Order Fluidigm
CD124	146Nd	Purified
CXCR2	147Sm	Order Fluidigm
CD16	148Nd	HIM Kit
PD-L2	149Sm	Purified
CD15	150Nd	Purified
CD14	151Eu	Order Fluidigm
CD13	152Sm	Order Fluidigm
CD62L	153Eu	Order Fluidigm
CD3	154Sm	HIM Kit
CD10	155Gd	Purified
PD-L1/CD274	156Gd	Order Fluidigm
CD11c	159Tb	Order Fluidigm
CD54	160Gd	Purified
CD33	161Dy	Purified
CD66b	162Dy	HIM Kit
CXCR3	163Dy	HIM Kit
CD161	164Dy	HIM Kit
CD24	166Er	HIM Kit
CCR7	167Er	HIM Kit
CD8	168Er	HIM Kit
CD32	169Tm	Order Fluidigm
CTLA-4/CD152	170Er	Order Fluidigm
CD20	171Yb	HIM Kit
CX ₃ CR1	172Yb	Order Fluidigm
HLA-DR	173Yb	HIM Kit
CD4	174Yb	HIM Kit
CXCR4	175Lu	Order Fluidigm
CD56	176Yb	HIM Kit
CD11b	209Bi	Order Fluidigm

Table 5. CyTOF antibody panel used for the characterization of PD-L2⁺ neutrophils

I.V Cell proliferation assay

PBMCs and neutrophils from healthy donors were isolated as described in Section *I. II of Material and Methods*. 1×10^6 Neutrophils were left unstimulated or stimulated with recombinant human GM-CSF (20 ng/ml, R&D Systems, USA), IL-4 (20 ng/ml, PeproTech, USA), or IFN γ (20ng/ml, R&D Systems, USA) alone or in combinations for 16-18 hours at 37°C. After stimulation, neutrophils were washed, resuspended in RPMI supplemented with 10%FBS and plated in a MW96 U bottom plate at a concentration of $50 \times 10^3/50\mu\text{l}$ or $100 \times 10^3/50\mu\text{l}$. PBMCs were resuspended at up $10 \times 10^6/\text{ml}$ in PBS and stained with 1 $\mu\text{L}/\text{ml}$ of Violet CellTracer™ stock solution (stock solution 5mM, final working solution 5 μM) to analyze lymphocyte proliferation. Cells were incubated for 20 min at 37°C and then washed with the medium to remove any free dye remaining in the solution. Stained PBMCs were activated with $\alpha\text{CD3}/\text{CD28}$ (1 $\mu\text{g}/\text{mL}$ αCD3 , 2 $\mu\text{g}/\text{mL}$ αCD28) and co-cultured 1:1 or 1:2 with neutrophils previously stimulated in a U-bottom 96-well plate at 37°C. Blocking studies were performed with 2,5 mg/mL $\alpha\text{PD-1}$ (CD279, GenScript #A01828-40) that was present throughout the incubation.

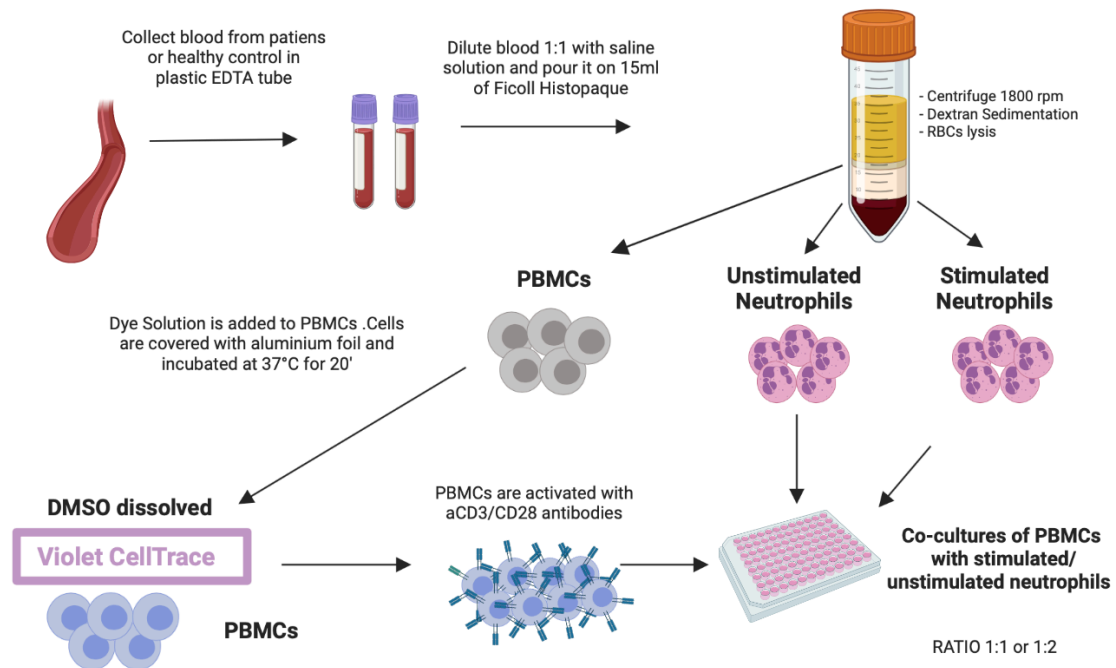


Figure 50. Schematic protocol used for cell proliferation assay. Made using Biorender.com.

After 3,5 days, 100 µl of supernatant from each well were stored at -80°C for cytokines analysis, while lymphocyte proliferation was assessed by dye dilution on a Cytoflex LX cytometer (Table 6) and analyzed using FCS express 7 flow (version 7.12.0007).

Human Panel – Cell Proliferation Assay				
Antigen	Fluorochrome	Company	Cat number	Dilution
CD45	BV510	BioLegend	304036	1:100
CD3	BV605	BioLegend	300460	1:100
CD4	BUV495	BD Biosciences	103239	1:100
CD8	APC eFluor 780	Invitrogen	1951528	1:100
CD69	PE	BD Pharmigen	555531	1:100
PD-1	PerCP-Cy5.5	BD Biosciences	561273	1:100
Live/Dead	IR	Backman Coulter	C36628	1:250

Table 6. Panel of antibodies used to quantify the cell proliferation after 3,5 days of co-cultures of lymphocytes with neutrophils.

I.VI Bioplex and ELISA

Supernatants from co-cultures were analyzed using a Bio-Plex multiplex cytokine assay (Bio-Rad Laboratories) or ELISA (HUMAN Duo Set ELISA R&D, IFN- γ #DY285B; PD-L2 #DY1224) for single proteins, according to the manufacturer's instructions. Concentrations were calculated according to a standard curve generated for the specific target and expressed as picograms/milliliters. The molecules examined included: IL-1 β , IL-2, IL-4, IL-10 and IL-12p70 using Bioplex and IL-4 and PD-L2 using ELISA.

I.VI May-Grünwald Giemsa Staining on neutrophils

May-Grünwald Giemsa Staining is a commonly used method for staining blood smears. Like other histological methods, it is based on electrostatic interactions between the dye and target molecules. The staining solutions contain methylene blue (a basic dye), related azures (also basic dyes) and eosin (acid dye). The nuclei of white blood cells and the granules of basophil granulocytes appear blue (stained with basic dyes), while red blood cells and eosinophil granules appear red (because of red color of eosin). The cytoplasm of white blood cells is light blue because of the low concentration of the RNA molecules.

Blood samples were collected from the patients or healthy donors in EDTA plastic tubes. Samples were lysaed and processed for two-channel sorting. Samples were stained for CD45+ CD16+ CD66b+ PD-L2+/- . Sorted cells were centrifuged at 6000 rpm and resuspended in 80µl of MACS Buffer. Cells were cytocentrifuged on slides using Cytospin at 800 rpm for 5 min (slow acceleration). The slides were then dried at room temperature for 15 min. Samples were then stained for 5 min with May-Grünwald stain diluted with an equal volume of distilled water. Slides were quickly washed with distilled water and placed for 15 minutes into Giemsa stain diluted with 9 volumes of distilled water. Finally, the slides were washed with distilled water, dried and observed under a light microscope. Images were acquired at 40X or 100X magnification using the Leica LasX software.

I.VII Immunofluorescence

Neutrophils were isolated as described above and plated in MW24 dishes with or without stimulation for 18hours. As for May-Grünwald Giemsa Staining, blood cells were cytocentrifuged on slides with Cytospin at 800 rpm for 5 min (slow acceleration) and slides were dried at room temperature for 15 min. Slides were then fixed with 4% paraformaldehyde in PBS at room temperature for 10 min and washed three times in PBS. Cells were blocked in *BLOCKING SOLUTION*: 5% normal goat serum (NGS, Sigma) or donkey serum (DKS, Sigma) depending on the secondary antibody, 0.02% saponin and 1% BSA in PBS. The primary antibodies were diluted in blocking solution and incubated overnight at 4°C. The cells were washed three times with PBS. The secondary antibodies were prepared in blocking solution and incubated for one hour at room temperature. Samples were incubated with Hoechst 33342 (Sigma) for nuclei counterstaining. The glasses were mounted on coverslip with DAKO or Prolong Gold (Invitrogen). Images were acquired using confocal microscopy LEICA Sp5 or Sp8 equipped with an HCX PL APO lambda blue 63.0x1.40 OIL UV objective. Stacks (1024X1024) were post-processed to generate maximal projections of Z-stacks (acquired with a 0.3 µm step or a 2 µm step).

Secondary antibodies used for all of the immunofluorescences are AlexaFluor
Invitrogen (1:1000):

- Goat or Donkey α Rabbit Alexa 488/546/633

- Goat or Donkey α Rat Alexa 488/546/647

I.VIII Lymphocytes/Neutrophils conjugates

Human neutrophils and PBMCs were isolated from the blood of healthy donors as described above (Material and Methods, I.III and I.IV). Neutrophils were plated in a MW24 in RPMI medium supplemented with 10% FBS and stimulated for 18 hours with IL4 (20 ng/ml) as described above. Lymphocytes were plated in a MW96 and activated overnight with α CD3/CD28 stimulation. The next day, neutrophils and lymphocytes were gently mixed together and plated on a glass (previously coated for at least 2 hours with poly-Lysine-L, 0,2 mg/ml) in a ratio 2:1, namely 10×10^3 neutrophils and 50×10^3 lymphocytes for each condition. The droplet was limited using a PAP pen for immunostaining. After 2-3 hours of co-culture at 37°C, cells were delicately fixed with 4% PFA for 8'. After the fixation, we proceed with the normal IF protocol described in paragraph IX.

IF - Primary Antibodies for human leukocytes				
Antibody	Host Specie	Company	Cat number	Dilution
CD16	Rabbit	ABCAM	AB183354	1:100
CD3	Rat	BioRad	mca1477	1:100
MPO	Mouse	ABCAM	AB25989	1:100
PD-L2 (CD273)	Rabbit	Invitrogen	PA5-20344	1:500
PD-L1 (CD274)	Rat	Invitrogen	14-5982-82	

Table 7. Primary antibodies used for IF on human leukocytes.

II. Mouse samples

II.1 EAE induction

EAE was induced in 8-10-week-old C57Bl/6 wild type mice by active immunization with an emulsion of myelin oligodendrocyte glycoprotein peptide 35-55 (MOG₃₅₋₅₅) in Complete Freund's adjuvant(CFA), followed by intravenous administration of pertussis toxin (500 ng) twice (at days 0 and 2) as previously described⁶⁸. A group of 11 mice was sacrificed every 7 days for each time point (7, 14, 21, and 24 d.p.i.) to study the kinetics of neutrophils during the disease. As controls, animals received the same treatment as EAE mice without the immunogen, MOG peptide, including complete CFA and Pertussis toxin (referred to as 'CFA'). Animals were scored daily by an operator blinded to treatment for clinical symptoms of EAE on a 0–5 scale⁶⁸ described in Figure 52.

Score	Clinical signs	Comments
0	No clinical signs	Normal mouse
0.5	Partially loss of tail tonus	Normal gait. Half of the tail or more has lost tonus. Absence of curling at the tip of the tail when mouse is handled
1	Paralyzed tail	Normal gait. Complete flaccidity of the tail
2	Moderate hind limb paraparesis	Hind limb weakness: Waddling gait; the posture of the hind legs when the mouse is placed at the edge of the cage is not adequate and it falls easily
2.5	Severe hind limb paraparesis	Severe hind limb weakness: Marked difficulty to right after placing on back
3	Partial hind limb paralysis	Inability to right within 5 s after placing on back. The mouse is unable to turn around. Dragging one hind limb
3.5	Hind limb paralysis	Dragging both hind limbs
4	Hind limb paralysis plus partial front leg paralysis	It has some mobility in one of the forelimbs
4.5	Tetraplegia, moribund	No movement
5	Death	

Figure 51. Clinical scores used to evaluate EAE. Giralt M., et al., *Myelin*. 2018. 227-232.

Every effort was made to minimize the number of animals used and their suffering. All procedures involving animals were performed in accordance with the animal protocol guidelines prescribed by the Institutional Animal Care and Use Committee (IACUC 1151) at the San Raffaele Scientific Institute (Milan, Italy).

II.II Intracardiac perfusion

First, the mice were anaesthetized by intraperitoneal injection of avertin (300 mg/kg). The mice were then placed with the abdomen facing up and secured on the four paws as wide as possible on surgical support. The skin was grabbed with forceps at the level of the diaphragm, thus by cutting through the ribs the heart was easily accessible. The right atrium was then cut, and a butterfly needle was placed into the left ventricle. A peristaltic pump with up to 0.5 ml/min flow allowed 25 ml of 1X saline solution with EDTA to flow through mouse systemic circulation to wash away all blood. Here, fresh brains and SCs were isolated for immune cell infiltration assessment using flow cytometry. For staining of tissue sections, perfusion continued to replace the buffer solution with approximately 25 ml/mice of cold 4% PFA fixative solution. The organs were carefully excised and maintained in ice-cold 4% PFA solution overnight (O/N) at 4°C. The day after, the organs were rinsed with 1X PBS for one hour at RT and then transferred to 30% sucrose solution until they sank. Sucrose was used to cryoprotect and prevent freezing artefacts and loss of tissue architecture. Organs were included in a cryo-embedding matrix such as OCT (CDK Italia) and stored at -80°C.

II.III Multiparametric analysis of mouse tissues by flow cytometry

Flow cytometry was performed on mouse blood, lymph nodes, CNS, and peritoneal cavity lavage cells. Blood samples were collected from the orbital sinuses. Ack Lysing Buffer (Gibco) was used to lyse the RBCs for 10 min. Axillary and inguinal lymph nodes and spleens were isolated from the mice and placed in ice-cold RPMI. To prepare single-cell suspensions from the spleens and lymph nodes, tissues were minced using sterile 70- μ m cell strainers. Spleen samples were then lysed with 2 ml of Ack Lysing Buffer for 2 min. Extracted brain and spinal cord tissues were incubated for 30 min with 0.4 mg/mL type IV collagenase (Sigma-Aldrich) and dissociated using a 19G syringe to obtain a homogeneous cell suspension. Finally, CNS cells were enriched using a Percoll gradient as previously described¹⁸². This was followed by centrifugation at 18000rpm for 30 min at 4°C. The myelin layer was removed, and the cell pellet was filtered and washed. Peritoneal cavity cells were isolated after peritoneal lavage with 10 ml of PBS1X. All samples were resuspended and counted. TruStain FcX Fc receptor blocking reagent (BioLegend) was used to prevent nonspecific staining signals. The cells were then labeled with fluorophore-conjugated antibodies diluted in Stain Buffer (BD).

Mouse Panel – EAE				
Antigen	Fluorochrome	Company	Cat number	Titer
CD3	FITC	BD Bioscience	555274	1:100
Trem2	PerCP	R&D System	FAB17291C	1:100
PD-1	PE-Cy7	BioLegend	135216	1:100
PD-L2	PE	BioLegend	107206	1:100
CD11b	PE-Cy5	BioLegend	101209	1:100
PD-L1	APC	BioLegend	124312	1:100
CD4	Alexa700	BioLegend	116022	1:100
CD11c	APC-Cy7	Blologend	117324	1:100
MHCII	BV421	Biologend	107620	1:200
CD45	BV510	BioLegend	103138	1:100
Ly6c	BV605	BioLegend	128036	1:100
Ly6g	BV650	BD Bioscience	740554	1:100
CD44	BUV395	BD Bioscience	740215	1:100
B220	BUV496	BD Bioscience	612950	1:100
SiglecH	BUV740	BD Bioscience	748293	1:100
Live/Dead	IR	Beckman Coulter	C36628	1:500

Table 8. Panel of antibodies used to analyze PD-L1 and PD-L2 expression on different population of leukocytes in mice with EAE.

Mouse Panel - CXCR2 expression in blood and CNS infiltrating cells				
Antigen	Fluorochrome	Company	Cat number	Titer
CD3	FITC	BD Bioscience	555274	1:100
CD45	PerCP	BioLegend	103130	1:100
PD-1	PE-Cy7	BioLegend	135216	1:100
PD-L2	PE	BioLegend	107206	1:100
CD11b	PE-Cy5	BioLegend	101209	1:100
PD-L1	APC	BioLegend	124312	1:100
CD4	Alexa700	BioLegend	116022	1:100
CD11c	APC-Cy7	Blologend	117324	1:100
MHCII	BV421	Biologend	107620	1:200
CXCR2	BV510	BD Bioscience	747815	1:100
Ly6c	BV605	BioLegend	128036	1:100
Ly6g	BV650	BD Bioscience	740554	1:100
CD44	BUV395	BD Bioscience	740215	1:100
B220	BUV496	BD Bioscience	612950	1:100
Live/Dead	IR	Beckman Coulter	C36628	1:500
Fc Block	-	BioLegend	101320	1:100

Table 9. Mouse panel for CXCR2 expression on circulating neutrophils and CNS infiltrating cells in EAE mice.

II.IV RT-PCR

Total RNA was extracted from brains, spinal cords, and lymph nodes of EAE mice with TRIzol™ Reagent (Invitrogen, 15596026). Genomic DNA was removed by treatment with DNase I type (QIAGEN). RNA concentration was measured on a NanoDrop spectrophotometer (Nanodrop® ND-1000 Spectrophotometer, Thermo Scientific, Roskilde, Denmark) and converted into cDNA using a high-capacity cDNA reverse transcription kit (Applied Biosystems). qRT-PCR was performed using a ThermoScript RT-PCR system (Invitrogen). IL-6 (Mm00446190_m1), IL-1β (Mm01336189_m1), MMP9 (Mm00442991_m1), CXCL1 (Mm00433859_m1), CXCL2 (Mm00436450_m1), CXCL3 (Mm01701838_m1), CXCL10 (Mm00445235_m1), SELP (Mm00441295_m1), ICAM (Mm00516023_m1) and gapdh (4352339E) mRNA levels were measured by real-time RT-PCR (Applied Biosystems, Invitrogen). The $2^{-\Delta\Delta CT}$ method was used to calculate relative changes in gene expression¹⁸³.

II.V Tissue immunofluorescence staining

SCs from healthy and EAE mice at different stages of disease were collected and frozen following the procedure described in *paragraph II.II* and used to prepare 15 μm sections. SC sections were washed two times with PBS1× and incubated in blocking solution (PBS1×, 5% or 10% serum of secondary Ab species with or without Triton 0.1% (depending on the nature of the antigen)), for up to one hour at room temperature. Primary antibodies were diluted in blocking solution (1% serum) and incubated at +4°C overnight, as suggested by the manufacturer's instructions. The following day CNS sections were rinsed in PBS1× three times for 5 min and incubated with fluorescent secondary antibodies (conjugated with Alexa Fluor 488, 546, or 633), diluted in blocking solution (1% serum). Slides were then washed three times in PBS1× for 5 min and incubated in DAPI for nuclei counterstaining (1:25,000; Roche Diagnostics Spa, Monza, Italy). Finally, slides were mounted with Dako or Fluoromount Gold (Invitrogen). The Leica SP5 and SP8 (Leica Microsystems, Milan, Italy) confocal microscopes were used for image acquisitions. Images were analyzed with Fiji software (NIH).

IF - Primary Antibodies for mouse tissues				
Antibody	Host Specie	Company	Cat number	Dilution
Ly6g	Rat	BD Pharmigen	551459	1:100
PD-L2 (CD273)	Rabbit	Invitrogen	PA5-20344	1:500
NeuN	Mouse	Millipore	mab377	1:500
Iba1	Goat	Novus Biological	Nb100-10-28	1:200
mCherry	Rabbit	Abcam	AB167453	1:200

Table 10. Primary antibodies used for IF on mouse tissues.

II.VI Isolation of murine neutrophils

Neutrophils were isolated from the BM of healthy adult C57BL/6J mice. After sacrifice, the tibias and femurs were surgically removed, and the medullary cavity was manually exposed in one extremity. To prevent premature early neutrophil activation, BM cells were rapidly flushed out of the bones in MACS Buffer (BSA 0.5% [Rockland], EDTA 2mM in PBS1X lacking Ca²⁺ and Mg²⁺) with a 30 Gauge ½ hypodermic needle. BM cells were pelleted, filtered with a 70µm strain and washed with MACS buffer. Bone marrow-derived mature neutrophils were isolated by negative selection using the Neutrophil Isolation Kit (Miltenyi Biotec, #130-097-658) following the manufacturer protocol. Neutrophils were finally washed, resuspended in RMPI medium supplemented with 10% FBS and counted. More than 90% of the isolated cells were Ly6G⁺ pure neutrophils as previously determined by flow cytometry. Freshly isolated neutrophils were rapidly used according to the experimental settings.

II.VII Transgenic mouse models

- PZTD mouse model

Rebecca Lee generated the PZTD mouse model to delete PD-L2 in a specific subset of B cells termed L2pB1 cells¹⁸⁴. To inducibly deplete L2pB1 cells, they inserted a diphtheria toxin receptor (DTR) gene in a duplicated exon 5 of the *Pdcd1lg2* gene, downstream of the 3' LoxP site. DTR was not expressed until the floxed region was removed by the specific Cre recombinase. Upon deletion of the floxed region by Cre recombinase, the PD-L2 gene ended at the stop codon of the duplicated exon 5, followed by the IRES-linked DTR gene. Consequently, PD-L2⁺ cells of interest were highly susceptible to diphtheria toxin. The expression of a human DTR on the surface of a mouse

cell allows for the ablation of specific cell types through the well-established mechanism of diphtheria toxin-mediated cell death¹⁷³. The genetic strategy used for the generation of this model is illustrated below (Figure 53) as well as the list of antibodies used for the characterization of leukocytes with multiparametric flow cytometry (Table 11).

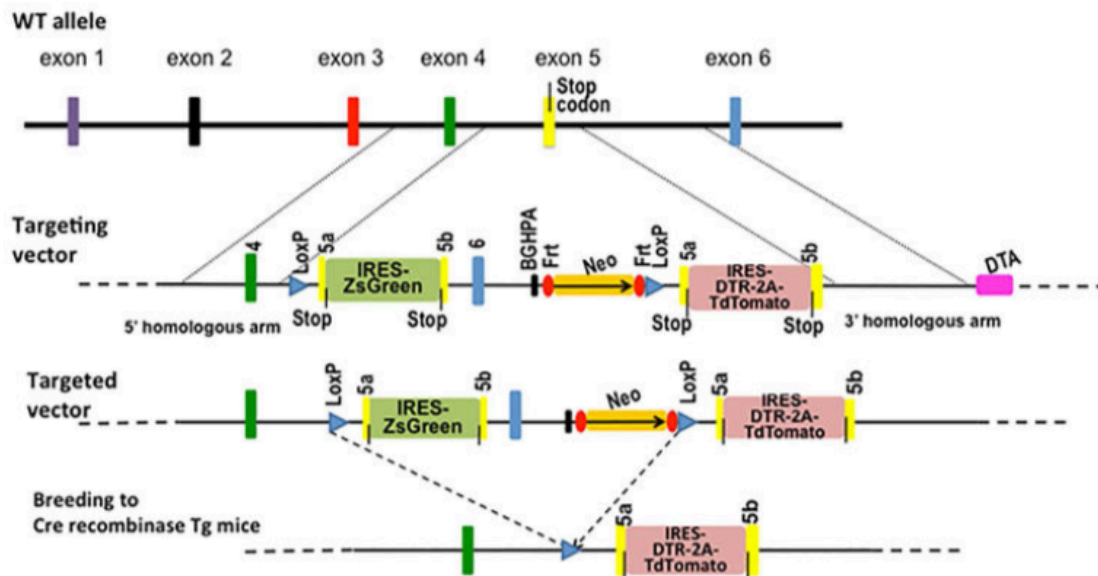


Figure 52. Genetic strategy used for the generation of PZTD mice.

Mouse Panel – CNS infiltrating cells in PZTD mice with EAE				
Antigen	Fluorochrome	Company	Cat number	Titer
Zs Green	FITC	-	-	Endo
PD-1	PE-Cy7	BioLegend	135216	1:100
PD-L2	PE	BioLegend	107206	1:100
CD11b	PE-Cy5	BioLegend	101209	1:100
PD-L1	APC	BioLegend	124312	1:100
CD11c	APC-Cy7	BIolegend	117324	1:100
MHC II	BV421	BioLegend	107620	1:200
CD45	BV510	BioLegend	103138	1:100
Ly6c	BV605	BioLegend	128036	1:100
Ly6g	BV650	BD Bioscience	740554	1:100
CD44	BUV395	BD Bioscience	740215	1:100
B220	BUV496	BD Bioscience	612950	1:100
Live/Dead	IR	Beckman Coulter	C36628	1:500
Fc Block	-	BioLegend	101320	1:250

Table 11. Panel of antibodies used to characterize infiltrating cells in the CNS of PZTD mice with EAE at 14 d.p.i.

- **Catchup mouse model (CRE specific for Ly6G locus)**

Falk Nimmerjahn and Matthias Gunzer reported that by modulating the neutrophil-specific locus Ly6G with a knock-in allele expressing Cre recombinase and the fluorescent protein tdTomato, they generated a “Catchup” mouse model that exhibits strong neutrophil specificity¹⁷⁵ (Figure 54).

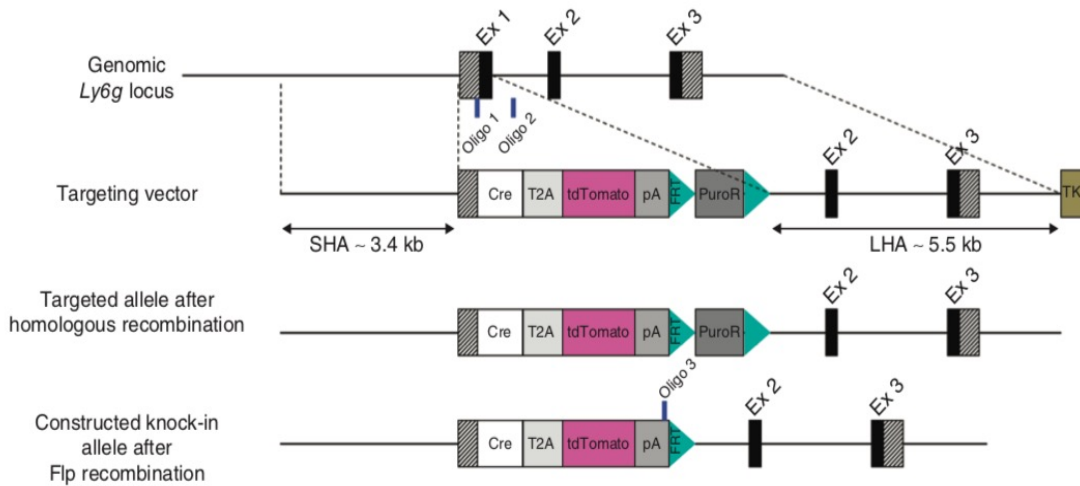


Figure 53. Genetic strategy used for the generation of Catchup mice.

For the characterization of Ly6g⁺ neutrophils circulating in blood of catchup mice, we used the following list of antibodies (Table 12):

Mouse Panel – Blood circulating cells of Catchup mice				
Antigen	Fluorochrome	Company	Cat number	Titer
CD3	FITC	BD Bioscience	555274	1:100
CD45	PerCP	BioLegend	103130	1:100
CD8a	PE Dazzle 594	BioLegend	100761	1:100
TdTomato	PE	BioLegend	107206	1:100
CD11b	PE-Cy5	BioLegend	101209	1:100
CD4	Alexa700	BioLegend	116022	1:100
Ly6c	BV605	BioLegend	128036	1:100
Ly6g	BV650	BD Bioscience	740554	1:100
B220	BUV496	BD Bioscience	612950	1:100
Live/Dead	IR	Beckman Coulter	C36628	1:500
Fc Block	-	BioLegend	101320	1:100

Table 12. Panel of antibodies used to characterize circulating cells in the blood of Catchup mice.

Crossing the Catchup mice with the PZTD mouse model, in the offspring only PD-L2⁺ neutrophils will be sensitive to killing by diphtheria toxin allowing for conditional deletion of PD-L2⁺ neutrophils.

- LysM-CRE mouse model (CRE specific for LysM locus)

The LysM mouse model was generated in 1999 by Clausen et al. Using the genetic strategy reported below, they generated mice that express Cre in myeloid cells due to targeted insertion of the cre cDNA into their endogenous M lysozyme locus. In double mutant mice harboring both the LysMcre allele and one of two different loxP-flanked target genes tested, a deletion efficiency of 83–98% was determined in mature macrophages and near 100% in granulocytes¹⁸⁵. LysM-CRE mice are extensively used since then to achieve the depletion of myeloid cells in transgenic mouse models.

Mouse Panel – PZTD x LysM EAE				
Antigen	Fluorochrome	Company	Cat number	Titer
PD-L2 PZTD	FITC	-	-	Endo
CD45	PerCP	BioLegend	103130	1:100
PD-1	PE-Cy7	BioLegend	135216	1:100
PD-L2/CRE ricombinated	PE/TdTomato	-	-	Endo
CD11b	PE-Cy5	BioLegend	101209	1:100
PD-L1	APC	BioLegend	124312	1:100
CD4	Alexa700	BioLegend	116022	1:100
CD11c	APC-Cy7	BioLegend	117324	1:100
CD3	BV421	BD Bioscience	558214	1:100
Ly6c	BV605	BioLegend	128036	1:100
Ly6g	BV650	BD Bioscience	740554	1:100
B220	BUV496	BD Bioscience	612950	1:100
Live/Dead	IR	BioLegend	101320	1:100
Fc Block				

Table 13. Panel of antibodies used to analyze different cell populations in PZTD x LysM mice with EAE.

Crossing the LysM-CRE mouse model with the PZTD mouse model, in the offspring only PD-L2⁺ myeloid cells will be sensitive to killing by diphtheria toxin allowing for conditional deletion of PD-L2⁺ myeloid cells, namely neutrophils but also

macrophages/monocytes and microglia cells. In Table 13, I reported the panel of antibody that will be used to analyze circulating and infiltrating leukocytes in mice with EAE.

III. Statistical analysis

Statistical analyses were performed using GraphPad Prism 9 software (GraphPad Software, San Diego, CA, USA). Results are expressed as the mean value \pm the standard deviation of the mean (SD) or standard error (SEM) for mouse experiments. Comparisons were made using the following statistical tests:

- One-way or Two-way Analysis of Variance (ANOVA)
- unpaired Student's t-tests

Followed by Tukey's or multiple comparison tests. p values lower than 0.05 were considered statistically significant and asterisks indicate significant increases: * $p \leq 0.05$; ** $p \leq 0.01$; *** $p \leq 0.001$.

REFERENCES

1. Manenti S, Orrico M, Masciocchi S, Mandelli A, Finardi A, Furlan R. PD-1/PD-L axis in neuroinflammation: new insights. *Front Neurol.* 2022;1045.
2. Kwon HS, Koh S-H. Neuroinflammation in neurodegenerative disorders: the roles of microglia and astrocytes. *Transl Neurodegener.* 2020;9(1):1-12.
3. DiSabato DJ, Quan N, Godbout JP. Neuroinflammation: the devil is in the details. *J Neurochem.* 2016;139:136-153.
4. Orihuela R, McPherson CA, Harry GJ. Microglial M1/M2 polarization and metabolic states. *Br J Pharmacol.* 2016;173(4):649-665.
5. He Y, Gao Y, Zhang Q, Zhou G, Cao F, Yao S. IL-4 switches microglia/macrophage M1/M2 polarization and alleviates neurological damage by modulating the JAK1/STAT6 pathway following ICH. *Neuroscience.* 2020;437:161-171.
6. Michael BD, Griffiths MJ, Granerod J, et al. The interleukin-1 balance during encephalitis is associated with clinical severity, blood-brain barrier permeability, neuroimaging changes, and disease outcome. *J Infect Dis.* 2016;213(10):1651-1660.
7. Hawkins BT, Davis TP. The blood-brain barrier/neurovascular unit in health and disease. *Pharmacol Rev.* 2005;57(2):173-185.
8. Tian L, Ma L, Kaarela T, Li Z. Neuroimmune crosstalk in the central nervous system and its significance for neurological diseases. *J Neuroinflammation.* 2012;9(1):1-10.
9. Prinz M, Jung S, Priller J. Microglia biology: one century of evolving concepts. *Cell.* 2019;179(2):292-311.
10. Davalos D, Grutzendler J, Yang G, et al. ATP mediates rapid microglial response to local brain injury in vivo. *Nat Neurosci.* 2005;8(6):752-758.
11. Fernandes A, Miller-Fleming L, Pais TF. Microglia and inflammation: conspiracy, controversy or control? *Cell Mol Life Sci.* 2014;71(20):3969-3985. doi:10.1007/s00018-014-1670-8
12. Lloyd AF, Miron VE. The pro-remyelination properties of microglia in the central nervous system. *Nat Rev Neurol.* 2019;15(8):447-458.

13. Tanaka T, Yoshida S. Mechanisms of remyelination: recent insight from experimental models. *Biomol Concepts*. 2014;5(4):289-298.
14. Bachiller S, Jiménez-Ferrer I, Paulus A, et al. Microglia in neurological diseases: a road map to brain-disease dependent-inflammatory response. *Front Cell Neurosci*. 2018;12:488.
15. Jha MK, Jo M, Kim J-H, Suk K. Microglia-astrocyte crosstalk: an intimate molecular conversation. *Neurosci*. 2019;25(3):227-240.
16. Rawji KS, Yong VW. The benefits and detriments of macrophages/microglia in models of multiple sclerosis. *Clin Dev Immunol*. 2013;2013.
17. Liddelow SA, Barres BA. Reactive astrocytes: production, function, and therapeutic potential. *Immunity*. 2017;46(6):957-967.
18. Iizumi T, Takahashi S, Mashima K, et al. A possible role of microglia-derived nitric oxide by lipopolysaccharide in activation of astroglial pentose-phosphate pathway via the Keap1/Nrf2 system. *J Neuroinflammation*. 2016;13(1):1-20.
19. Prajeeth CK, Kronisch J, Khoroshi R, et al. Effectors of Th1 and Th17 cells act on astrocytes and augment their neuroinflammatory properties. *J Neuroinflammation*. 2017;14(1):1-14.
20. Brosnan CF, Raine CS. The astrocyte in multiple sclerosis revisited. *Glia*. 2013;61(4):453-465.
21. Sofroniew M V. Astrogliosis. *Cold Spring Harb Perspect Biol*. 2015;7(2):a020420.
22. Tanuma N, Sakuma H, Sasaki A, Matsumoto Y. Chemokine expression by astrocytes plays a role in microglia/macrophage activation and subsequent neurodegeneration in secondary progressive multiple sclerosis. *Acta Neuropathol*. 2006;112(2):195-204.
23. Lassmann H. Mechanisms of white matter damage in multiple sclerosis. *Glia*. 2014;62(11):1816-1830. doi:10.1002/glia.22597
24. Nair A, Frederick TJ, Miller SD. Astrocytes in multiple sclerosis: a product of their environment. *Cell Mol life Sci*. 2008;65(17):2702.
25. Patel JR, Williams JL, Muccigrosso MM, et al. Astrocyte TNFR2 is required for CXCL12-mediated regulation of oligodendrocyte progenitor proliferation and differentiation within the adult CNS. *Acta Neuropathol*. 2012;124(6):847-860.

26. Mrdjen D, Pavlovic A, Hartmann FJ, et al. High-dimensional single-cell mapping of central nervous system immune cells reveals distinct myeloid subsets in health, aging, and disease. *Immunity*. 2018;48(2):380-395.
27. Van Hove H, Martens L, Scheyltjens I, et al. A single-cell atlas of mouse brain macrophages reveals unique transcriptional identities shaped by ontogeny and tissue environment. *Nat Neurosci*. 2019;22(6):1021-1035.
28. Jordão MJC, Sankowski R, Brendecke SM, et al. Single-cell profiling identifies myeloid cell subsets with distinct fates during neuroinflammation. *Science (80-)*. 2019;363(6425):eaat7554.
29. Goldmann T, Wieghofer P, Jordão MJC, et al. Origin, fate and dynamics of macrophages at central nervous system interfaces. *Nat Immunol*. 2016;17(7):797-805.
30. Nayak D, Zinselmeyer BH, Corps KN, McGavern DB. In vivo dynamics of innate immune sentinels in the CNS. *Intravital*. 2012;1(2):95-106.
31. Boven LA, Van Meurs M, Van Zwam M, et al. Myelin-laden macrophages are anti-inflammatory, consistent with foam cells in multiple sclerosis. *Brain*. 2006;129(2):517-526.
32. Ajami B, Bennett JL, Krieger C, McNagny KM, Rossi F. Infiltrating monocytes trigger EAE progression, but do not contribute to the resident microglia pool. *Nat Neurosci*. 2011;14(9):1142-1149.
33. Dobson R, Giovannoni G. Multiple sclerosis—a review. *Eur J Neurol*. 2019;26(1):27-40.
34. Dendrou CA, Fugger L, Friese MA. Immunopathology of multiple sclerosis. *Nat Rev Immunol*. 2015;15(9):545.
35. (IIBDGC) IIBDGC, Agliardi C, Alfredsson L, et al. Analysis of immune-related loci identifies 48 new susceptibility variants for multiple sclerosis. *Nat Genet*. 2013;45(11):1353-1360.
36. Belbasis L, Bellou V, Evangelou E, Ioannidis JPA, Tzoulaki I. Environmental risk factors and multiple sclerosis: an umbrella review of systematic reviews and meta-analyses. *Lancet Neurol*. 2015;14(3):263-273.
37. Popescu BFG, Lucchinetti CF. Pathology of demyelinating diseases. *Annu Rev Pathol Mech Dis*. 2012;7:185-217.

38. Kebir H, Ifergan I, Alvarez JI, et al. Preferential recruitment of interferon- γ -expressing TH17 cells in multiple sclerosis. *Ann Neurol Off J Am Neurol Assoc Child Neurol Soc.* 2009;66(3):390-402.
39. Hellings N, Barée M, Verhoeven C, et al. T-cell reactivity to multiple myelin antigens in multiple sclerosis patients and healthy controls. *J Neurosci Res.* 2001;63(3):290-302.
40. Smith KJ, Kapoor R, Hall SM, Davies M. Electrically active axons degenerate when exposed to nitric oxide. *Ann Neurol.* 2001;49(4):470-476.
41. Trapp BD, Nave K-A. Multiple sclerosis: an immune or neurodegenerative disorder? *Annu Rev Neurosci.* 2008;31:247-269.
42. Frischer JM, Bramow S, Dal-Bianco A, et al. The relation between inflammation and neurodegeneration in multiple sclerosis brains. *Brain.* 2009;132(5):1175-1189.
43. Ji Q, Castelli L, Goverman JM. MHC class I-restricted myelin epitopes are cross-presented by Tip-DCs that promote determinant spreading to CD8⁺ T cells. *Nat Immunol.* 2013;14(3):254.
44. Willing A, Leach OA, Ufer F, et al. CD 8⁺ MAIT cells infiltrate into the CNS and alterations in their blood frequencies correlate with IL-18 serum levels in multiple sclerosis. *Eur J Immunol.* 2014;44(10):3119-3128.
45. Birnbaum G. Making the diagnosis of multiple sclerosis. *Adv Neurol.* 2006;14:111-124.
46. Kimura K, Hohjoh H, Fukuoka M, et al. Circulating exosomes suppress the induction of regulatory T cells via let-7i in multiple sclerosis. *Nat Commun.* 2018;9(1):1-14.
47. Schneider A, Long SA, Cersaletti K, et al. In active relapsing-remitting multiple sclerosis, effector T cell resistance to adaptive Tregs involves IL-6-mediated signaling. *Sci Transl Med.* 2013;5(170):170ra15-170ra15.
48. Jiang W, Chai NR, Maric D, Bielekova B. Unexpected role for granzyme K in CD56bright NK cell-mediated immunoregulation of multiple sclerosis. *J Immunol.* 2011;187(2):781-790.
49. Poli A, Michel T, Thérésine M, Andrès E, Hentges F, Zimmer J. CD56bright natural killer (NK) cells: an important NK cell subset. *Immunology.*

- 2009;126(4):458-465.
50. Gold R, Giovannoni G, Selmaj K, et al. Daclizumab high-yield process in relapsing-remitting multiple sclerosis (SELECT): a randomised, double-blind, placebo-controlled trial. *Lancet*. 2013;381(9884):2167-2175.
 51. Kappos L, Wiendl H, Selmaj K, et al. Daclizumab HYP versus interferon beta-1a in relapsing multiple sclerosis. *N Engl J Med*. 2015;373(15):1418-1428.
 52. Mimpen M, Smolders J, Hupperts R, Damoiseaux J. Natural killer cells in multiple sclerosis: a review. *Immunol Lett*. 2020;222:1-11.
 53. Gross CC, Schulte-Mecklenbeck A, Wiendl H, et al. Regulatory functions of natural killer cells in multiple sclerosis. *Front Immunol*. 2016;7:606.
 54. Mishra MK, Yong VW. Myeloid cells—targets of medication in multiple sclerosis. *Nat Rev Neurol*. 2016;12(9):539-551.
 55. Goldenberg M. Multiple sclerosis Review. *Pharm Ther*. 2012;37(3):175-184.
 56. Frischer JM, Weigand SD, Guo Y, et al. Clinical and pathological insights into the dynamic nature of the white matter multiple sclerosis plaque. *Ann Neurol*. 2015;78(5):710-721.
 57. Brownlee WJ, Miller DH. Clinically isolated syndromes and the relationship to multiple sclerosis. *J Clin Neurosci*. 2014;21(12):2065-2071.
 58. Malekzadeh A, de Geer-Peeters V, De Groot V, Elisabeth Teunissen C, Beckerman H. Fatigue in patients with multiple sclerosis: is it related to pro-and anti-inflammatory cytokines? *Dis Markers*. 2015;2015.
 59. Lublin FD, Reingold SC. Defining the clinical course of multiple sclerosis: results of an international survey. *Neurology*. 1996;46(4):907-911.
 60. Lublin FD. New multiple sclerosis phenotypic classification. *Eur Neurol*. 2014;72(Suppl. 1):1-5.
 61. Brownlee WJ, Hardy TA, Fazekas F, Miller DH. Diagnosis of multiple sclerosis: progress and challenges. *Lancet*. 2017;389(10076):1336-1346.
 62. Bjartmar C, Wujek JR, Trapp BD. Axonal loss in the pathology of MS: consequences for understanding the progressive phase of the disease. *J Neurol Sci*. 2003;206(2):165-171.
 63. Yang JH, Rempe T, Whitmire N, Dunn-Pirio A, Graves JS. Therapeutic advances in multiple sclerosis. *Front Neurol*. 2022:1111.

64. Koritschoner RS, Schweinburg F. Induktion von Paralyse und Rückenmarksentzündung durch Immunisierung von Kaninchen mit menschlichem Rückenmarksgewebe. *Z Immunitätsf Exp Ther.* 1925;42:217-283.
65. Rivers TM, Schwentker FF. Encephalomyelitis accompanied by myelin destruction experimentally produced in monkeys. *J Exp Med.* 1935;61(5):689-702.
66. Kabat EA, Wolf A, Bezer AE. Rapid production of acute disseminated encephalomyelitis in rhesus monkeys by injection of brain tissue with adjuvants. *Science (80-).* 1946;104(2703):362-363.
67. Procaccini C, De Rosa V, Pucino V, Formisano L, Matarese G. Animal models of multiple sclerosis. *Eur J Pharmacol.* 2015;759:182-191.
68. Furlan R, Cuomo C, Martino G. Animal models of multiple sclerosis. In: *Neural Cell Transplantation.* Springer; 2009:157-173.
69. Stromnes IM, Goverman JM. Active induction of experimental allergic encephalomyelitis. *Nat Protoc.* 2006;1(4):1810.
70. Gold R, Linington C, Lassmann H. Understanding pathogenesis and therapy of multiple sclerosis via animal models: 70 years of merits and culprits in experimental autoimmune encephalomyelitis research. *Brain.* 2006;129(8):1953-1971.
71. Hofstetter HH, Shive CL, Forsthuber TG. Pertussis toxin modulates the immune response to neuroantigens injected in incomplete Freund's adjuvant: induction of Th1 cells and experimental autoimmune encephalomyelitis in the presence of high frequencies of Th2 cells. *J Immunol.* 2002;169(1):117-125.
72. Constantinescu CS, Farooqi N, O'Brien K, Gran B. Experimental autoimmune encephalomyelitis (EAE) as a model for multiple sclerosis (MS). *Br J Pharmacol.* 2011;164(4):1079-1106.
73. Bettelli E, Pagany M, Weiner HL, Linington C, Sobel RA, Kuchroo VK. Myelin oligodendrocyte glycoprotein-specific T cell receptor transgenic mice develop spontaneous autoimmune optic neuritis. *J Exp Med.* 2003;197(9):1073-1081.
74. Silvestre-Roig C, Hidalgo A, Soehnlein O. Neutrophil heterogeneity: implications for homeostasis and pathogenesis. *Blood.* 2016;127(18):2173-2181.
75. Summers C, Rankin SM, Condliffe AM, Singh N, Peters AM, Chilvers ER.

- Neutrophil kinetics in health and disease. *Trends Immunol.* 2010;31(8):318-324.
76. Mantovani A, Cassatella MA, Costantini C, Jaillon S. Neutrophils in the activation and regulation of innate and adaptive immunity. *Nat Rev Immunol.* 2011;11(8):519-531.
 77. Phillipson M, Kubes P. The neutrophil in vascular inflammation. *Nat Med.* 2011;17(11):1381-1390.
 78. Kolaczkowska E, Kubes P. Neutrophil recruitment and function in health and inflammation. *Nat Rev Immunol.* 2013;13(3):159-175.
 79. Lämmermann T, Afonso P V, Angermann BR, et al. Neutrophil swarms require LTB4 and integrins at sites of cell death in vivo. *Nature.* 2013;498(7454):371.
 80. Pillay J, Tak T, Kamp VM, Koenderman L. Immune suppression by neutrophils and granulocytic myeloid-derived suppressor cells: similarities and differences. *Cell Mol Life Sci.* 2013;70(20):3813-3827.
 81. Ley K, Hoffman HM, Kubes P, et al. Neutrophils: new insights and open questions. *Sci Immunol.* 2018;3(30):eaat4579.
 82. Rørvig S, Østergaard O, Heegaard NHH, Borregaard N. Proteome profiling of human neutrophil granule subsets, secretory vesicles, and cell membrane: correlation with transcriptome profiling of neutrophil precursors. *J Leukoc Biol.* 2013;94(4):711-721.
 83. Uriarte SM, Powell DW, Luerman GC, et al. Comparison of proteins expressed on secretory vesicle membranes and plasma membranes of human neutrophils. *J Immunol.* 2008;180(8):5575-5581.
 84. Cieutat A-M, Lobel P, August JT, et al. Azurophilic granules of human neutrophilic leukocytes are deficient in lysosome-associated membrane proteins but retain the mannose 6-phosphate recognition marker. *Blood, J Am Soc Hematol.* 1998;91(3):1044-1058.
 85. Leliefeld PHC, Koenderman L, Pillay J. How neutrophils shape adaptive immune responses. *Front Immunol.* 2015;6:471.
 86. Ng LG, Ostuni R, Hidalgo A. Heterogeneity of neutrophils. *Nat Rev Immunol.* 2019;19(4):255-265.
 87. Montaldo E, Lusito E, Bianchessi V, et al. Cellular and transcriptional dynamics of human neutrophils at steady state and upon stress. *Nat Immunol.* 2022:1-14.

88. Scapini P, Marini O, Tecchio C, Cassatella MA. Human neutrophils in the saga of cellular heterogeneity: insights and open questions. *Immunol Rev.* 2016;273(1):48-60.
89. Dumitru CA, Moses K, Trellakis S, Lang S, Brandau S. Neutrophils and granulocytic myeloid-derived suppressor cells: immunophenotyping, cell biology and clinical relevance in human oncology. *Cancer Immunol Immunother.* 2012;61(8):1155-1167.
90. Carmona-Rivera C, Kaplan MJ. Low-density granulocytes: a distinct class of neutrophils in systemic autoimmunity. In: *Seminars in Immunopathology*. Vol 35. Springer; 2013:455-463.
91. Bowers NL, Helton ES, Huijbregts RPH, Goepfert PA, Heath SL, Hel Z. Immune suppression by neutrophils in HIV-1 infection: role of PD-L1/PD-1 pathway. *PLoS Pathog.* 2014;10(3):e1003993.
92. Tsuda Y, Fukui H, Asai A, et al. An immunosuppressive subtype of neutrophils identified in patients with hepatocellular carcinoma. *J Clin Biochem Nutr.* 2012:12-32.
93. Fridlender ZG, Sun J, Kim S, et al. Polarization of tumor-associated neutrophil phenotype by TGF- β : “N1” versus “N2” TAN. *Cancer Cell.* 2009;16(3):183-194.
94. Li Y, Wang W, Yang F, Xu Y, Feng C, Zhao Y. The regulatory roles of neutrophils in adaptive immunity. *Cell Commun Signal.* 2019;17(1):1-11.
95. Marini O, Costa S, Bevilacqua D, et al. Mature CD10⁺ and immature CD10⁻ neutrophils present in G-CSF-treated donors display opposite effects on T cells. *Blood.* 2017;129(10):1343-1356.
96. de Kleijn S, Langereis JD, Leentjens J, et al. IFN- γ -stimulated neutrophils suppress lymphocyte proliferation through expression of PD-L1. *PLoS One.* 2013;8(8):e72249.
97. Bank U, Ansorge S. More than destructive: neutrophil-derived serine proteases in cytokine bioactivity control. *J Leukoc Biol.* 2001;69(2):197-206.
98. Woodberry T, Bouffler SE, Wilson AS, Buckland RL, Brüstle A. The emerging role of neutrophil granulocytes in multiple sclerosis. *J Clin Med.* 2018;7(12):511.
99. Stock AJ, Kasus-Jacobi A, Pereira HA. The role of neutrophil granule proteins in neuroinflammation and Alzheimer’s disease. *J Neuroinflammation.*

- 2018;15(1):1-15.
100. Wanrooy BJ, Wen SW, Wong CHY. Dynamic roles of neutrophils in post-stroke neuroinflammation. *Immunol Cell Biol.* 2021;99(9):924-935.
 101. Ruhnau J, Schulze J, Dressel A, Vogelgesang A. Thrombosis, neuroinflammation, and poststroke infection: the multifaceted role of neutrophils in stroke. *J Immunol Res.* 2017;2017.
 102. De Bondt M, Hellings N, Opdenakker G, Struyf S. Neutrophils: underestimated players in the pathogenesis of Multiple Sclerosis (MS). *Int J Mol Sci.* 2020;21(12):4558.
 103. Simmons SB, Liggitt D, Goverman JM. Cytokine-regulated neutrophil recruitment is required for brain but not spinal cord inflammation during experimental autoimmune encephalomyelitis. *J Immunol.* 2014;193(2):555-563.
 104. Németh T, Mócsai A. The role of neutrophils in autoimmune diseases. *Immunol Lett.* 2012;143(1):9-19.
 105. Wu F, Cao W, Yang Y, Liu A. Extensive infiltration of neutrophils in the acute phase of experimental autoimmune encephalomyelitis in C57BL/6 mice. *Histochem Cell Biol.* 2010;133(3):313-322.
 106. Kroenke MA, Chensue SW, Segal BM. EAE mediated by a non-IFN- γ /non-IL-17 pathway. *Eur J Immunol.* 2010;40(8):2340-2348.
 107. Aubé B, Lévesque SA, Paré A, et al. Neutrophils mediate blood–spinal cord barrier disruption in demyelinating neuroinflammatory diseases. *J Immunol.* 2014;193(5):2438-2454.
 108. Christy AL, Walker ME, Hessner MJ, Brown MA. Mast cell activation and neutrophil recruitment promotes early and robust inflammation in the meninges in EAE. *J Autoimmun.* 2013;42:50-61.
 109. Soulika AM, Lee E, McCauley E, Miers L, Bannerman P, Pleasure D. Initiation and progression of axonopathy in experimental autoimmune encephalomyelitis. *J Neurosci.* 2009;29(47):14965-14979.
 110. Steinbach K, Piedavent M, Bauer S, Neumann JT, Friese MA. Neutrophils amplify autoimmune central nervous system infiltrates by maturing local APCs. *J Immunol.* 2013;191(9):4531-4539.
 111. Brück W, Lucchinetti C, Lassmann H. The pathology of primary progressive

- multiple sclerosis. *Mult Scler J*. 2002;8(2):93-97.
112. Kostic M, Dzopalic T, Zivanovic S, et al. IL-17 and glutamate excitotoxicity in the pathogenesis of multiple sclerosis. *Scand J Immunol*. 2014;79(3):181-186.
 113. Ishizu T, Osoegawa M, Mei F-J, et al. Intrathecal activation of the IL-17/IL-8 axis in opticospinal multiple sclerosis. *Brain*. 2005;128(5):988-1002.
 114. Håkansson I, Tisell A, Cassel P, et al. Neurofilament levels, disease activity and brain volume during follow-up in multiple sclerosis. *J Neuroinflammation*. 2018;15(1):1-10.
 115. Guarnieri B, Lolli F, Amaducci L. Polymorphonuclear neutral protease activity in multiple sclerosis and other diseases. *Ann Neurol*. 1985;18(5):620-622.
 116. Bisgaard AK, Pihl-Jensen G, Frederiksen JL. The neutrophil-to-lymphocyte ratio as disease activity marker in multiple sclerosis and optic neuritis. *Mult Scler Relat Disord*. 2017;18:213-217.
 117. Naegele M, Tillack K, Reinhardt S, Schippling S, Martin R, Sospedra M. Neutrophils in multiple sclerosis are characterized by a primed phenotype. *J Neuroimmunol*. 2012;242(1-2):60-71.
 118. Owens T, Benmamar-Badel A, Wlodarczyk A, et al. Protective roles for myeloid cells in neuroinflammation. *Scand J Immunol*. 2020;92(5):e12963.
 119. Kasuga K, Yang R, Porter TF, et al. Rapid appearance of resolvins precursors in inflammatory exudates: novel mechanisms in resolution. *J Immunol*. 2008;181(12):8677-8687.
 120. Fox S, Leitch AE, Duffin R, Haslett C, Rossi AG. Neutrophil apoptosis: relevance to the innate immune response and inflammatory disease. *J Innate Immun*. 2010;2(3):216-227.
 121. Haschka D, Tymoszuk P, Bsteh G, et al. Expansion of neutrophils and classical and nonclassical monocytes as a hallmark in relapsing-remitting multiple sclerosis. *Front Immunol*. 2020;11:594.
 122. Khoroshi R, Marczyńska J, Dieu RS, et al. Innate signaling within the central nervous system recruits protective neutrophils. *Acta Neuropathol Commun*. 2020;8(1):1-13.
 123. Twomey JD, Zhang B. Cancer immunotherapy update: FDA-approved checkpoint inhibitors and companion diagnostics. *AAPS J*. 2021;23(2):1-11.

124. Darnell EP, Mooradian MJ, Baruch EN, Yilmaz M, Reynolds KL. Immune-related adverse events (irAEs): diagnosis, management, and clinical pearls. *Curr Oncol Rep.* 2020;22(4):1-11.
125. Zhang X, Lund H, Mia S, Parsa R, Harris RA. Adoptive transfer of cytokine-induced immunomodulatory adult microglia attenuates experimental autoimmune encephalomyelitis in DBA/1 mice. *Glia.* 2014;62(5):804-817.
126. Chen Q, Xu L, Du T, et al. Enhanced Expression of PD-L1 on Microglia After Surgical Brain Injury Exerts Self-Protection from Inflammation and Promotes Neurological Repair. *Neurochem Res.* 2019;44(11):2470-2481.
127. Zhao S, Li F, Leak RK, Chen J, Hu X. Regulation of neuroinflammation through programmed death-1/programmed death ligand signaling in neurological disorders. *Front Cell Neurosci.* 2014;8(SEP). doi:10.3389/fncel.2014.00271
128. Okazaki T, Maeda A, Nishimura H, Kurosaki T, Honjo T. PD-1 immunoreceptor inhibits B cell receptor-mediated signaling by recruiting src homology 2-domain-containing tyrosine phosphatase 2 to phosphotyrosine. *Proc Natl Acad Sci.* 2001;98(24):13866-13871.
129. Latchman Y, Wood CR, Chernova T, et al. PD-L2 is a second ligand for PD-1 and inhibits T cell activation. *Nat Immunol.* 2001;2(3):261.
130. Philips EA, Garcia-España A, Tocheva AS, et al. The structural features that distinguish PD-L2 from PD-L1 emerged in placental mammals. *J Biol Chem.* 2020;295(14):4372-4380.
131. Keir ME, Butte MJ, Freeman GJ, Sharpe AH. PD-1 and its ligands in tolerance and immunity. *Annu Rev Immunol.* 2008;26:677-704.
132. Liang SC, Latchman YE, Buhlmann JE, et al. Regulation of PD-1, PD-L1, and PD-L2 expression during normal and autoimmune responses. *Eur J Immunol.* 2003;33(10):2706-2716.
133. Ohigashi Y, Sho M, Yamada Y, et al. Clinical significance of programmed death-1 ligand-1 and programmed death-1 ligand-2 expression in human esophageal cancer. *Clin cancer Res.* 2005;11(8):2947-2953.
134. Yokosuka T, Takamatsu M, Kobayashi-Imanishi W, Hashimoto-Tane A, Azuma M, Saito T. Programmed cell death 1 forms negative costimulatory microclusters that directly inhibit T cell receptor signaling by recruiting phosphatase SHP2. *J*

- Exp Med.* 2012;209(6):1201-1217.
135. Said EA, Dupuy FP, Trautmann L, et al. Programmed death-1–induced interleukin-10 production by monocytes impairs CD4+ T cell activation during HIV infection. *Nat Med.* 2010;16(4):452.
 136. Salama AD, Chitnis T, Imitola J, et al. Critical role of the programmed death-1 (PD-1) pathway in regulation of experimental autoimmune encephalomyelitis. *J Exp Med.* 2003;198(1):71-78.
 137. Reynoso ED, Elpek KG, Francisco L, et al. Intestinal tolerance is converted to autoimmune enteritis upon PD-1 ligand blockade. *J Immunol.* 2009;182(4):2102-2112.
 138. Fife BT, Pauken KE, Eagar TN, et al. Interactions between PD-1 and PD-L1 promote tolerance by blocking the TCR–induced stop signal. *Nat Immunol.* 2009;10(11):1185.
 139. Nishimura H, Nose M, Hiai H, Minato N, Honjo T. Development of lupus-like autoimmune diseases by disruption of the PD-1 gene encoding an ITIM motif-carrying immunoreceptor. *Immunity.* 1999;11(2):141-151.
 140. Wang J, Yoshida T, Nakaki F, Hiai H, Okazaki T, Honjo T. Establishment of NOD-Pdcd1^{-/-} mice as an efficient animal model of type I diabetes. *Proc Natl Acad Sci U S A.* 2005;102(33):11823-11828. doi:10.1073/pnas.0505497102
 141. Nishimura H, Okazaki T, Tanaka Y, et al. Autoimmune dilated cardiomyopathy in PD-1 receptor-deficient mice. *Science (80-).* 2001;291(5502):319-322. doi:10.1126/science.291.5502.319
 142. Chauhan P, Lokensgard JR. Glial cell expression of PD-L1. *Int J Mol Sci.* 2019;20(7):1677.
 143. Magnus T, Schreiner B, Korn T, et al. Microglial expression of the B7 family member B7 homolog 1 confers strong immune inhibition: implications for immune responses and autoimmunity in the CNS. *J Neurosci.* 2005;25(10):2537-2546.
 144. Xiao Y, Yu S, Zhu B, et al. RGMB is a novel binding partner for PD-L2 and its engagement with PD-L2 promotes respiratory tolerance. *J Exp Med.* 2014;211(5):943-959.
 145. Hurrell BP, Helou DG, Howard E, et al. PD-L2 controls peripherally induced

- regulatory T cells by maintaining metabolic activity and Foxp3 stability. *Nat Commun.* 2022;13(1):1-14.
146. Carter LL, Leach MW, Azoitei ML, et al. PD-1/PD-L1, but not PD-1/PD-L2, interactions regulate the severity of experimental autoimmune encephalomyelitis. *J Neuroimmunol.* 2007;182(1-2):124-134.
147. Kroner A, Schwab N, Ip CW, et al. Accelerated course of experimental autoimmune encephalomyelitis in PD-1-deficient central nervous system myelin mutants. *Am J Pathol.* 2009;174(6):2290-2299.
148. Pawlak-Adamska E, Nowak O, Karabon L, et al. PD-1 gene polymorphic variation is linked with first symptom of disease and severity of relapsing-remitting form of MS. *J Neuroimmunol.* 2017;305:115-127.
149. Javan MR, Aslani S, Zamani MR, et al. Downregulation of immunosuppressive molecules, PD-1 and PD-L1 but not PD-L2, in the patients with multiple sclerosis. *Iran J Allergy, Asthma Immunol.* 2016;15(4):296-302.
150. Mohammadzadeh A, Rad IA, Ahmadi-Salmasi B. CTLA-4, PD-1 and TIM-3 expression predominantly downregulated in MS patients. *J Neuroimmunol.* 2018;323:105-108.
151. Arruda LCM, de Azevedo JTC, de Oliveira GL V, et al. Immunological correlates of favorable long-term clinical outcome in multiple sclerosis patients after autologous hematopoietic stem cell transplantation. *Clin Immunol.* 2016;169:47-57.
152. Schreiner B, Mitsdoerffer M, Kieseier BC, et al. Interferon- β enhances monocyte and dendritic cell expression of B7-H1 (PD-L1), a strong inhibitor of autologous T-cell activation: relevance for the immune modulatory effect in multiple sclerosis. *J Neuroimmunol.* 2004;155(1-2):172-182.
153. Koto S, Chihara N, Akatani R, et al. Transcription Factor c-Maf Promotes Immunoregulation of Programmed Cell Death 1-Expressed CD8⁺ T Cells in Multiple Sclerosis. *Neurol Neuroimmunol Neuroinflammation.* 2022;9(4).
154. Pittet CL, Newcombe J, Antel JP, Arbour N. The majority of infiltrating CD8 T lymphocytes in multiple sclerosis lesions is insensitive to enhanced PD-L1 levels on CNS cells. *Glia.* 2011;59(5):841-856.
155. van Nierop GP, van Luijn MM, Michels SS, et al. Phenotypic and functional

- characterization of T cells in white matter lesions of multiple sclerosis patients. *Acta Neuropathol.* 2017;134(3):383-401.
156. Gettings EJ, Hackett CT, Scott TF. Severe relapse in a multiple sclerosis patient associated with ipilimumab treatment of melanoma. *Mult Scler J.* 2015;21(5):670.
 157. Garcia CR, Jayswal R, Adams V, Anthony LB, Villano JL. Multiple sclerosis outcomes after cancer immunotherapy. *Clin Transl Oncol.* 2019;21(10):1336-1342.
 158. Lu BY, Isitan C, Mahajan A, et al. Intracranial Complications From Immune Checkpoint Therapy in a Patient With NSCLC and Multiple Sclerosis: Case Report. *JTO Clin Res Reports.* 2021;2(6):100183.
 159. Gerdes LA, Held K, Beltrán E, et al. CTLA4 as immunological checkpoint in the development of multiple sclerosis. *Ann Neurol.* 2016;80(2):294-300.
 160. Li C, Chen C, Kang X, et al. Decidua-derived granulocyte macrophage colony-stimulating factor induces polymorphonuclear myeloid-derived suppressor cells from circulating CD15+ neutrophils. *Hum Reprod.* 2020;35(12):2677-2691.
 161. Shan Z, Zhao Y, Zhang J, et al. FasL+ PD-L2+ Identifies a Novel Immunosuppressive Neutrophil Population in Human Gastric Cancer That Promotes Disease Progression. *Adv Sci.* 2021:2103543.
 162. Elghetany MT. Surface antigen changes during normal neutrophilic development: a critical review. *Blood Cells, Mol Dis.* 2002;28(2):260-274.
 163. Loke P, Allison JP. PD-L1 and PD-L2 are differentially regulated by Th1 and Th2 cells. *Proc Natl Acad Sci.* 2003;100(9):5336-5341.
 164. Maimone D, Gregory S, Arnason BGW, Reder AT. Cytokine levels in the cerebrospinal fluid and serum of patients with multiple sclerosis. *J Neuroimmunol.* 1991;32(1):67-74.
 165. Spitzer MH, Nolan GP. Mass cytometry: single cells, many features. *Cell.* 2016;165(4):780-791.
 166. Tanner SD, Baranov VI, Ornatsky OI, Bandura DR, George TC. An introduction to mass cytometry: fundamentals and applications. *Cancer Immunol Immunother.* 2013;62(5):955-965.
 167. Ornatsky O, Bandura D, Baranov V, Nitz M, Winnik MA, Tanner S. Highly

- multiparametric analysis by mass cytometry. *J Immunol Methods*. 2010;361(1-2):1-20.
168. Rowland BD, Bernards R, Peeper DS. The KLF4 tumour suppressor is a transcriptional repressor of p53 that acts as a context-dependent oncogene. *Nat Cell Biol*. 2005;7(11):1074-1082.
169. Condamine T, Dominguez GA, Youn J-I, et al. Lectin-type oxidized LDL receptor-1 distinguishes population of human polymorphonuclear myeloid-derived suppressor cells in cancer patients. *Sci Immunol*. 2016;1(2):aaf8943-aaf8943.
170. Zhang X, Yin X, Zhang H, et al. Differential expressions of PD-1, PD-L1 and PD-L2 between primary and metastatic sites in renal cell carcinoma. *BMC Cancer*. 2019;19(1):1-10.
171. Buderath P, Schwich E, Jensen C, et al. Soluble programmed death receptor ligands sPD-L1 and sPD-L2 as liquid biopsy markers for prognosis and platinum response in epithelial ovarian cancer. *Front Oncol*. 2019;9:1015.
172. Costantini A, Julie C, Dumenil C, et al. Predictive role of plasmatic biomarkers in advanced non-small cell lung cancer treated by nivolumab. *Oncoimmunology*. 2018;7(8):e1452581.
173. Buch T, Heppner FL, Tertilt C, et al. A Cre-inducible diphtheria toxin receptor mediates cell lineage ablation after toxin administration. *Nat Methods*. 2005;2(6):419.
174. Zu Hörste GM, Zozulya AL, El-Haddad H, et al. Active immunization induces toxicity of diphtheria toxin in diphtheria resistant mice—implications for neuroinflammatory models. *J Immunol Methods*. 2010;354(1-2):80-84.
175. Hasenberg A, Hasenberg M, Männ L, et al. Catchup: a mouse model for imaging-based tracking and modulation of neutrophil granulocytes. *Nat Methods*. 2015;12(5):445.
176. Huber S, Hoffmann R, Muskens F, Voehringer D. Alternatively activated macrophages inhibit T-cell proliferation by Stat6-dependent expression of PD-L2. *Blood, J Am Soc Hematol*. 2010;116(17):3311-3320.
177. Wu F, Zhao Y, Jiao T, et al. CXCR2 is essential for cerebral endothelial activation and leukocyte recruitment during neuroinflammation. *J*

- Neuroinflammation*. 2015;12(1):1-15.
178. Veenstra M, Ransohoff RM. Chemokine receptor CXCR2: physiology regulator and neuroinflammation controller? *J Neuroimmunol*. 2012;246(1-2):1-9.
179. Kurtzke JF. Multiple sclerosis in time and space-geographic clues to cause. *J Neurovirol*. 2000;6(2):S134.
180. Takahashi C, Au-Yeung A, Fuh F, et al. Mass cytometry panel optimization through the designed distribution of signal interference. *Cytom Part A*. 2017;91(1):39-47.
181. Zunder ER, Finck R, Behbehani GK, et al. Palladium-based mass tag cell barcoding with a doublet-filtering scheme and single-cell deconvolution algorithm. *Nat Protoc*. 2015;10(2):316-333.
182. Ginhoux F, Greter M, Leboeuf M, et al. Fate mapping analysis reveals that adult microglia derive from primitive macrophages. *Science (80-)*. 2010;330(6005):841-845.
183. Livak KJ, Schmittgen TD. Analysis of relative gene expression data using real-time quantitative PCR and the $2^{-\Delta\Delta CT}$ method. *methods*. 2001;25(4):402-408.
184. Lee R, Mao C, Vo H, Gao W, Zhong X. Fluorescence tagging and inducible depletion of PD-L2-expressing B-1 B cells in vivo. *Ann N Y Acad Sci*. 2015;1362(1):77.
185. Clausen BE, Burkhardt C, Reith W, Renkawitz R, Förster I. Conditional gene targeting in macrophages and granulocytes using LysMcre mice. *Transgenic Res*. 1999;8(4):265-277.

